The scientific case for DT operation in JET

Final report, of the Working Group at EFDA-JET on "Preparing a scientific case for DT operation in JET"

03 February 2011

Working group members:
G. Sips, C. Challis, H. Weisen

Outline:

A working group was formed in May 2010 to prepare the scientific case for DT operation in JET, planned for 2014-2015. The material is presented in the following chapters:

1. DT operation in JET
2. JET upgrades and preparation for DT
3. Diagnostic capabilities for DT
4. Fusion performance projections for JET DT operation
5. Isotope effects (H, D, T)
6. Alpha particle physics
7. RF heating scenarios and RF physics
8. Fusion Technology
9. DT campaign proposals

A summary of key points is given at the beginning of each chapter.

Contents **page**

Contents **page**

Terms of Reference

A working group was formed in May 2010 to prepare the scientific case for future DT operation in JET. The EFDA-JET Leader provided the working group with the following terms of reference:

"Establish the scientific potential of a DT Campaign on JET carried out after the exploitation of the ILW with particular reference to scenario development (isotopic effect), collective MHD instabilities and plasma wall interaction (tritium retention) in view of the preparation of the ITER exploitation. The programme should be developed on the assumption that the ILW is still in place, although the possible consequences of the replacement of the solid W base plate with a W-coated LBSRP should also be evaluated."

"Evaluate the maximum performance achievable (Q, fusion power/energy, etc.) on the basis of the extrapolation of the present JET results."

"Estimate the neutron budget that would be required to achieve the above two programme goals. Evaluate the impact on the programme of restricting operation to within the present neutron budget of 2x1021 as defined in the JIA."

"Evaluate the experimental preparatory activity to be made during the ILW exploitation period to ensure an effective execution of the DT Campaign."

"Assess the needs in the key programmatic interface areas (neutron budget, number of beam boxes in T, ICRF, LH, pellet & diagnostic requirements, etc.) identified by the working group on Maintaining JET Tritium Capability."

"Assess the impact on the proposed programme of the presently defined safety case restrictions, in particular with regard to the site tritium limit (90 g) and limits on the amount of tritium stored in systems outside the AGHS. "

"Preliminarily evaluate an optimal sequence of trace tritium, DD, full tritium and DT phases, in particular in the case of further enhancements installation in the pre DT shutdown (e.g. ECRH and RMP)."

"Provide an intermediate report at the beginning of October 2010 and a final report by December 2010."

"Composition of the group: G. Sips (Chair), H. Weisen, C. Challis. Advice of the JET and EFDA TF and TG will be sought."

Acknowledgements

The studies presented in this report would not have been possible with the input from several people from the Operator, from European Associations and from European Task Forces/Topical Groups. Their contributions are acknowledged in the table below.

Table: Collaborations during 2010

Study	**Collaboration**
Fuel retention. Is there a clear benefit in using tritium for retention and migration studies?	FT Task Force at EFDA-JET, S. Brezinsek (FZ-Jülich), R. Neu (IPP) and both for the EU-PWI, U von Toussaint (IPP)
ELMy H-mode plasmas at high Ip/BT: based on existing pulses and 0-D scalings.	I. Jenkins (CCFE) for TRANSP simulations, I. Nunes (EFDA-CSU)
Hybrid plasmas at high Ip/BT: based on 0-D scalings and investigation of uncertainties due to reduced beam penetration at high density with predictive modelling.	I. Jenkins (CCFE) for TRANSP simulations, J. Garcia (CEA) for CRONOS simulations, F. Crisanti (ENEA), ISM group of the ITM-EU Task Force.
AT plasmas at high Ip/BT: based on predictive modelling of performance at 35-40MW input power.	J. Bizarro (IST) for JETTO code calculations, X. Litaudon (CEA)
ICRH schemes in full tritium or 50:50 DT mix. Second harmonic tritium?	L-G Eriksson (European Commission), R. Koch (Belgium Association) + M-L Mayoral (CCFE)
LHCD: What can we learn from full tritium or 50:50 DT mix operation. Accessibility at higher pedestal density, essential in AT scenarios at high TF, or alpha particle effect (damping)?	L-G Eriksson (European Commission), T. Hoang (CEA)
MHD: This covers the alpha driven MHD as well as alpha losses due to MHD. Important areas are NTM's, AE's and sawteeth.	S. Pinches (CCFE), A. Fasoli (EPFL), S. Günter (IPP) and S. Sharapov (CCFE)
Isotope effects: A full tritium campaign can re-enforce or disprove hydrogen mass scaling for the L-H threshold, pedestal, core confinement, global confinement, transport, density limits, ELM size.	G. Cordey, D. McDonald (CCFE), Y. Martin (CRPP), K. Thomsen (European Commission), C. Angioni (IPP)
Diagnostics: Do we need upgrades before a tritium or DT campaign? What important issues could be addressed for ITER (neutron calibration)	A. Murari, F. Orsitto (ENEA), T. Donné (FOM, EU-TG)
Fusion Technology related tasks: Tile samples, dust collection, sample exposure to DT neutrons.	FT Task Force at EFDA-JET
Operator related tasks. Retaining JET's capability for DT. Diagnostics, JET activation, Planning.	K-D Zastrow (CCFE) D. Brennan (CCFE)

1. DT operation in JET

Key points:

A DT campaign in JET would address key aspects of the ITER research needs:

- An accurate measurement of tritium retention and tritium recovery (cleaning) from the ITER-like Wall and dust created by material erosion.
- The influence of isotope mass on access to H-mode and high confinement, on edge pedestal characteristics, ELMs and their mitigation and on "hybrid" and "steady state (ITB)" scenarios.
- The testing of the 2^{nd} harmonic tritium heating scheme with ICRF.
- The study of alpha particle behaviour, mainly for code validation of alpha driven instabilities.
- The test of DT relevant diagnostics and neutron calibration techniques.

Their collective results will provide the best possible basis for experiments on ITER.

The integrated optimization of ITER regimes of operation to steady high fusion performance in deuterium-tritium would:

- Represent the closest approach to ITER conditions.
- Would provide input and support for the development of integrated tokamak modelling tools for ITER.
- Would provide a 14 MeV neutron flux and fluence at the first wall level that is significantly larger than any other experiment before ITER.

Together with input from other experiments (in a step-ladder approach), this would address key aspects of the seven missions given in the Facility Review in 2008.

1.1 Rationale and objectives of future DT campaigns at JET

The JET facilities have played a substantial role in the development of the Physics Basis for the ITER design and in demonstrating the application of several technologies to fusion research. JET has capabilities that make it unique in the fusion programme and central to the operation and exploitation of ITER.

- it is the largest magnetic fusion device in operation and the one closest to ITER;
- it is unique in its capability for using tritium and deuterium mixtures and of confining the alpha particles produced in the fusion reactions;
- it is the only device capable of using beryllium; and
- it has a unique engineering capability and inherent flexibility in design, including remote handling for installation and maintenance;

Over the last five years, significant investments have been made on JET, in the context of the JET Enhancement Programme 2 (EP2), primarily to replace the cladding of the interior of the JET device with the same combination of materials (beryllium and tungsten; the ITER-Like Wall (ILW)) foreseen for ITER. The plasma facing materials now installed in JET reproduces, for the first time in a fusion device, that planned for the deuterium and deuterium-tritium phase of ITER operation

Together with other EP2 enhancements (detailed in Chapter 2) JET has significantly improved capabilities, such as a substantial upgrade of the main heating system, providing JET with the unique capability for the injection of high power hydrogen, deuterium, tritium and helium particle beams, crucial for the preparation of the non-nuclear regimes of operation in ITER and for performing hydrogen isotope scaling experiments (including tritium).

Operating JET with deuterium-tritium would be the final phase in a five year "*JET Programme in support of ITER*" to be developed along the following schedule:

Phase 1 (2011-2012), full characterisation of the ITER-like wall. Experiments during this phase will be carried out at moderate input power to reduce the risk of an early damage of the wall, while protection systems are still being commissioned. Any damage the ITER-like Wall would preclude taking meaningful samples in an intervention planned for the second half of 2012.

Phase 2 (2013-2014), expansion of the ITER regimes of operation. Experiments during this phase will concentrate on the development of ITER regimes of operation towards high performance, fully exploiting the EP2 enhancements. High priority will be given to operation with a hot plasma edge under conditions closest to ITER.

Phase 3 (2015), DT campaigns with both full tritium and deuterium-tritium operation. During this phase, the experiments using tritium and deuterium-tritium mixtures address key aspects of operating with different hydrogen isotopes and demonstration of ITER regimes of operation in DT.

The phased exploitation of JET represents a coherent approach along the three main axes shown in Fig. 1.1 and addresses, 10 years in advance, many of the challenges that ITER will encounter.

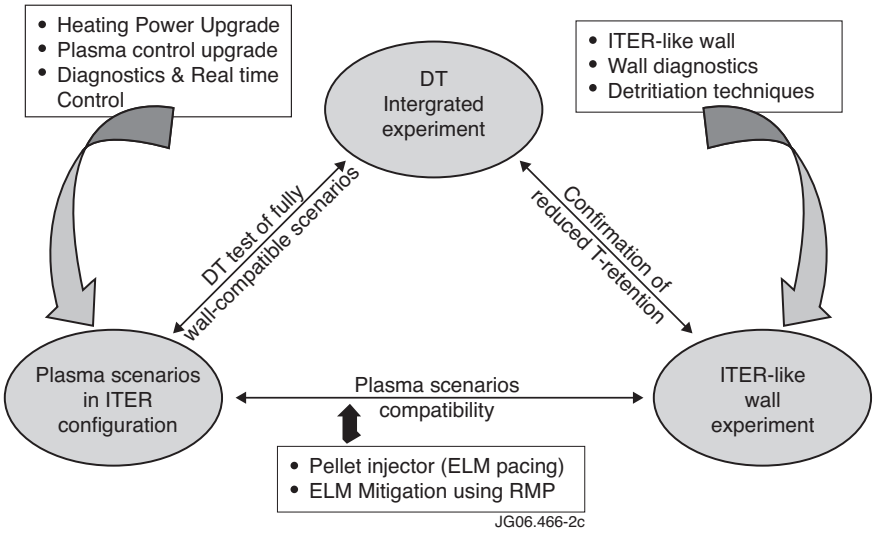

Fig. 1.1: The characterisation of the ITER-like Wall, the development of scenarios for ITER and a DT campaign are an integrated approach at JET to providing input for ITER

The key elements of the deuterium-tritium campaign at JET are summarized below.

Demonstration of low fuel retention. The choice of beryllium and tungsten as plasma facing materials for the DT phase of ITER is motivated in large part by the need to minimize tritium retention in the ITER vacuum vessel. Much of this analysis will be performed in deuterium plasmas, but subsequent DT experiments will provide more accurate determination of the short and long term fuel retention and spatial distribution of the retained fuel.

Demonstration of effective means of fuel recovery. ITER relevant techniques such as wall baking to ~320°C and ion cyclotron wall conditioning (ICWC) will be tested to provide confirmation that the ITER requirements for control of the in-vessel tritium inventory can be satisfied.

Investigation of material erosion, migration and dust (containing tritium). Erosion and migration of plasma facing materials are associated with two phenomena of critical importance to ITER, the retention of fuel (see above) and the formation of dust. In ITER, dust could potentially form a major part of the mobile tritium inventory. Following campaigns using tritium in JET, the dust produced can be collected characterised and analysed using the radioactive decay of tritium as an accurate tracer for the retention and removal of tritium.

Assessment of the influence of isotope mass on access to H-mode and high confinement: Most DTE1 data relate to plasma scenarios in non-stationary conditions. No data are available with an ITER-like metal wall, which is likely to provide a significantly different operating environment than the carbon wall in DTE1. Vessel conditions are also known to affect the L-H threshold, justifying a revisit of the isotope effects on the transition in the ILW. The isotope dependence of the H-mode power threshold can be better documented than in DTE1 thanks to enhanced diagnostic capability and the enhanced neutral beam capability in hydrogen. The DTE1 investigation was mostly focussed to the H-mode access. In 2015 a special attention will be given to the requirements for "H=1"access to confirm that the expected plasma conditions for high fusion power are readily accessible in ITER with the installed heating power.

Assessment of the influence of isotope mass on edge pedestal characteristics, ELMs and their mitigation. In addition to the consideration made for the isotope scaling of the H-mode threshold, it should be noted that the DT campaign together with the enhanced diagnostic and heating capabilities will allow a characterization of the isotopic dependence of the pedestal characteristics. With potentially higher pedestal pressures in tritium, ELM size (energy-loss per ELM) is likely to scale unfavourably with isotope mass, requiring optimisation of ELM mitigation techniques. Moreover, in JET, ELM mitigation requirements can be compared in helium, hydrogen, deuterium and tritium plasmas.

Assessment of the influence of isotope mass on "hybrid" and "steady state (ITB)" scenarios. No data with tritium are available at all from the DTE1 experiment for the hybrid and steady-state regimes that have been substantially progressed on JET over the last 15 years and are one of the main research items of future JET campaigns. Hybrid and steady state scenarios (in most cases with an internal transport barrier) are foreseen as the main vehicles for developing very long pulse operation in ITER. Both involve some degree of profile control to allow access to further improvements in energy confinement beyond H-mode levels. A detailed assessment on JET of the isotope dependence of transport and internal transport barrier access in such scenarios would not only accelerate their implementation in ITER, but would also provide the stronger basis for a choice of the possible upgrade of the heating systems in ITER, to be decided already during the first few years of ITER operation.

Test of ICRF scenarios for heating of DT plasmas: Specific ICRF heating scenarios have been proposed for ITER, based on the coupling to the second cyclotron harmonic of tritons or the fundamental cyclotron resonance of an injected He^3 minority. The effectiveness of such scenarios for plasma heating in ITER can be demonstrated and quantified only in DT plasmas at JET. Particular emphasis on demonstration of the 2^{nd} harmonic tritium scheme is required to ensure that a reliable ICRF heating scheme is available for DT operation in ITER, without the use of ^{3}He, or a well documented minimum level of ^{3}He.

Study of alpha particle behaviour: In ITER, alpha particles provide significant (dominant for Q>5) heating of the plasma. Deuterium-tritium experiments in JET would provide several MW of alpha heating in stationary conditions that could be used to validate theoretical models and codes for alpha particle driven instabilities as well as for developing strategies for the optimum hydrogen isotope mix and heating to burn in ITER. The exact amount of fusion alpha particles that can be obtained in stationary conditions will depend on the achievements during Phase 2; although it is expected to significantly exceed that achieved in the 1997 campaign (see Chapter 4).

Demonstration of DT relevant diagnostics and neutron calibration techniques: Several diagnostics at JET are purpose built for a deuterium-tritium campaign (see Chapter 3) and include a wide range of detectors, spectrometers and neutron cameras, all with direct relevance for ITER. They provide the alpha birth profile and allow discriminating between neutrons from DD, DT and TT reactions for inferring fuel ratios. The availability of a 14MeV neutron detection system at JET, together with the ITER-like Wall, offers an excellent opportunity to address the development of an optimized neutron calibration strategy for ITER, which is essential in estimating the fusion power production, but is also

critical to determining the tritium fuel burn-up, an important input to the tritium accounting procedure in ITER.

By operating JET in deuterium-tritium, the collective results obtained in the areas given above, will provide the best possible basis for experiments on ITER itself in support of a ITER Research Plan that has an aggressive step-wise approach to Q=10.

1.2 Deuterium-tritium experiments at JET in the context of the European Fusion Facilities Review gap analysis

The case for DT operation in JET should also be seen in the context of the wider fusion research effort in Europe (and world-wide). A Review of the EU Facilities carried out by an international panel reported in October 2008, outlined a roadmap that included a systematic gap analysis in terms of medium to long term R&D needs, organised in seven missions (introduced by EFDA):

I. Burning Plasmas.
II. Reliable Tokamak Operation.
III. First wall materials & compatibility with ITER/DEMO relevant plasmas.
IV. Technology and physics of Long Pulse & Steady State.
V. Predicting fusion performance.
VI. Materials and Components for Nuclear Operation.
VII. DEMO Integrated Design: towards high availability and efficient electricity production.

The Panel concluded that "*JET is the most relevant device for support to ITER until new devices with improved capabilities become available.*" Fig. 1.2 gives an overview of the JET parameter space compared. The specific contributions of deuterium-tritium experiments at JET to the first six missions can be summarised as follows:

Burning Plasmas (Mission I): JET is the only device in operation capable of producing significant isotropic pressure of fusion born alpha particles. A DT experiment at JET will be able to produce values of beta alpha close to the ones expected in ITER i.e. $\beta_\alpha(0)\sim1.2\%$, $v_\alpha/v_A\sim1.9$. Despite the difference in ρ^*_α, these experiments may allow model validation (in conjunction with the TAE antenna system) and the development of diagnostic techniques. The assessment of what can be validated by JET is being presently carried out by the ITPA group on Fast Particles and will be detailed at a later stage.

Reliable Tokamak Operation (Mission II): The integrated optimization of ITER regimes of operation (including ELM control or suppression) to high current, high fusion performance deuterium-tritium plasmas, together with appropriate power handling in the ITER-like Wall environment would represent the closest approach to an ITER-like plasma regime in advance of ITER operation. The triggering of NTM's in H-mode and hybrid plasmas and their effect on alpha particles that need to be explored and documented in DT plasmas at relevant values of normalised beta. Moreover, specific techniques for machine conditioning and fuel removal (320^{o}C baking and ICWC) will be tested.

First wall materials & compatibility with ITER/DEMO relevant plasmas (Mission III): The maximisation of performance and component lifetime in ITER includes the development of techniques to control power loads to metallic

plasma facing components. It is crucial that this is carried out in deuterium-tritium plasmas with the ITER-like Wall at JET, since some key aspects of the ITER standard scenario (ELMy H-mode), such as the H-mode threshold, ELM regime and access, ELM size has been shown to depend on the isotopic mass composition.

Technology and physics of Long Pulse & Steady State (Mission IV): The study of long pulse and steady state operation demands improvements in physics and technologies. JET is equipped with ~22MW heating for 40s and an LHCD system capable of aiding in the development of ITER relevant plasma scenarios. Hence, $\tau_{pulse} > \tau_R$ can be achieved in various ITER scenarios, addressing key issues in terms of current profile evolution and equilibration. Physics issues are addressed under isotope scaling experiments as no information is available from the DTE1. However, technology issues can be addressed with deuterium operation only

Predicting fusion performance (Mission V): JET almost symmetrically spans the gap between present mid-size tokamaks and ITER, with access the parameter range closest to ITER. JET's contribution has been to extend the available parameter space in the relevant dimensionless parameters. JET DT experiments will address issues such as the isotope effect on global (core + edge) confinement in the different ITER regimes of operation. Together with results from other devices, JET will provide input and support in the development of integrated tokamak modelling tools for ITER.

Materials and Components for Nuclear Operation (Mission VI): The tritium inventory in JET is at least 3 orders of magnitude larger than any other tokamak experiment with unique handling and processing technologies for activated, tritiated, or beryllium contaminated components. Also, the 14 MeV neutron flux in excess of 10^{12} n/s·cm^2 and a fluence in excess of 10^{14} n/cm^2 on the first wall level are significantly larger than any other experiment before ITER, allowing the development of neutron diagnostics using the real neutron fusion spectrum and activation test of reactor relevant materials (mainly used for diagnostics in ITER). The activation of the JET device (and samples) will provide (code) validation of shutdown dose rate calculations under fusion-relevant DT conditions for ITER.

1.3 Previous DT campaigns at JET

JET has been designed from the outset for deuterium-tritium (DT) operation and has comprehensive tritium processing and remote handling systems. JET is now the only experiment able to operate with tritium.

Significant controlled fusion power was first produced during the Preliminary Tritium Experiment (PTE) in JET in 1991, when a hot ion H mode plasma containing 11% tritium in deuterium produced 2 MJ of fusion energy, with a peak fusion power P_{DT} =1.7 MW and a fusion power gain $Q_{in} = P_{DT}/P_{in}$ =0.12. Tritium usage and neutron production were deliberately kept low during the PTE in order to limit vessel activation so that a pumped divertor could be installed three months later during a manned intervention. Meanwhile, TFTR operated with DT mixtures and, using 50%

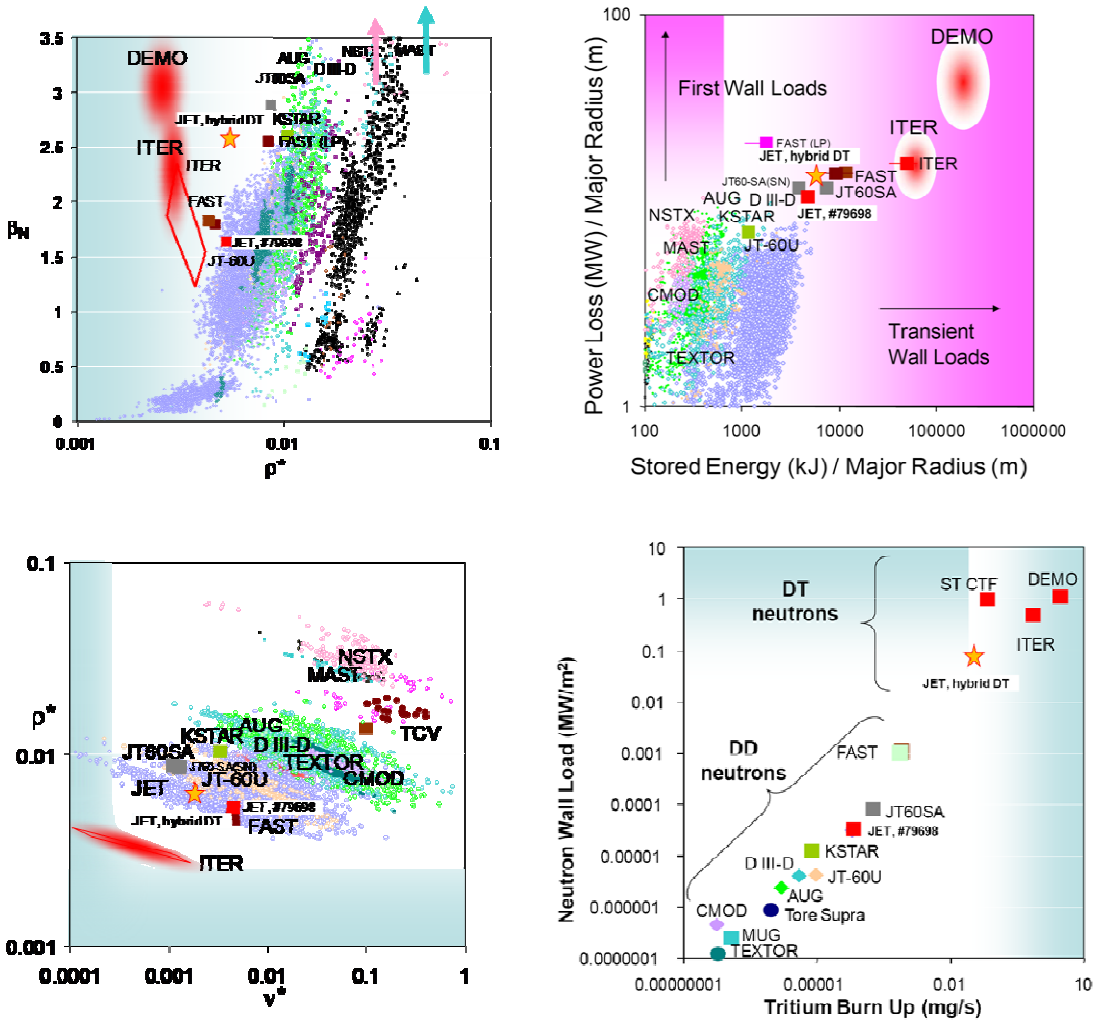

Fig.1.2: The data shown are from a large database for tokamaks worldwide, as used in the Facility Review in 2008. The definition of the dimensionless parameters used, are as specified in the Facility Review report: $\beta_N = \beta\, a\, B_T\, I_P^{-1}$, $\rho^* \sim 0.0096\sqrt{T_e}\, a^{-1} B_T^{-1}$, $\nu^* \sim 10^{-22}\, n_e\, R_0\, q_{95}\, T_e^{-2}$.

Two specific JET data points are shown in the graphs:

(1) A high current ELMy H-mode discharge from 2009 (#79698), at $I_p = 4.5MA/B_T = 3.6T$, $\langle n_e \rangle_{vol} = 9.1x10^{19} m^{-3}$, $\langle T_e \rangle_{vol} = 2.7keV$, $a_m = 0.94m$, $R_m = 2.92m$, $Z_{eff} = 2.0$ *and* $\beta_N = 1.4$; *and*

(2) A DT projection as described in Chapter 4 (hybrid DT), at $I_p = 3.5MA$, $B_T = 3.45T$, $\langle n_e \rangle_{vol} = 5.6x10^{19} m^{-3}$, $\langle T_e \rangle_{vol} = 5.0keV$, $a_m = 0.93m$, $R_m = 2.93m$, $Z_{eff} = 2.1$ *and* $\beta_N = 2.5$.

The JET data are also compared with projections from future devices such as JT-60SA, FAST, CTF, ITER and DEMO (the values used for these devices in the plots are from the Facility Review Report).

Top-left: *Overview the normalised beta as function of the normalised gyro-radius ρ*.*
Top-right: *The power loss to the first wall as function of the plasma stored energy (both normalised to the machine major radius).*
Bottom left: *The achievable normalised gyro-radius ρ* versus plasma collisionality ν*.*
Bottom-right: *The neutron wall loading achievable for a given tritium burn-up rate (mg/s) for deuterium experiments (including FAST and JT-60SA), and DT experiments (including JET, ST-CTF, ITER and DEMO).*

deuterium and 50% tritium, produced 10.7 MW of fusion power and a fusion gain Q_{in} =0.27, transiently, in the super-shot regime. This limiter tokamak also explored improved confinement in the so-called enhanced reversed shear (ERS) regime, but the performance improvements achieved in deuterium could not be translated to DT.

Prior to DTE1, JET developed a range a capabilities to enable operation and maintenance of JET with tritium and activation by DT fusion reactions. For DTE1, a total budget of 2.5×10^{20} DT neutrons was set to limit the subsequent activation of the vessel, constraining the number of DT shots consuming a large number of neutrons (long pulse, high performance shots). During DTE1, the JET torus was pumped continuously through by the on-site closed circuit Active Gas Handling System (AGHS) and was supplied with tritium (and deuterium) by the gas introduction and neutral beam (NB) systems. The tritium was stored in uranium beds and reprocessed in the AGHS to a purity of 99.4% by gas chromatography. The site inventory of 20 g of tritium was reprocessed eight times by the AGHS, making the equivalent of 99.3 g of tritium available for DTE1, permitting a significant number of tritium and DT experiments.

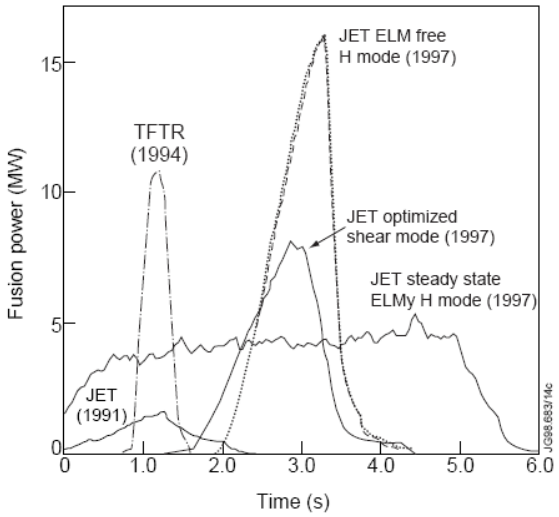

Fig. 1.3: Fusion power development in JET (1991 and 1997) and TFTR (1993 to 1997).

The results obtained during DTE1 still form the basis of extrapolations to ITER in the areas of confinement, plasma performance, plasma wall interaction and a range of hydrogen isotope dependencies found during DTE1 in 1997.

In addition the JET DT experiments produced record fusion power and energy:

- 16.1 MW transiently in an ELM free H mode, with Q=0.62 (see Fig. 1.4b);
- 8.2 MW, transiently, in the optimized shear mode of operation ; and
- 4 MW in a steady state ELMy H mode discharge, at Q=0.18, with a total of 22MJ fusion energy produced in a single discharge (see Fig. 1.4a).

These can be compared to the results from PTE at JET and TFTR (see Fig. 1.3).

JET was designed with sufficient plasma current that alpha particles, at their birth energy of 3.5 MeV, have orbital excursions away from their mean magnetic flux surfaces which are at most 10% of the plasma minor radius. For typical electron temperatures of ~10 keV, more than 95% of the alpha power is transferred to the electrons. During DTE1 fusion heating was observed in JET, in the absence of

Toroidal Alfvén Eigenmode instabilities. The alpha pressure in the DTE1 experiments reached $\beta_\alpha(0) \approx 0.7\%$ for $v_\alpha/v_A \approx 1.6$, the main reason for not observing TAE's was the high background pressure of the discharges.

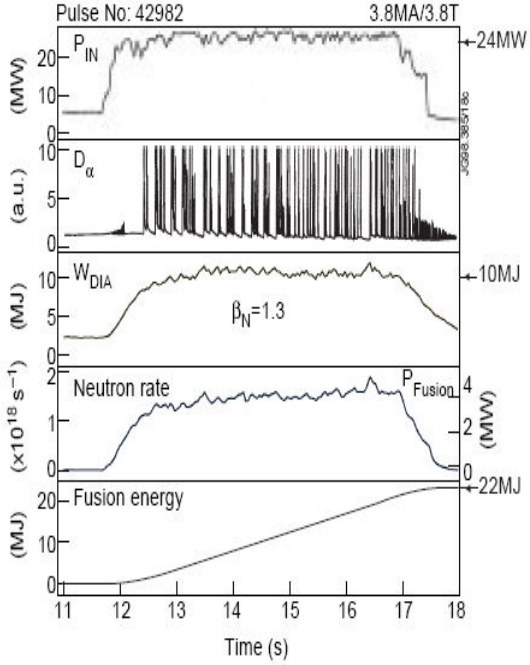

Fig. 1.4a: Time traces of a 3.8 MA, 3.8 T ELMy H mode pulse during DTE1 which produced a world record 22 MJ of fusion energy.

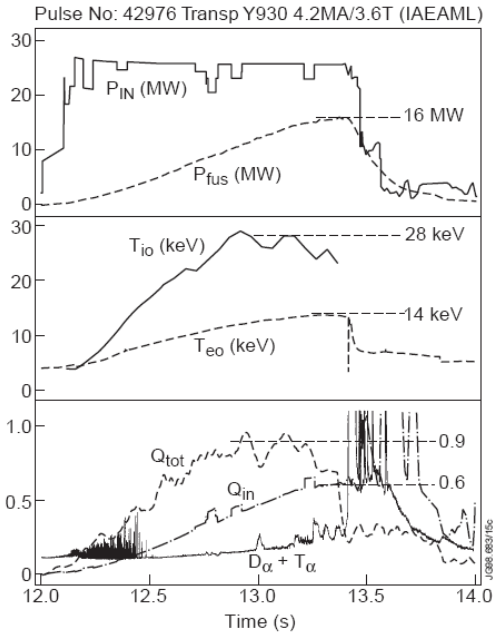

Fig. 1.4b: Various time traces for the highest fusion yield hot ion H mode discharge during DTE1. From top to bottom: Input and fusion power; central ion and electron temperatures; ratios of fusion to loss power minus particle heating power, Q_{tot}, and of fusion to input power Q_{in}; and $D_\alpha + T_\alpha$ intensity.

In 2003, trace tritium experiments were conducted on the JET, demonstrating the continued readiness of JET to perform experiments with tritium for scientific studies. During these experiments 9g of tritium was available, with 5g fed into the machine. The evolution of the tritium spatial distribution was detected in 'trace' quantities (typically $n_T/(n_D + n_T) < 3\%$) used in these experiments, by observation of the 14MeV neutron emission. Detailed observation of evolution of the tritium content associated with events such as sawtooth collapses, neo-classical tearing modes and edge localized modes were documented, while tritium transport was studied for several operation regimes in JET.

The shutdowns that followed DTE1 were completely (exchange of the Mk IIa divertor to the Mk II Gasbox divertor in 1998) or predominantly performed by remote handling. EFDA-JET has maintained and upgraded its remote handling capability. The current shutdown with the complete exchange of the wall and divertor by remote handling demonstrates the high level of in-vessel remote handling capability of the JET facilities.

2. JET upgrades and preparation for DT

Key points:

The recent JET enhancements (EP2) fully support DT operation at JET:

- The ITER-like Wall is designed to allow high input power and maintenance by remote handling.
- The availability of high power neutral beam operation in hydrogen (16MW), deuterium (34MW), tritium (35MW) and helium (24MW) for 20s.
- The ICRH systems would provide ~7MW and LHCD ~3MW in addition, to provide ~45MW for DT operation.
- The limits on power handling of the Be-wall and W-divertor are expected not to restrict the JET operating space with the available input power, provided the ELM energy loss is kept below ~0.6MJ.

For the execution of the DT campaigns at JET:

- We assume that the solid tungsten divertor tiles are replaced by tungsten-coated CFC divertor tiles before the start of the deuterium-tritium campaigns.
- The ITER-like antenna is not refurbished before DT operation (potentially 2-4MW of ICRH in H-mode and 4-6MW in L-mode).
- For 100% tritium operation ~60g of tritium are required, for a DT campaign ~40g (the amount of tritium currently on-site is ~6.3g).
- With the use of Active Gas Handling Systems, nitrogen seeding will not be allowed, unless operational solutions are found.
- There are two options for DT campaigns (from a vessel activation perspective):
    1. With a DT neutron budget up to $3x10^{20}$ (similar to DTE1), allowing manned entry into the vessel after 1-2 years; or alternatively
    2. With a DT neutron budget up to $17x10^{20}$ (JET Implementing Agreement limit), only allowing remote handling operation afterwards.

The recent JET enhancements (EP2) include the installation of the ITER-Like Wall and a substantial upgrade of the neutral beam heating systems. In this Chapter these upgrades are reviewed in the context of DT operations at JET:

- Details of the ITER-like wall are given. The careful design of the ITER-like Wall should allow operation at high input power (required for some of the DT experiments)
- The capabilities of the upgraded neutral beam systems and their tritium capability are given, together with the ICRH and LHCD system capabilities.
- The operational limits for the ITER-like Wall are given, based on data available, in the areas of the power loads to the divertor regions, the limits set by the maximum allowable surface temperature, the energy limits and the limits posed by ELM energy losses for the tungsten divertor.
- This together with the technical preparation required to enable operation with tritium and calculations for the neutron activation of the JET vessel during DT.

2.1 The ITER like Wall

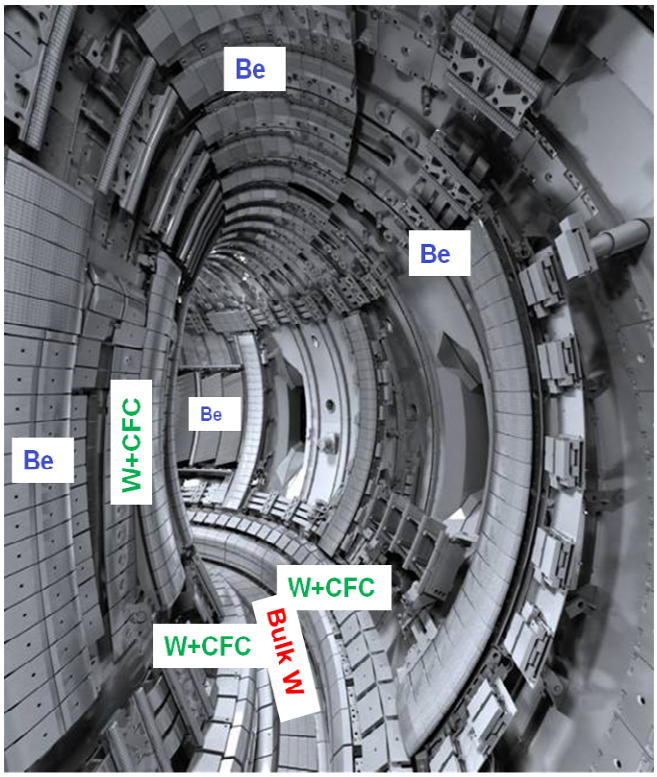

Fig. 2.1: The new ITER-like Wall at JET. The main chamber is covered with beryllium tiles and tungsten coated CFC-tiles for high heat flux components used to protect the wall from shine-trough of the neutral beam injection. The lower divertor consists of tungsten coated CFC-tiles and a row of, segmented, full-tungsten tiles.

In the current shutdown, a full replacement of the presently carbon based first wall will result in a mainly beryllium main chamber and a tungsten divertor (see Fig. 2.1).

One of the key engineering boundary conditions to the design of the ILW is the need to re-use the existing support structures. Therefore, disruption loads due to the use of materials far more conductive than CFC had to be reduced. This was achieved by slicing the tile assemblies and introducing new carriers or modifying the design of existing carriers. In detail:

- Beryllium inner and outer wall limiters: The beryllium limiters have to be compatible with plasma loads during plasma ramp up and ramp down, hence larger format limiter tiles compared to existing ones are used to minimise wastage of wetted surface needed to shadow edges, slice tiles to reduce eddy current loads, remove plasma facing holes (hiding the fixings of one tile behind the following tile till a top hat covers the last ones) wherever possible to maximise front power handling, introduce castellation (to reduce thermal stresses in hot regions and further reduce eddy loads) and shadow edges;
- The beryllium top dump plate: Replace full coverage of rounded edge flat tiles with discreet ribs of bidirectional tile assemblies to give better defined area of interception;
- NBI shine-through and re-ionisation loads: these are increased by the NBI upgrade and had to be accommodated. Normal NBI shine through on inner wall use W-coated CFC and exploit the change of geometry needed for the sliced Be tile to ensure the NBI footprints are away from plasma loads and to increase slightly tile thickness and improve energy density capacity;
- The design had to offer safe paths to Radio Frequency (RF) driven image currents in limiters and protections surrounding the RF antennas, while the design had to account for Lower Hybrid (LH) sheath loads in the vicinity of the launcher;
- The strike point loads will have to be adjusted to fit the limits imposed by the new divertor materials. A solid tungsten tile for the outer strike point (tile 5) will be used, employing a high level of segmentation with four independent toroidal stacks. Each bulk W row of divertor tiles has 6 mm thick lamellae perpendicular to the toroidal direction to minimise the eddy loads, while the plasma facing surface raised by a few millimetres to make space for modified support system. The rest of the divertor uses tungsten coated CFC tiles with a design that is identical to the carbon tiles;
- Add main chamber thermocouples (and re-install divertor ones) to be able to monitor thermal loads and manage operation accordingly.

In order to make space for the carriers holding the beryllium tile assemblies in the main chamber, the inner wall and the dump plate have moved closer to the plasma. Consequently, low triangularity configurations will have slightly smaller minor radius and therefore boundary safety factor for the same plasma current and toroidal field, while high triangularity configuration may need to be adjusted to avoid interaction with the upper inner wall protections and the dump plate.

2.2) Heating systems during DT

2.2.1) Neutral beam injection

Until 2009, two neutral beam injected boxes provided JET with a maximum of ~24 MW with a mixture of 80kV and 130kV for the injection energy, with a maximum pulse length of 10 seconds.

The EP2 neutral beam project is currently installing improved beam source configurations, replacements of the beam ducts by water cooled components and other upgrades to the beam line. As a result, the beam power and pulse length will both

increase from 2011 onwards. The increase in power comes from accelerator modifications, allowing injection of all sources at 125kV, changes to the beam source to allow more power in the $^1/_2$ and $^1/_3$ beam energy components and an increase in beam current. The projections for operation in deuterium are given in Fig. 2.2.

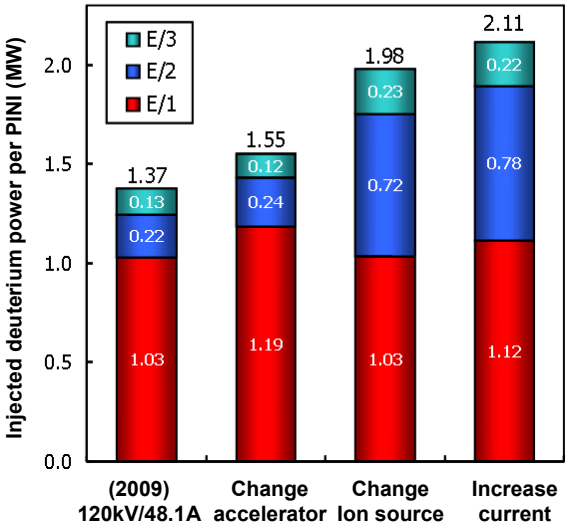

Fig. 2.2a: Various stages of the neutral beam source upgrades. The power increase is calculated for deuterium operation. E/1, E/2 and E/3 are the contribution (in MW) of the full, half and 1/3 energy components of the beam species.

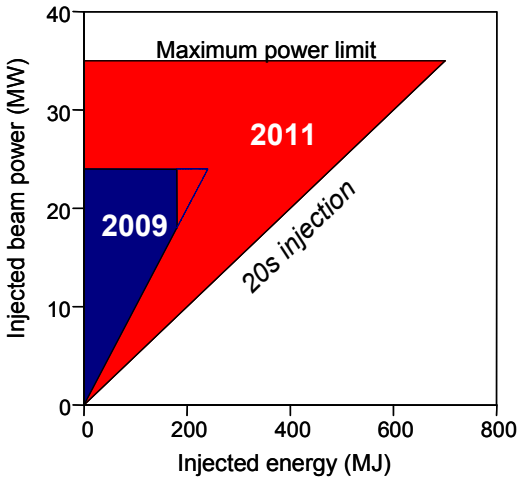

Fig. 2.2b: The increase, from 2011 onwards, of the total power and injected energy from both neutral beam boxes, compared to the capability of the neutral beam injection systems in 2009.

Prediction of injected tritium power:
The injected beam power for tritium has been calculated by modelling the ion source and applying known cross-sections for collision processes in the neutraliser. For an injection energy of 118 kV (limited by the maximum available current in tritium, 45A), the maximum power per PINI is ~2.2MW, given a maximum total power available (from 2 beam boxes) of ~35MW. For tritium, the dominant (>60%) component for the beam is at full energy. For deuterium the full energy contribution is only 53%.

Table 2.I: JET NBI parameters after the completion of EP2 NBE project

Parameter	Gas species			
	H_2	D_2	T_2	^4He
Maximum beam energy (keV)	90	125	118	120
Maximum beam current (A)	50	65	45	42
Maximum power per PINI (MW)	1.0	2.16	2.2	1.56
Maximum power per NIB (MW)	8.0	17.3	17.6	12.5
Maximum total power (MW)	**16.0**	**34.6**	**35.2**	**25.0**

The EP2 upgrade of the neutral beam system also allows significant power injection in hydrogen and helium. For hydrogen, ~40% of the injected power injected comes

from the ½ energy component. The increase in full energy component going from hydrogen to deuterium and to tritium, would allow a close match of the beam power deposition profile for the different hydrogen isotopes. An overview of the values that could be achieved using all 16 beam sources is given below. This is a considerable improvement compared to 2009, which should be exploited in an experimental programme leading to tritium and DT operation.

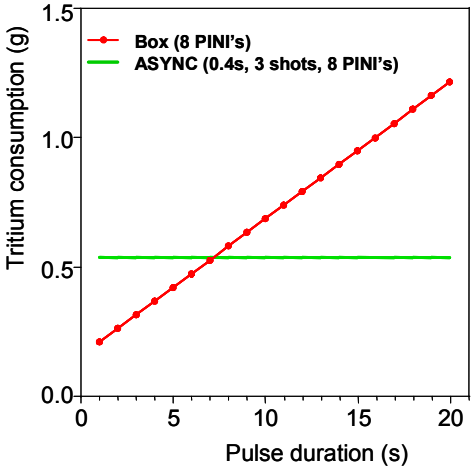

Fig. 2.3: Predicted NBI tritium gas consumption per neutral beam injection box (8 sources) for ASYNC operation (NBI without plasma) and SYNC operation (NBI into plasma)

The daily tritium consumption for the neutral beam system has been assessed. Allowing for 3 ASYNC shots each operational day, gives a daily ASYNC tritium consumption of 0.54 g (duration of 0.4 s for all 8 sources, with a conservative estimate for the arc stabilisation time of 3 seconds). For high power operation (using all 8 sources), the consumption is calculated versus pulse duration, as shown in Fig. 2.3. For a typical 10s heating pulse, the 8 PINI's would consume 0.69 g (or 2.6 barl) of tritium gas.

The maximum tritium inventory allowed outside the Active Gas Handling Systems at JET is 11g, with the main storage on the neutral-beam and divertor cryo-pumps. Putting 50% of this gas limit on the neutral beam cryo-pumps would allow *7 full power pulses (17.6 MW) for each operational day* from 1 neutral beam injection box for a heating pulse length of 10s, including ASYNC conditioning.

With the new wall in JET, the neutral beams system will have to prevent overheating of the areas affected by neutral beam shine-through:

- First of all the beam line injection trajectories will be changed. Before 2011, there were two configurations: (a) standard alignment of the 8 PINI's in each beam box aiming at the axis of the device, and (b) up-shifted alignment aiming predominantly at the centre of the plasma (which is typically 25-30 cm above the horizontal axis). Starting in 2011, the beam injection angle will use 'mixed' alignment, with PINI's 1, 6 & 7 in up shifted alignment and PINI's 2-5 & 8 in standard alignment. This will avoid two sources hitting the same spot on the inner wall (normal beams) or outer limiters (for tangential beams); and
- Second, the minimum density allowed we be revised, and in most cases be increased from values used up to 2009. The precise values are not known at present, but as an indication, the plasma current in H-mode will need to be above 1.5MA to be able to inject NBI for more than a few seconds and still stay below the Greenwald density limit.

For the projections of DT performance in Chapter 3, the neutral beams use the 'mixed' alignment configuration.

2.2.2) ICRH

The power delivered by four A2 antennas of the ICRH system is expected to provide routinely about 4MW in H-mode and about 8MW in L-mode for an antenna voltage of 30kV. During DTE1, the A2-antennas were conditioned up to 35kV, potentially increasing the available power to 5.5MW in H-mode and ~11MW in L-mode.

The ITER-like antenna

The ITER like antenna is currently not operational. It could be refurbished to provide 2-4 MW in H-mode and 4-6 MW in L-mode, to have more ICRH power available (in for example the ICRH physics studies presented in Chapter 7 of this report). Such a repair however, consisting of furbishing the Vacuum Transmission Lines, replacing all capacitors in the systems, re-instating the power transmitters and (if possible) re-arranging the connection to the antenna to allow poloidal pairing of the antenna-straps, is not planned at the moment.

2.2.3) LHCD

LHCD was not allowed in previous DT campaigns due to concerns of neutron damage to the LHCD window protection system. This is now evaluated to be safe for future DT campaigns. A power level of ~3MW from LHCD would be available to provide current profile shaping for hybrid and steady state scenarios.

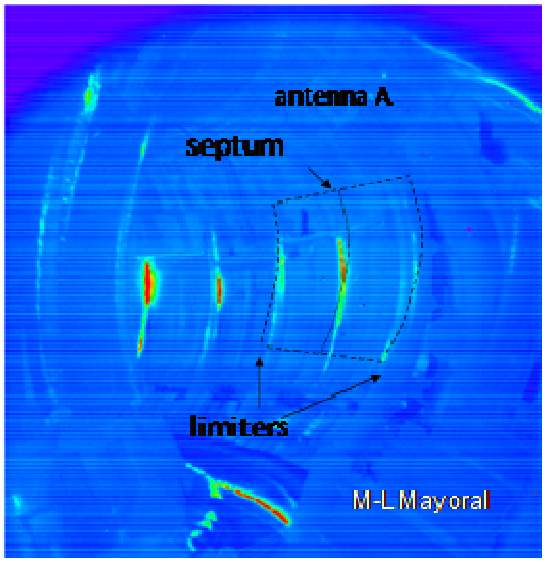

Fig. 2.4a: Wide angle view of ICRH antenna A and the protection limiters

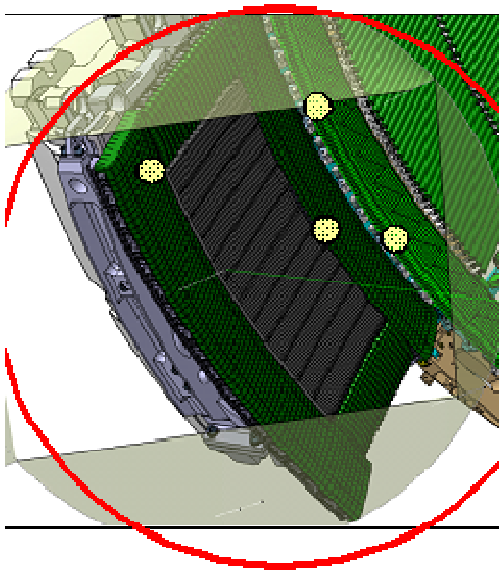

Fig. 2.4b: Protection camera view of the LHCD antenna

In parallel to the installation of the ITER-like Wall a suite of visible and infrared cameras will be installed with dedicated views of the antennae and discrete poloidal limiters (see Fig. 2.4). It will be possible to make fast measurements of heat and particle loads combined with a sophisticated capability to measure and control hot spots in real time, to allow maximum safe operation of the ICRH antennae and the LHCD launcher. These systems will be available for full tritium operation, but can not provide data during DT (see diagnostics, Chapter 3).

Table 2.II: Summary of the JET heating capabilities during future DT campaigns

Maximum values	I_p *(MA)*	B_T *(T)*	P_{NBI} *(MW)*	P_{ICRH} *(MW)*	P_{LHCD} *(MW)*
DTE1, 1997	3.8	3.8	22.5	3 – 10*	not allowed**
DT 2015	4.5	4.0	34-35	4 – 8* 8 – 14***	3

**: Values for H-mode and L-mode respectively*
***: Not allowed in DTE1 due to concerns of neutron damage to the LHCD window protection systems (now evaluated to be safe for future DT campaigns).*
****: Including the ITER-like antenna with ~2-4MW in H-mode, ~4-6MW in L-mode.*

2.3 Material and operational limits for the ITER-like Wall

Summary: With the possible exception of ELMs at the highest plasma currents where some mitigation may be required, the power handling limits of the Be-wall and W-divertor are expected not to (significantly) restrict the JET operating space for DT operation.

With the ILW and upgrades to the auxiliary heating power, the JET wall will go from being almost indestructible to making the material driven operational constraints predicted for ITER a more immediate reality for JET.

The expected operating space in JET with a Be-wall and tungsten-coated CFC divertor tiles depends on three limits:

- Maximum allowable surface temperature for steady state power loads;
- Energy limits for the bulk tiles and fixings; and
- Damage to the tungsten coatings due to transient power loads (e.g. ELMs).

The beryllium melting temperature is $1278^{o}\pm5^{o}$C, and the tiles are designed to have the surface temperature ~200^{o}C below melting when the castellation root temperature equilibration temperature is <600^{o}C. A surface temperature limit of 900^{o}C will be used during operation. For thermally thick components (generally the case), this translates to $20MWm^{-2}s^{1/2}$ (equivalent to a heat pulse of $6MW/m^2$ for 10s for a cold start at 200^{o}C). Transient heat loads from disruptions pose the highest risk to local melting, hence a strategy with a progressive increase in maximum plasma current is proposed for 2011 (starting at 2.5MA) and onwards, together with an optimisation of disruption mitigation systems.

For W-coated CFC, the most stringent temperature limit is imposed by W-carbide formation, which increases non-linearly with temperature (e.g. diffusion coefficient of C in W increases 100 times between 900^{o}C and 1200^{o}C and another 10 times between 1200^{o}C and 1600^{o}C). Initially the surface temperature will be limited to 1200^{o}C, equivalent to ~$10MWm^{-2}s^{1/2}$. In addition, to avoid surface damage and excessive erosion of the coated tile, the ELM loads during the 2011-2012 will be limited to ~$150kJ/m^2$ at the target. This limit will be used until detailed data on retention have been taken and the coatings have been checked in a subsequent shutdown. The energy capability of the W-coated CFC tiles remains unchanged from previous campaigns.

So far, the divertor energy capability (typically 90-120 MJ) has not been challenged (see section below), but with an increase of the heating power by ~20% and duration by a factor of 2, sweeping of the strike point should be used to spread the input energy over more than one divertor tile.

Initially the surface temperature of the bulk W row of divertor tiles will be limited to 1200°C to avoid re-crystallisation completely. Later this limit will be relaxed to 2200°C, translating to ~20-35MWm^{-2}s$^{1/2}$, which corresponds to 90MJ/m^2 for typical heat pulse durations. At this point, the maximum allowable temperature for the (inconel) supports (some parts are limited to 350°C) will drive a lower energy density limit, ~70MJ/m^2 or less depending on the performance of the clamping system. The high level of segmentation (four independent toroidal stacks and heat path mainly vertical within each stack) makes the energy handling of the bulk W row of tiles more sensitive to the toroidal and poloidal spread of the heat load. The energy capacity scales with the number of stacks among which the energy is divided, making strike point sweeping an attractive option. The energy capacity of each stack is proportional to its Toroidal Wetted Fraction (TWF), so with TWF ~ 70% the stack energy limit is ~50MJ.

For this report we assume that the solid tungsten divertor tiles will be deliberately melted as part of the ITER divertor qualification tests by 2013, and be replaced by tungsten-coated CFC divertor tiles (well) before the start of a deuterium-tritium campaign. The energy limit for the CFC tile is 254MJ.

2.3.1) Experimental data from 2008-2009 (carbon wall and carbon divertor)
A survey of thermocouple measurements taken during C20-C27 (for the period 2008-2009, including #72200-#79900) shows that:

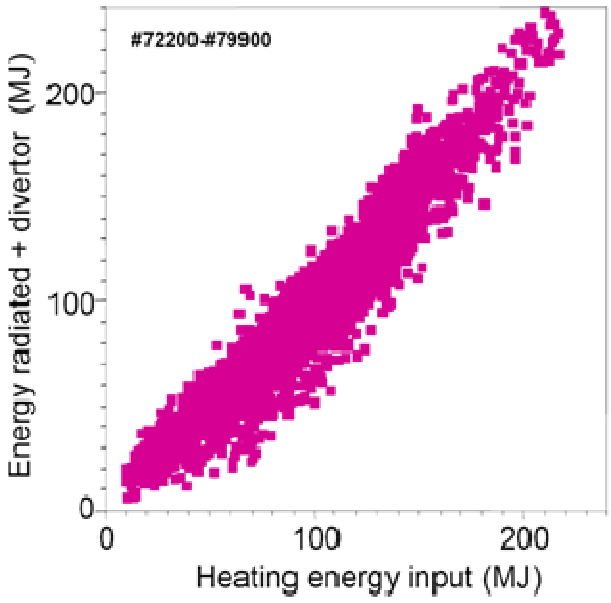

Fig. 2.5: The measured total radiated energy from the plasmas (during the 2008-2009 experimental campaigns) added to the total energy conducted to the divertor target is compared to the total heating energy of the plasma

- The maximum heating energy applied (E_{OHMIC}+E_{NBI}+E_{ICRH}+E_{LHCD}) during these campaigns was 230MJ;
- A good energy balance is found; comparing the total heating energy and the energy to the divertor targets + radiated power (see Fig. 2.5);

- No more than 50% of the heating energy goes to the outer target (sum over tile 5, tile 6, tile 7 and tile 8 using thermocouple data, see Fig. 2.6);
- No more than 20% of the heating energy goes to the inner target (sum over tile 1, tile 3 and tile 4 using thermocouple data, see Fig. 2.6);
- Typically, between 30% and 50% of the heating energy is radiated (this includes radiation during ELMs, see Fig 2.6);
- No more than 30% of the input energy ever arrives at tile 5, with an observed maximum of 70MJ, see Fig. 2.6; and
- Moreover, at high input energy there is significant spreading of the energy in the outer divertor (no more than 40% of the input energy is ever found in one toroidal row of divertor tiles).

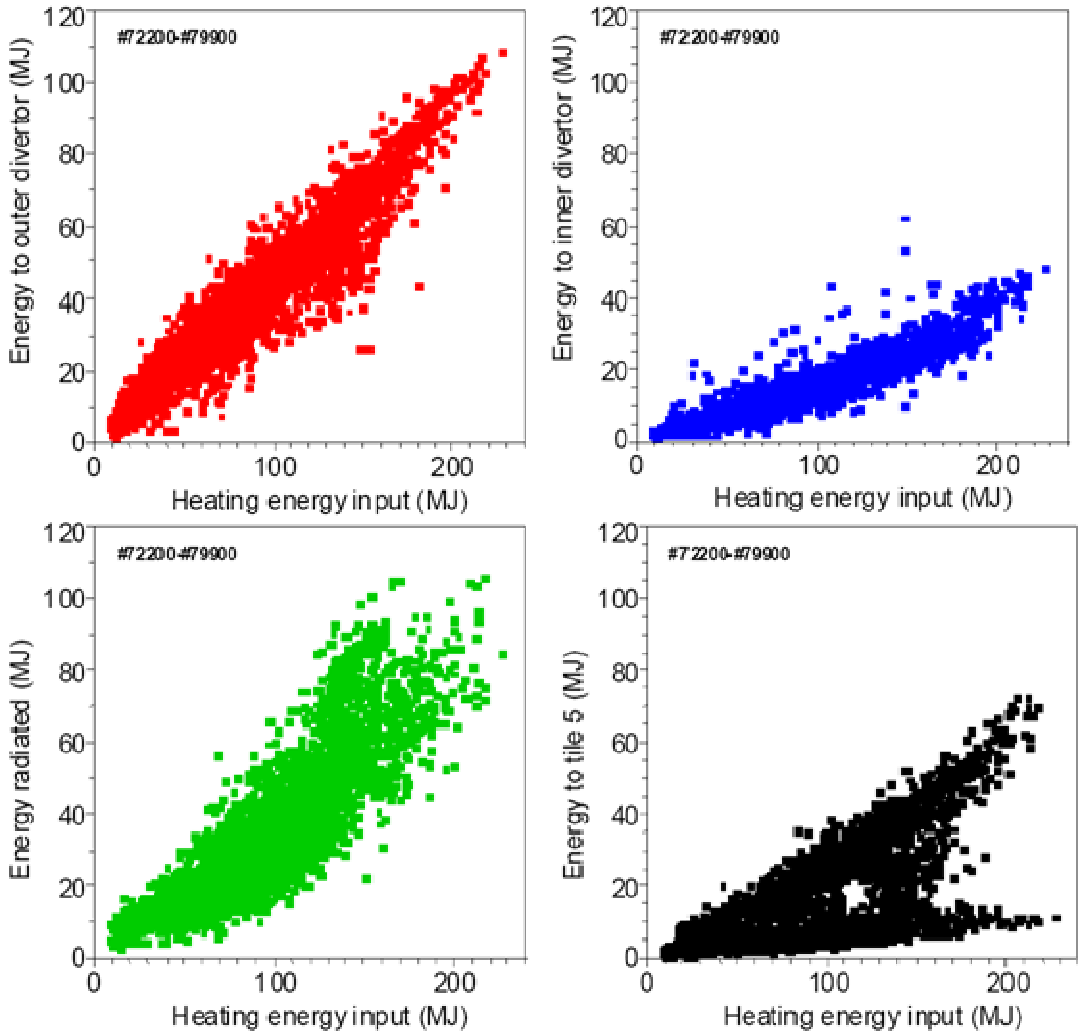

Fig. 2.6: The range of heating energy input to the plasma (during the 2008-2009 experimental campaigns), is compared to the total energy conducted to the outer divertor target (top-left), to the total energy conducted to the inner divertor target (top-right), the energy radiated from the plasma (lower-left), and the energy conducted to tile 5 (the solid tungsten tile in 2011) only (lower-right)

All of the analyses is based, of course, on operation in a carbon machine and predominantly for discharges without extrinsic impurities for radiation enhancement.

In a metal machine, the level of intrinsic radiation may be lower and thus the power load on the divertor could be somewhat higher.

2.3.2) Maximum allowable surface temperature for steady state power loads

For steady state power loads to the first wall and the divertor in particular, we assume a power scrape-off length of 1 cm in the plasma midplane, typical of H-modes in JET. Using this, the energy and power limits have been calculated for tile 5; the table summarises the limits for tile 5 for several cases:

- Two limits for the surface temperature: 1200°C and 2200°C (with a starting temperature of 200°C);
- Static configurations or using sweeping of the divertor strike points. A sweep of 4Hz over ½ the (poloidal) length of tile 5 = 12.5cm;
- Two values (1° and 4°) of the field angle on tile 5. A high current configuration at q_{95}~3 has a field line angle of 1°. Sweeping eliminates the dependence on field line angle;
- Two assumptions for the energy input to tile 5: Namely 50% and 30% of the heating energy.

Table 2.III: Surface limits for a W-coated tile 5, starting temperature = 200 °C

Maximum T_{surf} (°C)	**Strike point sweep**	**Power limits ($MWs^{1/2}$)**	**Maximum heating time at 40 MW**
50% of the heating energy to tile 5 (conservative)			
1200	no	23 – 64*	0.35 - 2.6 s
1200	12.5 cm	81	4.1 s
2200	no	46 - 128*	1.3 – 10 s
2200	12.5 cm	162	16.4 s
30% of the heating energy to tile 5 (in line with 2008-2009 data)			
1200	no	37 – 106*	0.85 - 7 s
1200	12.5 cm	135	11.4 s
2200	no	75 - 212*	3.5 – 28 s
2200	12.5 cm	270	45 s

**: For two values (1° and 4°) of the field angle on tile 5. Sweeping eliminates this dependence.*

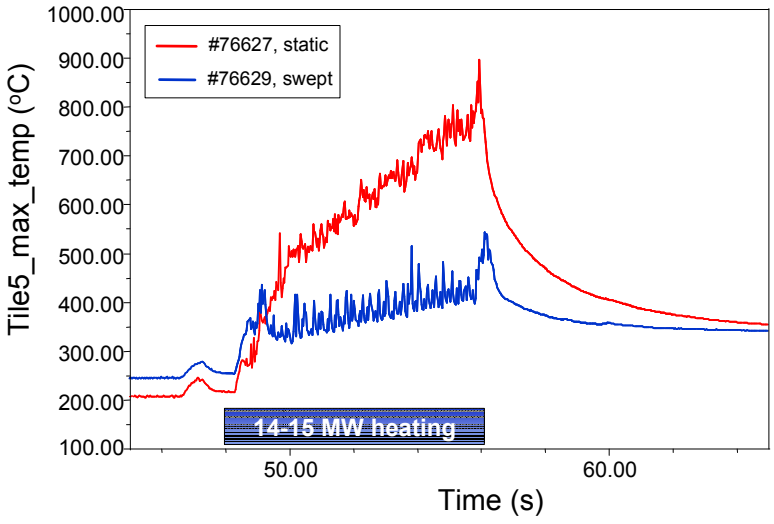

Fig. 2.7: The evolution of the maximum surface temperature of tile 5 (outer strike point) for a static plasma configuration (red) and a plasma configuration using sweeping of the divertor strike points (blue). The neutral beam heating phase is indicated.

Strike point sweeping at 4Hz has already been tested successfully in the preparatory experiments for the ILW (see Fig. 2.7). It has been shown that good density control can be maintained while sweeping over the outer half of tile 5 (12.5cm sweep). By sweeping the power is spread over a much larger area compared to the power scrape-off length at the outer strike point. In case 50% of the heating energy goes to tile 5, sweeping increases the limit to 81 $MWs^{1/2}$ for a maximum surface temperature of 1200°C and to 162 $MWs^{1/2}$ for a maximum surface temperature of 2200°C. Therefore, sweeping is considered a requirement for high power, long pulse operation with the ILW and gives sufficient headroom to fully explore the JET operating space. An example on the use and effect of sweeping is given in Fig. 2.7.

2.3.3) Energy limits for the bulk CFC tiles and fixings

The total deposited energy to a divertor tile is limited by the temperature rise of the inconel fixings, which must stay below 700°C. Assuming a starting temperature of 150°C (first pulse with the vessel at 200°C) and taking the new, slightly modified geometry to be implemented in the ILW, 245 MJ are required to raised the bulk temperature of tile 5 to the limit of the inconel fixings. In case 30% of heating energy goes to tile 5, both the surface temperature (if >1500°C is allowed) and bulk energy limits are not reached at 40MW input power for 20s.

Table 2.IV: Bulk tile 5 limits (limited by inconel fixings)

Assumption	**Heating energy limit**	**T_{surf} at bulk limit (40MW, sweeping)**
50% of heating energy to tile 5 (conservative)	490 MJ	1930 °C
30% of heating energy to tile 5 (in line with 2008-2009 data)	817 MJ	1540 °C

2.3.4) Maximum tolerable ELM energy loss for tungsten-coated CFC

The ELM resilience of (thin) W coatings has already been tested in JET operation from 2007 to 2009 by the insertion of a coated tile 5 (outer strike point, horizontal target) in one toroidal location. After removal from the machine during the present shutdown (2010), there was no exposure of the carbon substrate evident in ion beam analysis of this tile. As an example of the largest ELM loads to which this test tile was subjected, the average ELM energy of the discharges from the high current development programme is plotted versus plasma current in Fig. 2.8.

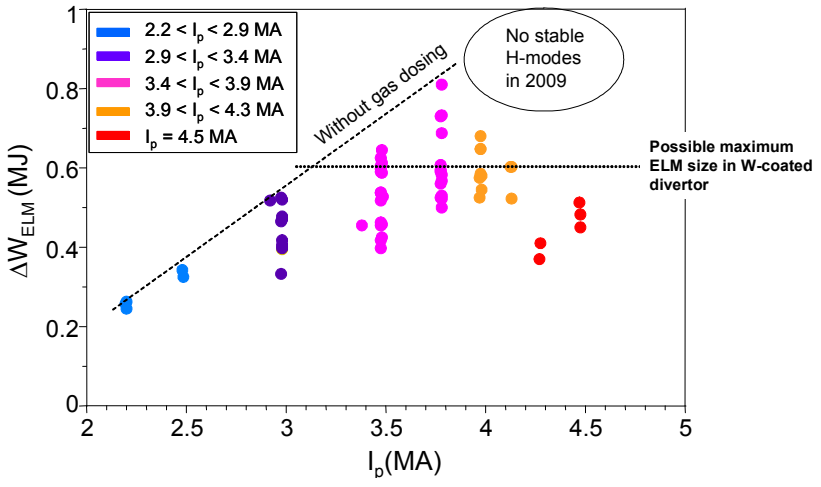

Fig. 2.8: The averaged ELM energy loss, during the heating phase as function of the plasma current (the variation of the ELM energy during the heating phase is within ~20%).

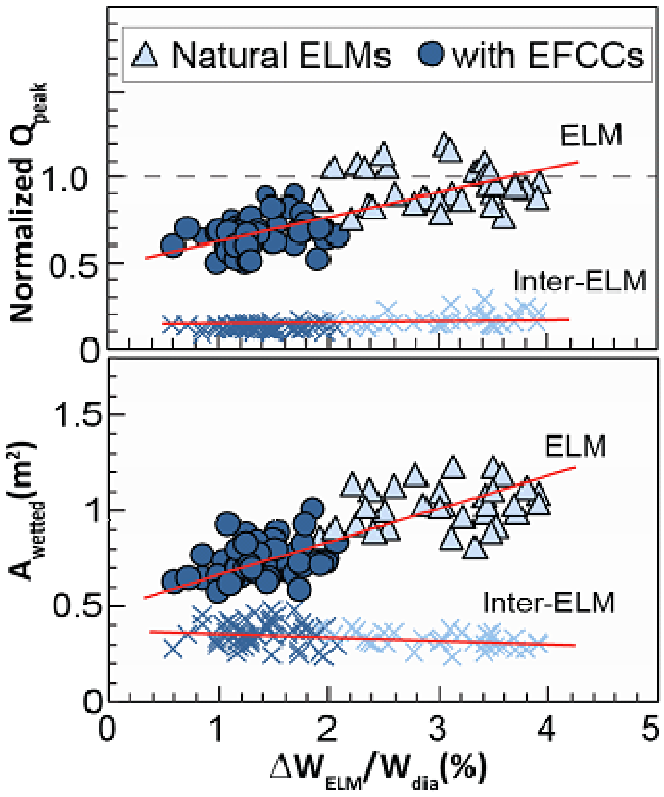

Fig. 2.9: The peak energy flux during ELMs and in-between ELMs is plotted against the relative energy loss for the ELMs (upper figure). The area over which the energy is deposited (A_{wetted}) in the outer divertor, increase with the relative ELM size as displayed in the lower figure.

The first ELM-simulation tests on the coatings being used in the ITER-like Wall have just been completed in Judith I (July 2010). The electron beam was applied as a 1 ms "square" pulse and coating destruction was observed to consistently occur at 150 kJ/m^2, after several 1000 cycles. Further tests are to be conducted on Judith II using a more representative temporal form, which may lead to a higher, more realistic, damage threshold. For now, assuming 35% of the ELM energy goes to the outer divertor and a midplane power scrape-off length of 3 cm during ELMs [T. Eich, PSI 2010, see Fig. 2.9], the energy density on tile 5 would be 70-190 kJm^{-2} per MJ of ELM loss energy. Therefore, 150 kJ/m^2 could be exceeded for ELMs in excess of 0.8-2.2 MJ, depending upon the plasma configuration. For the inner divertor, the situation is much less clear as it has not been possible to measure either the total energy deposited by ELM or the deposition width due to coatings on the carbon tiles. In a very conservative estimate, we assume that all of the remaining ELM energy (65%) is deposited on the inner divertor and that the target energy deposition profile on the inner divertor is the same as that on the outer divertor, the threshold for ELM damage of W coatings could be a low as 0.6 MJ. This value is plotted in Fig. 2.8 for comparison with the existing data. This is conservative in two aspects: (1) a fraction of the order 5-10% of the ELM energy is deposited on the main chamber and (2) beryllium migrated from the main chamber will form deposits at the inner strike region, "protecting" the W-coating.

During the 2009 campaigns it was necessary at the highest plasma currents (3.8-4.5MA) to use gas fuelling to keep the discharge quasi-steady (avoiding compound ELMs). The compound ELMs are thought to be due to the destruction of surface layers on the (carbon) inner divertor tiles and/or due to a lack of input power.

2.4 Technical preparations for a tritium campaign at JET

To ensure that JET maintains its tritium capability a working group was set up in 2005 to examine the options and priorities for the necessary work. This group considers all issues associated with maintaining the tritium capability: Technical, health physics, emergency planning, waste management, training and manning, safety case and schedule and costs.

Maintaining the tritium capability on a machine like JET is a complex process that requires careful planning for both the requirements of the machine and those who are going to operate it. The clear definition of the future DT programme would help to refine this planning and enable the operator to focus on the tasks required to deliver it.

As some of the enhancements have a lead time of up to several years, a detailed list of work has been compiled. Key items are:

- Increase of the tritium gas fuelling rate by installing additional Gas Introduction Modules for tritium gas fuelling;
- Tritium feeds to both neutral beam boxes, whilst maintaining the injected power at a 16-18 MW level per box (for details on neutral beam capabilities during the DT campaign, see section 2.2);
- Tritium Accountancy: Improvements proposed in tritium accountancy (instrumentation and procedures). These will be tested during the ILW retention studies in 2011-2012;
- Making the pellet injector exhaust systems tritium compatible. Otherwise this system needs to be isolated and cannot be used for fuelling or ELM pacing (using deuterium pellets);
- Upgrades to the tritium pumping capability: New mechanical pumps for the fore vacuum, tritium compatible Sterling pumps for the exhaust crown, modifications to the diagnostic crown and purchase of portable de-tritiation systems;
- Replace outdated control units in AGHS. These were specified in 1990 as proven technology. Compatible hardware has been identified and installed as phase 1 of the upgrade. Phase 2 is underway at reduced cost (£1.3M-£750K), with phase 3 completion in time for the next DT campaign;
- Improve diagnostics, upgrade essential diagnostics for a DT neutron environment and remove non compatible diagnostics (vacuum systems not compatible with the use of tritium or neutron damage);
- Improve and re-instate the biological shield;
- Train (new) staff for tritium operation; and
- Purchase 50-55 g of tritium (presently 6.3 g is on site). The present cost of tritium is ~£22.000/gram (including 10% shipping costs). The 50-55g can be delivered in 5g batches, and should start 2 years before the DT campaign.

The JET technical capabilities for tritium will need to be fully rehearsed in deuterium in 2012 or 2013 at the latest (test phase duration of ~2 weeks). Preparations and investments are on-going in time for campaigns with tritium in 2014-2015.

Limitations: Amount of tritium, restrictions to use of nitrogen
The amount of tritium currently on site is 6.3g, this would be sufficient for a trace tritium experiment, but not for 100% tritium or 50:50 D:T operation. The requirement

to purchase 50-55g of tritium comes from estimates of the tritium consumption for one week (4 operation days) of DT or full tritium operation of JET.

Table 2.V: Estimates for tritium use during 1 week of operation

Experiment	**Estimated tritium use**
Full tritium campaign	
Load up the wall to 100% T	12-15 g
100% tritium campaign. (long campaign is possible since yield is lower)	up to 60 g
50:50 deuterium-tritium campaign	
Load up the wall to 50% T/(D+T)	4-5 g
Moderate yield RF campaign (no tritium injection by beams)	5-10 g in addition
High density operation at 50:50 (with only half of the beam power in tritium)	25-30 g in addition

The maximum tritium inventory allowed outside AGHS, on the neutral-beam cryo-pumps, on the divertor cryo-pumps and on other cryo-pumps is 11g. When this limit is reached, (some of) the cryo-pumps need to be regenerated overnight.

Reprocessing of the gas mixtures by AGHS, typically takes ~3 days. Although improvement to AGHS have been made since DTE1 to allow simultaneous gas chromatography and tritium accountancy, an operation cycle of 4 days of plasma operation interleaved by 3 days of reprocessing is still sensible.

Restrictions to use of nitrogen: Uranium beds are used during the tritium and DT campaigns (or a rehearsal in deuterium). Nitrogen used in the plasma (for seeding) will react with the uranium in the storage beds to form uranium-nitride, which is stable for the typical temperature cycles used during operation of the storage beds. The formation of uranium-nitrate significantly reduces the storage capability for hydrogen gases by the uranium beds. Operational solutions maybe found to remove the nitrogen before storage on the uranium beds at JET. However, until such solutions are demonstrated it is recommended NOT to use ANY additional nitrogen when the uranium beds are used for supplying JET with deuterium and tritium. This may have severe consequences for the scenarios at JET that use seeding to reduce the power loads to the divertor (e.g. use only neon gas for seeding).

2.5 Neutron activation

In JET, the 2.45 MeV DD neutrons and 14.1 MeV DT neutrons produce isotopes of cobalt, chromium and manganese, activating the JET vessel at different levels and with different half life durations. An overview of the activation levels is given in Table 2.VI.

Table 2.VI: Vessel activation increase for each 1x10^{18} DD neutron dose, 1x10^{20}DT neutron dose and half life

	Cobalt-57	***Cobalt-58***	***Cobalt-60***	***Chromium-51***	***Manganese-54***
1x10^{18} 2.45 MeV, DD neutrons	1x10^{-14} μS/h	18.7 μS/h	0.13 μS/h	0.03 μS/h	0.02 μS/h
1x10^{20} 14.1 MeV, DT neutrons	26 μS/h	7013 μS/h	94 μS/h	32.2 μS/h	17.6 μS/h
DT/DD activation ratio	2.6x10^{15}	375	723	1110	838
Half Life	271 days	71 days	1925 days	28 days	312 days

For typical temperatures in JET plasmas the <σv> for the D+T → ^{4}He+n reaction is two orders larger than the <σv> for the D+D → ^{3}He+n reaction. When this is combined with the increased vessel activation rate of the 14.1 MeV neutrons from the DT reaction compared to the 2.45 MeV DD reactions, then DT operation results in a much larger increase in radiation levels at JET. Data for the T+T → ^{4}He+n+n reaction are more uncertain for temperatures in the range 5-20keV. Within uncertainties the <σv> for the TT reaction is similar to the DD neutron producing reaction.

A limit on the total DT neutrons allowed set by JET Implementing Agreement is 2.0x10^{21}. The total amount of DT neutrons left for future operations needs to take into account the DT neutrons used in previous JET DT campaigns = 3.0x10^{20}, leaving 1.7x10^{21} DT neutrons for future experiments (see Table 2.VII).

Manned entry into the vessel is allowed for vessel activation levels of less than 350μSv/hour. For emergency repairs an activation limit for vessel entry is 1mSv/hour. The limit for whole body to workers has been limited in recent shutdowns to 2mSv, in line with practice in other industries. Hence, difficult manual repairs would have to wait as only simple manual emergency repairs can take place at activation levels in the range 0.35-1 mSv/hour.

Table 2.VII: The level of DT neutrons used during the PTE, DTE1 and TTE campaigns at JET compared to the maximum DT neutron limit allowed under the JET Implementing Agreement, together with the remaining number of DT neutrons for future campaigns.

Campaign	***DT neutrons***
PTE (1991)	2.0x10^{18}
DTE1 (1997)	2.4x10^{20}
TTE (2003)	4.0x10^{18}
JIA* limit	2.0x10^{21}
Remaining for JET	1.7x10^{21}

* JIA=JET Implementing Agreement

The vessel activation for a DT campaign and the decay of the vessel activation can be calculated, taking into account the activation data for 5 isotopes and their respective half lives. This was done for an instantaneous DT neutron dose of $1x10^{20}$, $3x10^{20}$, $5x10^{20}$, …, $17x10^{20}$, for a baseline (non-decaying) vessel activation of 100μSv. These calculations show that a future DT campaigns should either aim for a DT neutron budget similar to DTE1 ~ $3x10^{20}$, in order to allow manned entry (<350μSv/hour) into the vessel within 2 years following a DT campaign, or alternatively use a DT neutron budget in the range 5-$17x10^{20}$ that allows only remote handling operation in the vessel.

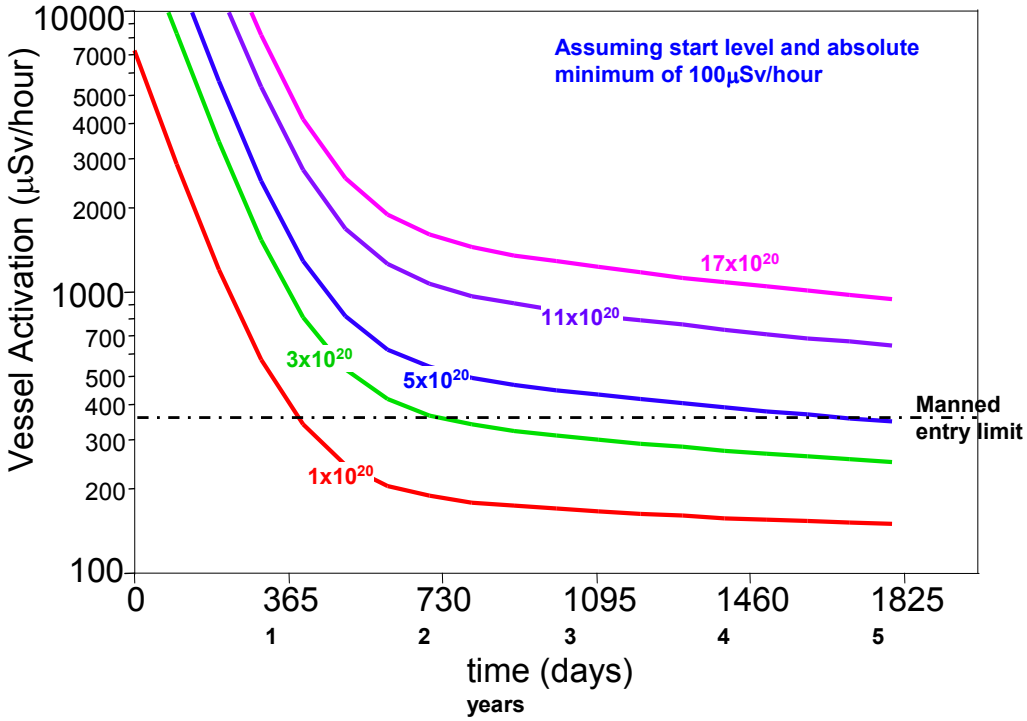

Fig. 2.10: The vessel activation resulting from a DT campaign at JET, for various levels of DT neutrons. The activation is calculated for an instantaneous dose of 14 MeV neutrons, with a vessel background level of 100υS/hour. The limit of 350μS/hour for manned entry into the vessel is indicated (dash-dotted line).

3. Diagnostic capabilities for DT

3.1. Profile diagnostics
3.2. Fluctuation diagnostics
3.3. JET neutron and fast particle diagnostics
3.4. The active TAE antennae
3.5. Diagnostics for protecting the ITER-like Wall
3.6. Recommendations for diagnostics and possible ITER relevant tests

Key points:

- Since DTE1, the JET diagnostics for profile measurements have been substantially upgraded in spatial and temporal resolution and new diagnostics, e.g. High Resolution Thomson Scattering and reflectometer systems, have been installed to provide accurate measurements of the core and pedestal, in experiments on isotope dependence, the documentation of ITER-regimes of operation in DT and heating and confinement studies.
- JET diagnostics for fusion products (neutrons, gamma rays, lost alpha scintillators and TAE antennae) are of direct relevance to ITER. They provide information on the alpha population, alpha losses and allow discriminating between neutrons from DD, DT and TT reactions for inferring fuel ratios.
- A number of (minor) upgrades and some new diagnostics may be considered leading up to DT operation.

3.1 Profile diagnostics

An overview table with the most important profile diagnostics, with improvements since DTE1 is shown below. Details for the main systems are described further below.

Table 3.I: Overview of the profile measurement capabilities in JET with various diagnostics and their resolution in space and time, compared to the capability during DTE1 in 1997

Parameter	**Diagnostics**	**Spatial/time resolution during DTE1**	**Spatial/time resolution in 2011**	**Comments**
T_e	Thomson scattering	12cm/1s	1.5cm/50ms	Now two systems
T_e	ECE	2cm/<1ms	2cm/<1ms	Better radial coverage
n_e	Thomson scattering	10cm/1s	1.5cm/50ms	Now two systems
n_e	Reflectometry	-	<1cm/<0.1ms	new
T_i	CXRS (main) CXRS (edge)	10cm/50ms -	6-10cm/20ms 2-3cm/20ms	Better edge coverage
v_ϕ v_ϕ, v_{pol}	CXRS (main) CXRS (edge)	10cm/50ms -	2-3cm/20ms 2-3cm/20ms	v_{pol} new
q	MSE	-	10cm/20ms	Limited usage
q	Polarimetry	-	Line int./0.1ms	Constraint for EFIT

Thomson Scattering:
JET currently operates, in addition to the core LIDAR, a High Resolution Thomson Scattering System (HRTS), which became fully operational in 2009. The LIDAR has a repetition rate of 5 Hz and a resolution of ~10cm. HRTS provides a ~2 cm spatial resolution over most of the profile, with a repetition rate of 20 Hz. In the pedestal region the instrument function width is narrower, ~1.5cm with a spacing of ~1.7cm. Experiments for resolving the pedestal involve a radial sweep of the last closed flux surfaces by a few cm. The HRTS diagnostic provides an excellent tool for decomposition of the electron stored energy into a pedestal and a core contribution, as pedestal widths at JET are typically ~ 2.5cm or less. DTE1 results indicated that pedestal and core contribution have a different isotope scaling, however the spatial resolution was only ~12 cm. It is not clear however, whether the pedestal gradients are resolved adequately using the HRTS system. To this end, various advanced analysis techniques are being developed. Pedestal gradients can be measured with greater accuracy using the edge LIDAR (currently mothballed for lack of JOC resources) and the swept frequency reflectometer (for density only). Any observation of an isotope dependence of the pedestal heights and gradients would be of great fundamental physics interest.

Electron Cyclotron Emission (ECE):
The heterodyne electron cyclotron emission diagnostic now features 96 channels (upgraded from 48), which are available in real time and have a spatial resolution of ~2 cm and a time resolution of <1ms. These channels cover 2/3 of the plasma diameter (up to half the radius on the high field side). Their high S/N ratio and time resolution makes them particularly valuable for studying MHD activity, as may be associated with fast particle modes, as well as ELMs, which behaved very differently depending on the background isotope in DTE1. Unfortunately the system cannot reliably provide measurements in the pedestal because of optical depths limitations. However it is an important diagnostic for internal transport barriers, the physics of which may depend on isotope composition.

Ion temperature, ion density and ion rotation profiles
The ions are diagnosed with the present tangentially viewing horizontal core CXRS system with a spatial resolution of ≤10 cm and a temporal resolution of 20 ms. The system routinely provides impurity ion temperature, toroidal rotation and density profile measurements. From 2011 onwards, beryllium will be the main species used for this diagnostic. Should however beryllium densities be insufficient for a reliable measurement, neon may be puffed into the plasma for the purpose of providing a trace impurity for the measurement. JET also has a vertical CXRS system with opposing lines for accurate poloidal flow measurements with high spatial resolution in the edge (~2cm). This system will be very valuable for L-H transition and edge pedestal physics in the various isotope campaigns.

Plasma equilibrium
Constraints for improving the post-pulse equilibrium reconstruction using EFIT can be obtained from MSE and from polarimetry. The JET MSE system has relied in the recent past on using one neutral beam source at higher injection energy than the others in the same beam box in octant 4. From C27 onwards, all neutral beam sources will have the same energy. As a result, MSE can only obtained reliable information when a single source is in use for one neutral beam injection box (7 sources not in use), i.e. at relatively low total NBI power. Modulating the neutral beam source used by MSE will be tested in 2011-2012. The impact of the more reflective metallic inner wall will also need to be evaluated.

As a result, polarimetry will be the main diagnostic routinely providing constraints for improving the equilibrium reconstruction in the plasma core. The polarimeter allows measurements of both the Faraday rotation and the Cotton-Mouton angle and is currently under refurbishment. New calibration algorithms have been developed to improve the quality and the reliability of the measurements (M Gelfusa et al, Review Scientific Instruments 81, 2010, 1). The potential of the polarimetric measurements to contribute to a better determination of the equilibrium has therefore increased significantly (M.Gelfusa et al Meas. Sci. Technol. 21, 2010, 115704). Improvements in data analysis also allow the line integrated density to be determined from the polarimeter and so to be used to resolve ambiguities in the Far Infrared interferometer line density measurements resulting from fringe jumps. The polarimeter will be very valuable for the real time equilibrium code EQUINOX (D.Mazon et al, FST 58, 2010).

Swept frequency reflectometer

This diagnostic consists of 4 O-mode and 2 X-mode instruments, which together cover the range 30-150GHz, giving access to the entire profile, including the scrape-off layer. It has sub-centimetre spatial resolution, particularly at the edge, where it measures density pedestal widths (~1cm) with resolution that is significantly below HRTS. It is extremely valuable for diagnosing the edge pedestal density profiles, the scrape-off layer (for ICRH and LH studies) and density gradients near internal transport barrier in advanced scenarios.

3.2 Fluctuation diagnostics

The measurement of the dependence of turbulence scales on isotope mass may help resolving the question of whether transport is Bohm or gyro-Bohm like. This issue is still under debate and in particular was not resolved by isotope experiments in DTE1 due to poor data quality. Currently available and planned diagnostics should be able to provide these measurements, as well as ELM behaviour. In a DT campaign these diagnostics will also allow measuring the radial structure of TAE's, if unstable TAE's are found:

- *Swept frequency reflectometer:* With its time resolution of 15μs, it allows detailed studies of the ELM dynamics and drift wave turbulence in the main plasma. This instrument is likely to be essential for investigating the differences in pedestal and ELM behaviour seen with different isotopes in DTE1; however turbulence measurements in the pedestal area appear not to be possible using this instrument.
- *Correlation reflectometer:* Currently a new scannable two frequency correlation reflectometer is scheduled to be commissioned in 2011. It will allow measurements of the radial correlation function for drift wave fluctuations and of TAE's, if observed around a single radial position with a resolution (for each of the two sample positions) of ~1mm and a time resolution (for a correlation measurement) of some 10ms. If successful, additional channel pairs can be implemented.
- Edge fluctuation measurements, such as produced by ELMs, blobs and turbulence will also be possible using the fast visible *wide angle tangential camera* with 250'000 frames/sec using an intensifier to be purchased (may not be DT compatible) and the *Li-beam* system (not DT compatible), which is undergoing an upgrade for edge fluctuation measurements, featuring up to 20 channels.
- Should MSE be confirmed not to be useable in the current conditions, the viewing line might be useable for Beam Emission Spectroscopy, potentially allowing the measurement of MHD fluctuations.

3.3 JET Neutron, Isotopic Composition and Fast Ion Diagnostics

Diagnostics for fusion products are undoubtedly the most important for a DT campaign, setting JET apart from any other device in the world. These diagnostics are of direct relevance to ITER.

<u>Neutron counters</u>

JET is equipped with a set of neutron counters for time resolved measurements of the total neutron yield (both 2.45 and 14 MeV neutrons). They consist of fission chambers, Si diodes and CVD diamond detectors. The main method for the calibration the neutron counters is the activation technique, which has provided very

good results and therefore the JET system is considered to be the reference for ITER. For calibration, a ^{252}Cf source should be deployed inside the torus by using the MASCOT robot. This calibration (KN1 monitors and KN2 activation diagnostic) will take approximately one week.

Two neutron cameras, one vertical (9 channels) and one horizontal (10 channels) allow tomographic reconstructions of the neutron emissivity. The 2D neutron emissivity distribution sensitively depends on fast D & T ion orbit types (see examples in Fig. 3.1) and is expected to contribute to understanding the effect of MHD relaxations on fast particles. The neutron cameras feature dual detectors in each channel (Ne213, Bicron418) for discriminating between 2.45 (D-D) and 14 MeV (DT) neutrons. They are currently being upgraded with a high time resolution digital acquisition system, allowing the data to be post-treated for better spectral discrimination and for resolving the 11.3 MeV T-T neutrons. Any two of these three neutron energies are in principle sufficient for determining the D/T density ratio profiles, as foreseen in ITER. Usage of the 11.3 MeV neutrons (together with 14MeV neutrons) may have the advantage (over 2.45 MeV D-D neutrons) of a lesser spectral pollution by scattered and slowed-down DT neutrons.

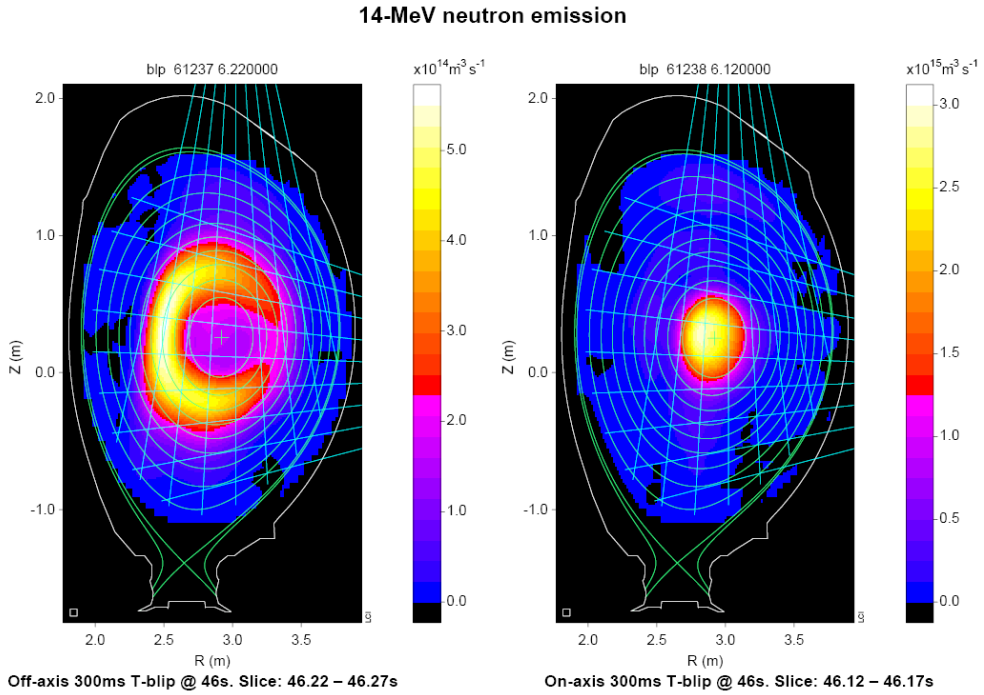

Fig. 3.1: Tomographic reconstruction of data obtained with JET neutron cameras in a trace tritium experiment. Left: Off-axis tritium NBI-blip. Right: On-axis tritium NBI-blip.

The neutron spectra of the 14 MeV neutrons can be measured with the Magnetic Proton Recoil spectrometer (MPR, currently only enabled for ITER) and the spectra of the 2.45 MeV neutrons with the time of flight TOFOR spectrometer. The neutron spectra can also be obtained from various compact spectrometers with more modest access requirements and which provide complementary information and are meant to qualify ITER-relevant technologies. The present set of compact neutron spectrometers comprises the following detectors: NE213, Stilbene and CVD mono-crystalline diamond diodes.

Neutron spectrometers are not the mainstream ion temperature diagnostics in JET. However, the core ion temperature and toroidal angular rotation can be obtained from neutron spectra. These spectrometers too, can provide measurements of the D/T density ratio and information on the confined alphas via the neutron spectrum knock-on tails. Although not important for ion temperature measurements in JET, neutron spectrometers are an important option for ITER, because the ITER diagnostic neutral beam does not penetrate to the centre and the heating beams cannot be used for charge exchange spectroscopy because of the vanishingly low CX cross section at 1MeV.

Isotopic composition

In addition to the new cameras, a Neutral Particle Analyser is specifically devoted to the measurement of the plasma isotopic composition. The diagnostic can measure all the hydrogen isotopes simultaneously. Unfortunately, during the TTE campaign, the detection system was found to be too sensitive to the neutron background. To provide accurate measurements, the detection section of the diagnostic should be upgraded along the lines of the project already completed for the high energy NPA.
A complete design for a Fast Wave reflectometer for mass density profile measurements has been completed in the framework of the EP2 diagnostic upgrade studies (L. Cupido et al, RSI 79, 2008, 10F106). The diagnostic could therefore be manufactured and installed with a relatively limited budget, to test one more candidate technique for ITER. The TAE antennae (see below) also measure mass density as a by-product and hence can provide information on the isotope composition.

Fast ion distributions

Alpha particle distributions in particular, are measured mainly with a specific neutral particle analyser and by gamma ray spectrometry. Gamma rays are emitted in many collisions between fast ions. The broadening of the gamma lines can be related to the fast ion energy distribution (Kiptily et al, Nucl. Fusion 50, (2010) 084001). The $^{9}Be(^{4}He,n\gamma)^{12}C$ reaction, which has a 1.7 MeV threshold and produces 4.44 MeV gammas, is a candidate for alpha particle distribution measurements (Kiptily Fusion Technology 18 (1990) 583). The 16.7 MeV gammas from the $D(T,\gamma)^{5}He$ reaction (a branch of the main DT reaction) provide an alternative for alpha birth profile measurements. The wide range of gamma ray spectrometers (NaI, LaBr, BGO, HPGe) at JET, equipped with ^{6}LiH neutron-attenuators (the horizontal BGO detectors have to be equipped with LiH-attenuator for DT-plasmas) constitute by far the most relevant and flexible set of gamma ray detectors in the world.

The fast alpha-particle spatial distribution can be obtained from the gamma-ray cameras using CsI(Tl)-detectors, which share the collimators with the neutron detectors. A demonstration of this method has already been obtained on JET in a measurement of the 2D distribution of 3rd harmonic ICRH-accelerated ^{4}He-beam ions and D-minority heating, using reactions with Be and C impurities (Fig. 3.2, Kiptily et al, NF 45, 2005 L21).

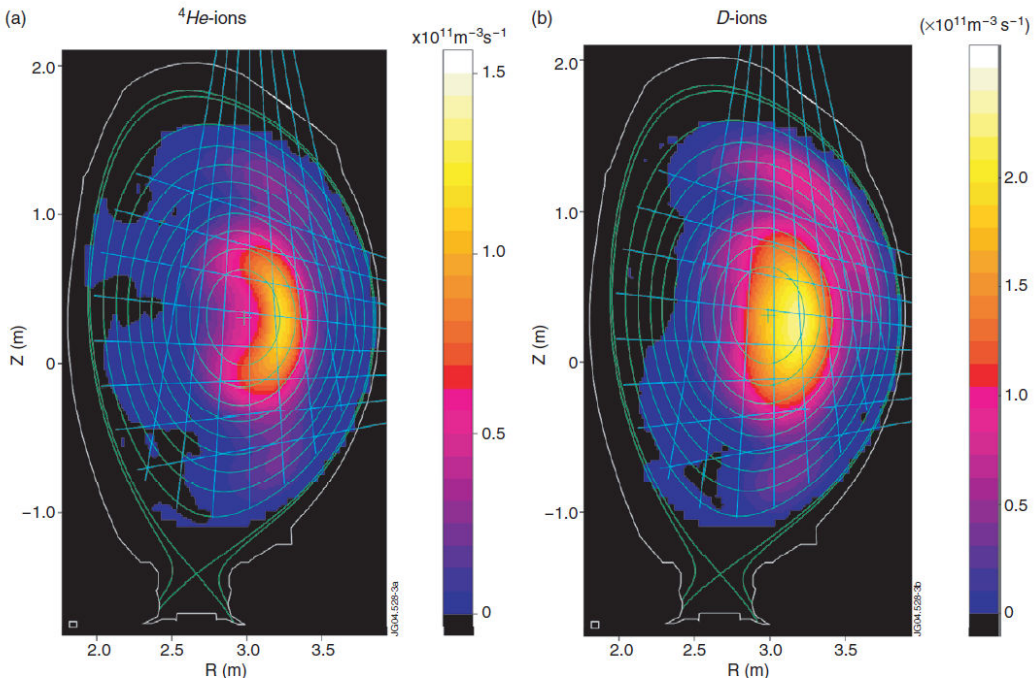

Fig. 3.2: From Kiptily et al, NF 45, 2005 L21. Tomographic reconstructions of 4.44MeV γ-ray emission from the reaction ^{9}Be(^{4}He,nγ)^{12}C (left) and 3.09MeV γ-ray emission from the reaction ^{12}C(D,pγ)^{13}C (right) deduced from simultaneously measured profiles. The different distributions for fast ^{4}He and D ions are explained by differences in the orbits for the two species.

When used for gamma rays, the neutron cameras must be equipped with attenuators for reducing the neutron background by two orders of magnitude. The vertical camera is being upgraded with attenuators suitable for a full DT campaign and by faster scintillators. For the horizontal camera the present attenuator is not considered adequate to shield from 14 MeV neutrons and will have to be upgraded if its detectors are to be used in DT.

Fast particle losses

FP losses can be investigated with a Scintillator Probe as it allows the detection of lost ions at a single position outside the plasma, and provides information on the lost ion pitch angle in the range 35° to 85° (~5% resolution) and its gyro-radius between 3 and 14 cm (~15% resolution) with a time resolution of 2 ms. The scintillator probe at JET is located 28 cm below the mid-plane of the machine. The examples in the figure below show that different MHD modes lead to differences in the ion loss patterns. This diagnostic will shortly be equipped with fast scintillators and a fast CCD camera for better investigating the effects of MHD instabilities.

A further fast ion loss diagnostic is provided by a set of 9 stacked thin foil Faraday Cups at 5 different poloidal positions below the equatorial plane at the low field side. These detectors achieve energy resolution (in the range 0-7MeV for alpha particles) by the usage of a stack of 4 different foils (Fig. 3.4).

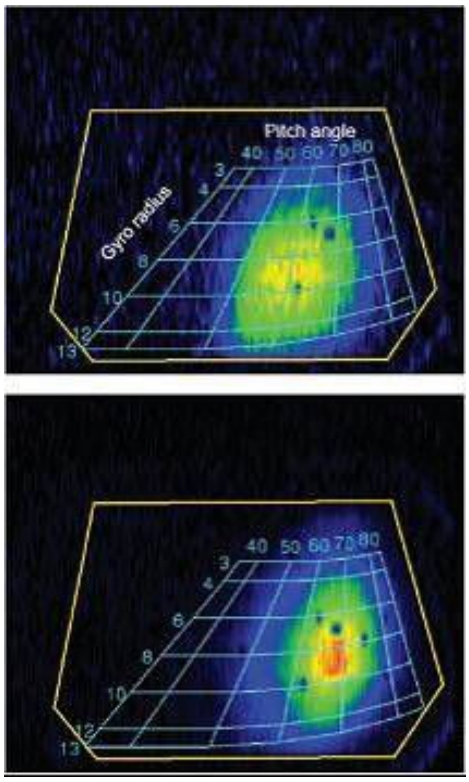

Fig. 3.3: JET discharge #66380, I_P = 2.5 MA, B_T = 2.7T. Footprints of fast protons lost at the SP during periods when TAE and precessional fishbones are unstable (top); tornado and TAE modes are unstable (bottom). (Kiptily et al Nucl. Fusion 49 (2009) 065030)

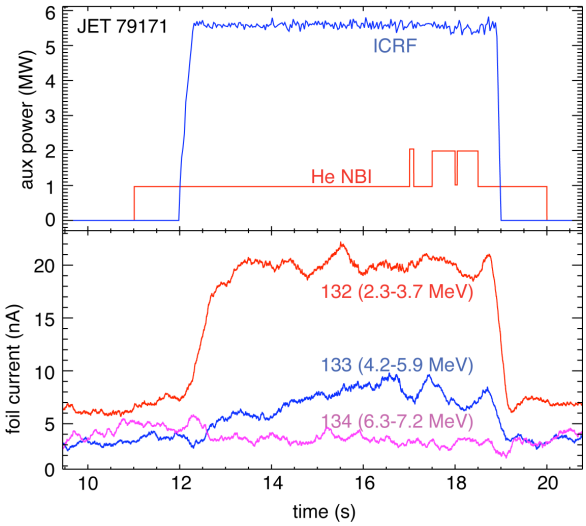

*Fig. 3.4: Lost alpha-particle measurements. Auxiliary heating power and thin foil Faraday Cup currents for a JET discharge with ^{4}He NBI and third harmonic RF heating of the injected ^{4}He. The signals show diminishing current at increasing energy, as expected. There is essentially no current in foil 134, indicating also the absence of RF pickup. (D. Darrow et al RSI **81**, 2010, 10D330)*

3.4 The active TAE antennae

During the DT campaign in JET and at sufficient plasma background pressure some TAE's disappearing from the Alfven Eigenmode (AE) spectrum altogether, as was the case in DTE1. Whether stable modes actually exist, that could be unstable in the corresponding scenario in ITER, or whether there are simply no modes can be addressed using the active TAE antennae at JET.

The antenna system is capable of exciting AE's over a wide range of frequencies (50-500 kHz) and toroidal mode numbers (n=0-15) and has been used extensively in C26-

27 (T. Panis et al. Nucl. Fusion 50, 2010, 084019). The diagnostic automatically sweeps a given frequency range and after detecting a mode, track this mode by performing small sweeps across the resonance. The line widths of the resonances provide the effective damping rates (damping rate minus growth rate). The most unstable modes in the presence of alpha particles are expected in the intermediate n-range (3-10). Experimentally, the growth rate can be obtained by measuring the difference between two modes with the same poloidal mode number, but opposite toroidal mode numbers, because only one of the two interacts with alphas, whereas both of them experience the same plasma damping. Growth rates and damping rates can be used to validate (or invalidate) fast particle models in view of ITER predictions. In addition, the diagnostic provides a measure of the mass density in the region where the mode is localised, which can be used to determine the D/T ratio.

3.5 Diagnostics for the protecting the ITER-like Wall

Part of the diagnostic improvements being made in parallel to the installation of the ITER-like Wall, is a suite of visible and infrared camera views of plasma-facing components. It will be possible to make fast measurements of heat and particle loads on divertor and on most of the limiters, allowing detailed 3D information to be obtained. In addition, as part of the protection system for the wall, a sophisticated capability to measure and control hot spots in real time is being implemented. This is important for safely developing high performance, high input power scenarios. However it is almost certain that the cameras used for viewing and protecting the ITER-like wall will not be available during a DT phase, unless protective measures are implemented.

3.6 Recommendations for diagnostics and possible ITER relevant tests

With the assessment of the diagnostic capabilities for a DT campaign at JET, various shortcomings and recommended upgrades were identified, as well as test that could be undertaken in preparation for ITER. This list may not be complete:

1 The main systems which are not tritium and/or DT compatible two VUV spectrometers, the lithium beam diagnostic, the time-of-flight neutron spectrometer (TOFOR, for DD neutrons), all but one of the X-ray cameras and the visible and infrared surveillance and protection cameras. Most of these will have to be removed during the last shutdown before the DT campaign, while some may remain until they fail. A complete list of system has already been compiled by the operator, together with severity and fixes, where possible.

2 Given the importance of the safe operation with the ITER-like Wall, the options for (ITER) relevant protection (shielding, special fibres, optical relaying) for at least some of the cameras by should be investigated.

3 Bringing the edge LIDAR into service again should be considered for best edge resolution and for a proof-of-principle test of the laser detritiation technique, by vaporising possible Be/T co-deposits in sample areas in the inner divertor.

4 JET also has a vertical CXRS system with opposing lines for accurate poloidal flow measurements with high spatial resolution in the edge (~2cm). This system will be very valuable for L-H transition and edge pedestal physics in the various isotope campaigns. Unfortunately the system has been close to dormant since 2009 for lack of staff, which is why we recommend bringing it back into operation.

5 Ways of allowing the use of MSE despite the upgrade of the neutral beams to sources with equal beam energy should be researched.

6 Beam emission spectroscopy (BES) is a successful diagnostic in other devices, allowing a measurement of large scale fluctuations, such as associated with MHD modes. It may be worth considering using the port currently dedicated to MSE for BES in case the use of MSE is irrevocably compromised.

7 The current version of EFIT is outdated and rather unsatisfactory. It uses an inadequately coarse spatial grid and inadequate constraints for e.g. the current profile, which cannot be representative of H-modes. An overhaul of EFIT is overdue irrespectively of a future DT campaign.

8 A new calibration of the neutron counters with a moveable in-situ ^{252}Cf source (~2MeV) should be foreseen. In addition to preserving the accuracy of JET neutron diagnostics in the DD neutron energy range, this would constitute a test for a proposed ITER calibration technique (albeit not at 14MeV) and to benchmark neutron transport codes and analysis techniques.

9 In the case of an expression of interest by ITER, a more ambitious and challenging neutron calibration using a 14MeV neutron source (miniature accelerator), as proposed for ITER, should be considered (see chapter 8).

10 Tests and cross-comparisons of the various neutron detector and spectrometers in a DT campaign will be of great value for ITER and sufficient resources should be made available. The detectors may include new concepts not currently on JET, such as a monitor based on the activation of water (see chapter 8).

11 The Neutral Particle Analyser for measuring the isotope composition must be upgraded to cope with the enhanced neutron background.

12 The active TAE diagnostic is to be (and should be) upgraded in a collaboration involving CRPP, MIT, Brazil and CCFE in order to improve the S/N ratio and operational flexibility by allowing e.g. to track more than one mode at a time.

13 Various new diagnostics have been proposed for DT, but are currently not being implemented. They include:
- A Fast Wave Reflectometer for mass density measurements.
- An Ion Cyclotron Emission diagnostic.
- A Coherent Thomson Scattering Diagnostic for alpha particle measurements

4. Fusion performance projections for JET DT operation

Key points:

- Extrapolation of JET plasma performance to DT operation with the EP2 power upgrade leads to the following estimates for total fusion gain:
  - Q~0.16-0.2 for ELMy H-mode plasmas at 4.5MA/3.6T (based on existing plasmas at 3.8-4.5MA)
  - Q~0.3-0.5 for hybrid plasmas at 3.5-4.1MA/3.45-4.0T (extrapolating from existing plasmas at 1.7MA/2.0-2.3T)
  - Q~0.1-0.4 for AT plasmas at 1.8-3.4MA/2.7-3.5T (supplementing results from existing plasmas with predictive modelling benchmarked at 1.9MA/3.1T)
- To obtain Q_{DT}~1, it would be necessary to achieve H_{98}~1.55-1.8 at high plasma current (4MA).
- ELMy H-mode and hybrid extrapolations are based on plasma scenarios that have been already achieved in steady conditions for several energy confinement times. The duration of steady Advanced Tokamak plasma conditions would need to be extended compared with present experiments.
- Key elements for the extrapolation would need to be investigated to validate these projections prior to a DT campaign:
  - potential for high H at high plasma current and high density
  - density and impurity control
  - q-profile control
  - disruption risk
  - stability of NTMs and kink modes
  - impact of sawteeth and fishbones
  - ILW compatibility

As this Chapter presents an extensive analyses of fusion performance projections for the various ITER regimes of operation (sections 4.2, 4.3 and 4.4), a detailed summary is provided below

Detailed summary

Building on the extensive scenario development programme at JET to prepare for the operation of ITER, we assume here that existing plasma scenarios can be developed using the maximum available heating power. Hence, it is assumed that the performance achieved in ELMy H-mode, hybrid and advanced tokamak (AT) scenarios can be extrapolated to high magnetic field at the same q_{95} as present experiments. In addition it is assumed that hybrid plasmas can be developed to lower q_{95} (~3) to allow exploitation at the high plasma currents that are accessible in ELMy H-mode scenarios (≥3.5MA).

The two tools used to extrapolate fusion performance using scaled profiles from existing reference deuterium experiments were TRANSP and JETFUSE. TRANSP was first used to make an interpretive simulation of reference plasmas as a test of the validity of the fusion yield calculation. Then the simulations were modified to include: mixed deuterium-tritium plasma and beams; conserved plasma profile shapes (n_e, T_e, T_i, ω_ϕ…); and scaled global parameters (I_P, B_T, P, $<n_e>$, W_{th}…) following various 0-D assumptions. The TRANSP simulations presented in this report were made by Ian Jenkins. JETFUSE is a spreadsheet based, single time-slice fusion yield calculator, which has been benchmarked against experimental data and TRANSP simulations. JETFUSE has been used to perform scans of 0-D parameters that would be time consuming to obtain by multiple TRANSP runs.

To investigate the uncertainties in core fusion performance due to reduced beam penetration at high density, CRONOS simulations were performed for the hybrid scenario by Jeronimo Garcia using density profiles and temperature pedestal values scaled from the reference plasmas. The core temperature profiles were predicted using a Bohm/GyroBohm model coupled with an internal transport barrier (ITB) model based on a threshold condition in terms of magnetic shear and ω_{ExB} flow shear, as described in [Tala T. *et al* 2006 *Nucl. Fusion* **46** 548]. The modelling method was benchmarked against reference deuterium experiments on JET.

For AT plasmas, an extrapolation from previous JET experiments to deuterium ITB plasmas at high plasma current, magnetic field and heating power has already been performed using JETTO by João Bizarro and published in [Litaudon X. *et al* 2007 *Nucl. Fusion* **47** 1285]. In this case, the strong interdependence of the current drive and transport necessitated the self-consistent prediction of temperature, density, current density and rotation profiles, based only on assumed initial conditions and pedestal values. Again the Bohm/GyroBohm plus ITB transport model was used from [Tala T. *et al* 2006 *Nucl. Fusion* **46** 548]. This procedure was also benchmarked against reference deuterium experiments on JET. The final extrapolation to deuterium-tritium plasma and beams was made using JETFUSE assuming the same plasma profiles and heating power.

The ELMy H-mode has the most robust basis for extrapolation due to the recent high plasma current experiments in deuterium [Nunes I. *et al* 2010 IAEA EXC/P8-03]. It is expected that $Q_{DT,total}$~0.16-0.2 should be achievable, comparable with the DTE1 results. But the increased neutral beam heating power expected due to the EP2 upgrade opens the prospect for a significant increase in the steady fusion power provided that compatibility with the ITER-like wall can be achieved without degrading the core plasma performance and deleterious effects of MHD can be avoided at higher normalised β.

It is considered that the hybrid scenario provides the best prospect for steady high Q_{DT} operation, provided that the good stability and improved confinement achieved during the 2008/9 experimental campaigns (i.e. $H_{IPB98(y,2)}$~1.3 and β_N~3 at I_P~1.7MA) can be extended to high plasma current and magnetic field (reduced q_{95}~3) and maintained despite any measures that may be required to achieve compatibility with the ITER-like wall. A key uncertainty concerns the density dependence of confinement, but taking a range of assumptions for the extrapolation to 4.1MA/4.0T, the predictions give a range of uncertainty for $Q_{DT,total}$ of the order 0.3 to 0.5.

For the purpose of extrapolating AT scenarios predictive simulations have been performed to investigate the potential plasma performance if the high input power available from the EP2 neutral beams were to produce ITBs at large plasma radius (ρ~0.7) giving access to $H_{IPB98(y,2)}$~1.7. If this were achievable, such a plasma is predicted to generate $Q_{DT,total}$~0.27-0.38 at β_N~3 using 45MW of heating at 2.3MA/3.5T. Such a high normalised confinement has not previously been maintained in steady conditions at JET and plasmas with steep temperature and density gradients due to ITBs can also be limited in terms of fusion performance due to MHD instabilities and impurity accumulation. It may be possible to increase the plasma current in order to mitigate the need for such a high normalised confinement, and the achievement of $Q_{DT,equivalent}$~0.4 has been reported from earlier JET deuterium ITB experiments at high plasma current (3.4MA), although the duration was limited to ~1s. It is considered, therefore, that $Q_{DT,total}$~0.4 represents an upper limit on the range of uncertainty for ITB scenarios. For comparison the estimated $Q_{DT,equivalent}$ for recent JET AT plasmas at lower plasma current (1.8MA) is of the order 0.1-0.14 maintained for ~5s. Despite being the extrapolation with the greatest uncertainty of the three plasma scenarios in terms of possible fusion yield and potential for sustainment, it may be of interest for AE investigations due to the potential for significant alpha pressure in the plasma core with $q_{minimum}$ above unity.

Key elements for the extrapolation would need to be investigated to validate these predictions prior to a DT campaign both experimentally and through further modelling activities. Areas of importance include: potential for high $H_{IPB98(y,2)}$ at high current and high density; density and impurity control; q-profile control; disruption risk; stability of NTMs and kink modes; impact of sawteeth and fishbones; ILW compatibility at high heating power; etc. The potential for performance improvements in the hot-ion H-mode regime used to achieve the record Q_{DT} in DTE1 have not been examined in detail due to the transient nature of the plasmas used in previous JET DT campaigns. However, it should be noted that new techniques are now available for plasma edge control (e.g. vertical kicks, pellets, EFCCs, etc.). The potential for further improvement of this route to high Q in the light of improvements in

understanding and control of the plasma edge could be assessed in deuterium experiments prior to a DT campaign.

Estimations in this report suggest that $H_{IPB98(y,2)}$~1.55-1.8 would be required at high plasma current (4MA) to achieve Q~1. This would represent an increase in normalised confinement by a factor of almost 2 compared with the recent ELMy H-mode experiments at high plasma current. Even if the recent improvements in the normalised confinement of JET hybrid plasmas could be extended to high plasma current, the projected fusion yield would not reach the required level for Q~1. Therefore proposals for a future JET DT campaign should be assessed on the basis of more modest projections from existing experiments such as those discussed above.

4.1 Scenario development in preparation for a DT campaign

The development of ITER scenarios at JET is envisaged to take place sequentially in D, T and then DT plasmas, so that any isotope effects can be evaluated during the development phase (see also lessons learned from DTE1 in section 2.2).

The relatively high confidence that we presently have for ELMy H-modes and their exploitation in ITER is due to the reproducibility of these regimes on multiple machines of different sizes. It should be noted that this confidence has been achieved despite the absence of a complete, first-principles theoretical model of the edge transport barrier and therefore of the behaviour of the H-mode. Nevertheless, the implementation of even the baseline scenario on ITER will have to be done in an integrated manner, simultaneously respecting all the additional boundary conditions associated with ITER operation. To achieve this the ITER Research Plan foresees a step-wise approach to Q=10 with limited time available for optimising NTM and ELM control, divertor detachment, plasma species mix, burn control, etc., all of which must be reliably and simultaneously integrated before the plasma performance can be pushed towards high fusion yield. An integrated demonstration of high performance in JET will significantly reduce the risk of a delay in achieving the main fusion power mission of ITER.

The situation with regard to fully non-inductive scenarios, which are likely to require improved core confinement as well as edge transport barriers, is quite different. There is presently no firmly established regime that can be confidently extrapolated to the conditions of ITER. The development of such scenarios and validation in terms of machine size scaling and wall compatibility has the potential to save substantial time in ITER. The ITER Research Plan does not envisage allocating significant experimental time to the development of advanced modes of operation before the Q=10 mission is achieved. Therefore decisions concerning upgrades to the ITER heating systems that are intended to enhance plasma performance in advanced modes will rely strongly on results from other machines and the input they provide to modelling codes.

4.1.1 ELMy H-mode scenario

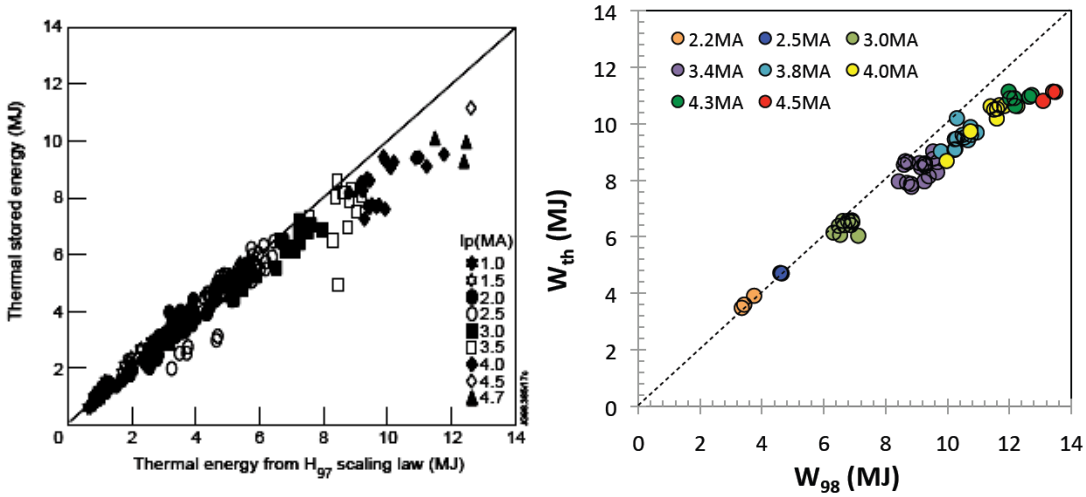

Fig. 4.1: (left) Thermal stored energy for JET pulses performed in 1996-1999 versus thermal stored energy predicted by the 1997 ELMy H-mode scaling law and (right) thermal stored energy versus the thermal energy predicted by the 1998 ELMy H-mode scaling law for recent experiments. Symbols denote plasma current. [from Horton L.D. et al 1999 Nucl. Fusion 39 993 and Nunes I. et al 2010 IAEA EXC/P8-03]

JET ELMy H-mode experiments have contributed strongly towards the validation of the baseline scenario for ITER operation (Scenario 2). In a summary of the results obtained on ELMy H-modes [Horton L.D. *et al* 1999 *Nucl. Fusion* **39** 993] it has been observed that the achievement of H~1 requires the application of sufficient heating power to maintain stationary type I ELMs. Although the extrapolation of this condition to ITER is difficult due to the present uncertainty in the prediction of the power necessary to obtain H-mode in an ITER sized device, the best JET DT plasmas had a higher ratio of input power to threshold power than is expected for ITER. Even so, the confinement of the highest plasma current DT plasmas was degraded compared with the ITERH97P(y) ELMy H-mode scaling. This may have been due to a lack of available input power (25 MW during DTE1) or a departure from one of the parameter dependencies in the scaling (e.g. I_P, B_T or n_e).

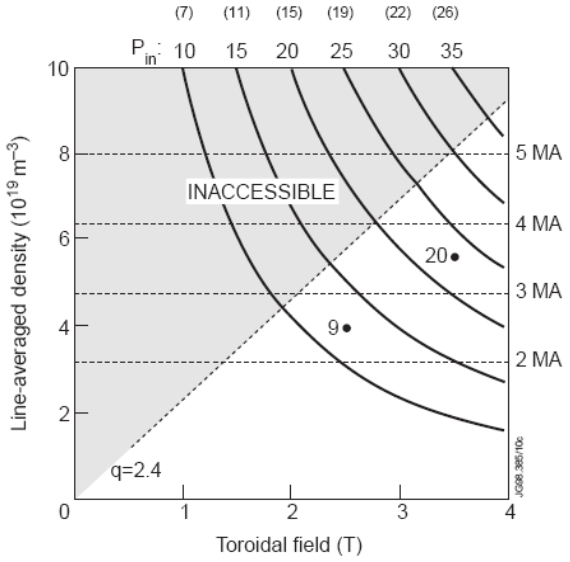

*Fig. 4.2: Operating space diagram for stationary ELMy H modes in JET. Operation at high current is limited to discharges above q_{95} = 2.4, the lower right half of the diagram. The plasma density is assumed to be 50% of the Greenwald limit. This places a limit on the power necessary to maintain the discharge in H mode, $P_{LH} = 0.45 B_T n_e^{0.75} R^2$. The input power for deuterium and, in brackets, DT is shown at the top. The two experimental points indicate where there is an observed loss of confinement. [from Horton L.D. et al 1999 Nucl. Fusion **39** 993]*

In more recent experiments during 2009 (Nunes I. *et al* 2010 IAEA EXC/P8-03) safe operation was again demonstrated at high plasma

current (up to 4.5MA/3.6T). These experiments also show degraded confinement in plasmas above 3.5MA compared with the more recent global confinement scaling. This relative loss of confinement appears to be shared between the edge confinement barrier and the plasma core. The similarity between these results and the DTE1 high current ELMy H-mode behaviour is striking despite the comparison being made with the IPB98(y,2) scaling in the case of the more recent plasmas. The maximum available heating power was similar in both sets of experiments, but gas fuelling was different. The DTE1data illustrated were without gas fuelling. At the highest plasma current in the 2009 experiments it was necessary to use gas fuelling to keep the plasma quasi-steady (avoiding compound ELMs). The compound ELMs are thought to be due to the destruction of surface layers on the (carbon) inner divertor tiles and/or to a lack of input power. As the gas fuelling also reduced the plasma confinement, it is planned to re-assess high current performance with the metal divertor tile surfaces of the ILW where the requirements for gas fuelling may be different. If these experiments prove successful in terms of avoiding compound ELMs and achieving quasi-steady, high confinement, it is possible that an interesting operating space will become accessible. However, it is probable that the ELM size will become larger, perhaps reaching an ELM energy of 1-2 MJ. At such large ELM energy it is expected that ELM mitigation techniques will be needed to reduce the transient power flux to the divertor (see section 4.5). The ability to mitigate ELMs in this situation is one of the objectives for 2011-2013 campaigns, using the external error-field correction coils, vertical kicks or pellet pacing.

4.1.2 Hybrid scenario

The hybrid scenario has been developed at JET based on the achievements in earlier experiments on AUG and DIII-D. During the 2008-2009 campaigns the confinement was improved in the JET hybrid scenario by optimising the target q-profile using the ohmic circuit. In these experiments a plasma current overshoot was used to prepare a target q-profile and produce a wide region of low magnetic shear around the plasma centre with q_0 close to 1. Examples are given in section 4.2.1 below. These plasmas can obtain $H_{IPB98(y,2)}$~1.3 at β_N~3 at q_{95}~4 for many τ_E or ~τ_R. Hybrid plasmas were obtained at different plasma currents and developed at low triangularity and high triangularity.

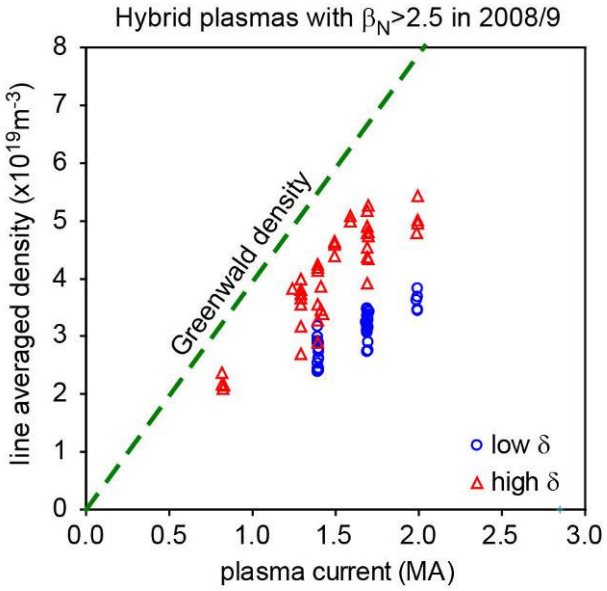

Fig. 4.3: Line averaged density versus plasma current at time of peak β_N for JET hybrid plasmas during 2008/9 where β_N exceeded 2.5.

An overview of the densities obtained as a function of plasma current is given in the figure. It is noticeable that the density is systematically higher for high triangularity plasmas compared with cases as low triangularity. Also the

density tends to increase with plasma current at similar values of β_N for each plasma shape so that $n/n_{Greenwald}$ remains roughly constant.
So far the development of JET hybrid plasmas with improved normalised confinement has been has been performed in the domain $I_P \leq 2MA$. The increase in the available NBI power due to the EP2 upgrade (up to 35 MW of beam power in DT) will allow access to high β_N at higher plasma current and lower ρ^*, thus extending results from DIII-D and AUG and permitting studies of the ρ^* dependence of NTM stability and control in preparation for hybrid operation in ITER [for the ρ^* dependence of NTM stability see, for example, Buttery R.J. *et al* 2007 EPS P-1.137].

4.1.3 Non-inductive, advanced tokamak scenario

Developing candidate plasma scenarios that extrapolate to steady-state ITER operation at Q=5 provides some of the most demanding performance challenges of all the ITER scenarios being developed at JET. The simultaneous requirement for excellent normalised confinement and good stability has to be combined with efficient non-inductive current drive and wall compatibility. Since DTE1, when transient ITBs with extreme pressure gradients were used to generate high fusion power, the development has been towards plasmas with a broader pressure profile capable of access to high β_N whilst deriving as much confinement as possible from the edge transport barrier [see Mailloux J. *et al* 2010 IAEA EXC/1-4]. This has led to the achievement of $H_{IPB98(y,2)} \sim 1.2$ and $\beta_N \sim 2.7$ for more than $10\tau_E$ and plasma conditions were achieved where the bootstrap current provides up to 45% of the total plasma current.

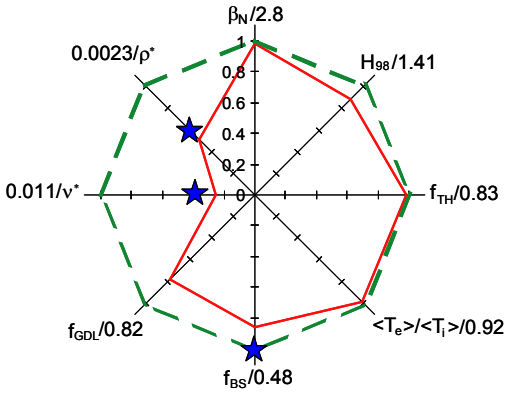

Fig. 4.4: Dimensionless parameters for shot 78052 1.8MA/2.7T normalised to notional ITER steady-state targets. The stars represent an extrapolation to B=3.45T assuming upgraded EP2 NBI power. [from Mailloux J. *et al* 2010 IAEA EXC/1-4*]*

The q-profile used in these AT experiments typically had weak magnetic shear near the plasma centre with $q_{minimum} \sim 2$, which has the potential for much better core fast ion confinement than plasmas with deeply reverser shear or a 'current-hole'. The use of 'weaker' ITBs with more modest local pressure gradients inside the plasma allows steady plasma performance to be maintained until the slowly evolving q-profile reaches an unfavourable shape for stability with $q_{minimum}$ too far below 2 [see Maget P. *et al* 2010 *Nucl. Fusion* 045004].

The development of AT plasmas in configurations with high triangularity (approaching that of ITER) has led to higher density plasmas ($n/n_{Greenwald} \sim 0.6$) with $\langle T_e \rangle \sim \langle T_i \rangle$, the latter being favoured by the addition of ICRH power in the plasma core. With the additional heating power due to the EP2 NBI upgrade it is expected that ρ^* and ν^* can be further reduced to achieve the closest approach yet to the dimensionless parameters of ITER.

4.2 JET DT fusion yield projections for ELMy H-mode plasmas

ELMy H-mode plasmas with regular type I ELMs typically achieve $H_{IPB98(y,2)}$~1 on JET. However, as was shown in section 4.1.1, the available deuterium reference plasmas at high plasma current have somewhat degraded confinement compared with the IPB98(y,2) scaling. Therefore the performance extrapolation for ELMy H-mode operation in DT has been performed in two ways:

- Extrapolate directly from a high current plasma (#79698, 4.5MA/3.6T) with degraded confinement ($H_{IPB98(y,2)}$~0.85), simply replacing deuterium by DT for the plasma and beams
- Extrapolate indirectly from a plasma with slightly reduced plasma current (#74176, 3.8MA/3.0T) and good confinement ($H_{IPB98(y,2)}$~1), by increasing I_P, B_T, in the simulation to reach 4.5MA/3.6T and scaling the temperature profiles to maintain $H_{IPB98(y,2)}$~1

This approach allows an assessment of the potential DT performance of ELMy H-mode plasmas based on the achievements at high current as well as an indication of the potential gain if $H_{IPB98(y,2)}$~1 can be reached in this domain. The results also give some indication of the range of DT fusion performance that might be expected given the uncertainty in the value of $H_{IPB98(y,2)}$ that might be accessible with the ILW. The TRANSP simulations presented in this section were performed by Ian Jenkins.

4.2.1 ELMy H-mode extrapolation to DT

The interpretive TRANSP simulation for #79698 slightly underestimates the plasma stored energy compared with the diamagnetic measurement, and the neutron yield is slightly overestimated. Note that the small amount of ICRH heating (~2.5MW) is not included in the simulation, which can account for some of the missing stored energy in the simulation. But this does not explain the overestimation of the neutron yield. The neutron yield discrepancy may be due to some effect such as the anomalous diffusion of fast ions generated by the neutral beams. For simplicity it is assumed here that an equivalent discrepancy can be expected in the case of a DT plasma and the fusion yield from the DT simulation can be discounted by the ratio of the measured and simulated fusion yield in the deuterium reference case.

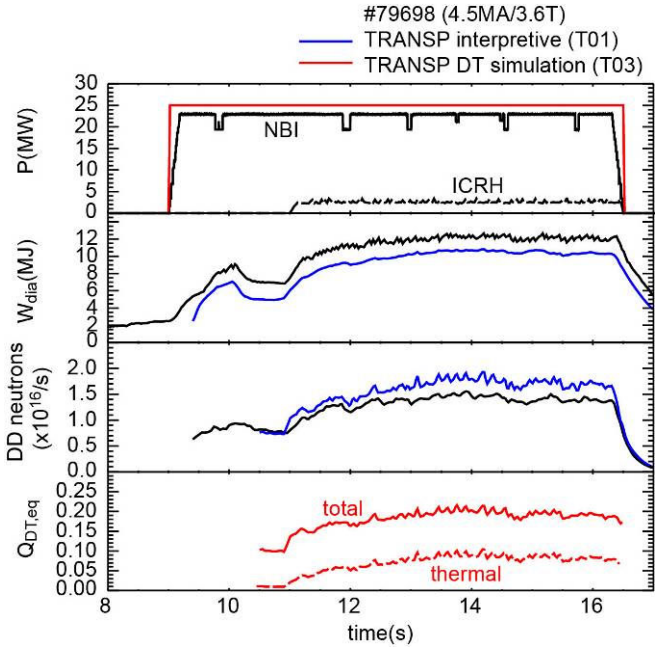

Fig. 4.5: Heating power, stored energy and neutron yield for ELMy H-mode pulse #79698 (black), results of an interpretive simulation (blue) and DT simulation assuming the same density and temperature profiles (red).

The DT simulation based on #79698 has slightly higher neutral beam power than the original pulse to compensate for the missing ICRH power. The assumed DT beam specification is:

- D beams at 124keV (52% full energy power, 38% half energy power)
- T beams at 118keV (58% full energy power, 29% half energy power)

Note that this specification was based on early predictions of the EP2 beam performance and that the most recent predictions can be found in [Ćirić D. *et al* 2010 SOFT]. The beam power is divided equally between the deuterium and tritium beams and the plasma is close to 50:50 D:T.

The extrapolation gives $Q_{DT,equivalent}$~0.2 directly from the simulation, which scales to $Q_{DT,equivalent}$~0.16 when the neutron discrepancy of the interpretive simulation is taken into account. Here Q is simply the ratio of the total fusion power divided by the neutral beam heating power injected into the tokamak. No credit is taken for α-heating or any mass dependence of confinement. The result is roughly consistent with the DTE1 observation of Q~0.18 for steady ELMy H-mode experiments at high current [Horton L.D. *et al* 1999 *Nucl. Fusion* **39** 993].

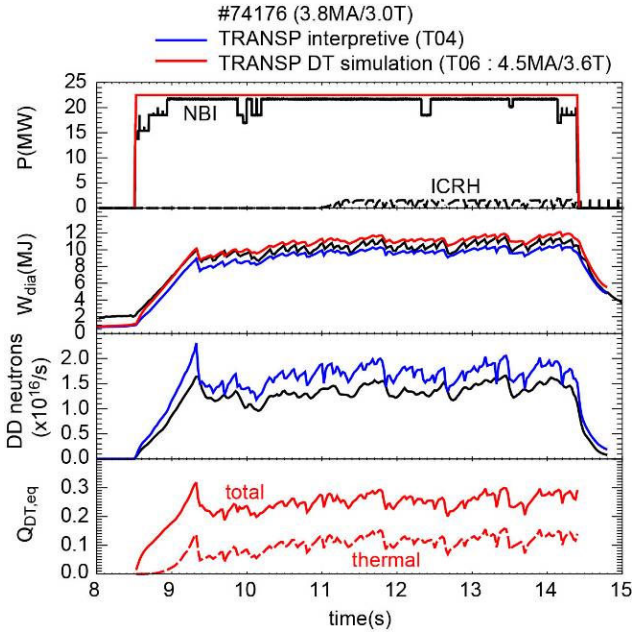

Fig. 4.6: Heating power, stored energy and neutron yield for ELMy H-mode pulse #74176 (black), results of an interpretive simulation (blue) and DT simulation assuming the same $H_{IPB98(y,2)}$ and input power at 4.5MA/3.6T profiles (red).

To assess the fusion yield potential if $H_{IPB98(y,2)}$~1 could be achieved at high plasma current, a second TRANSP simulation was performed based on #74176. The interpretive simulation shows similar results to #79698, with the slight underestimation of the diamagnetic stored energy and slight overestimation of the neutron yield. To estimate the fusion performance of a DT plasma with $H_{IPB98(y,2)}$~1 at higher plasma current the magnetic field and plasma current were increased at constant q_{95} to reach 4.5MA/3.6T. The density was conserved, but $<T_i>$ and $<T_e>$ were both increased to maintain $H_{IPB98(y,2)}$ for the same

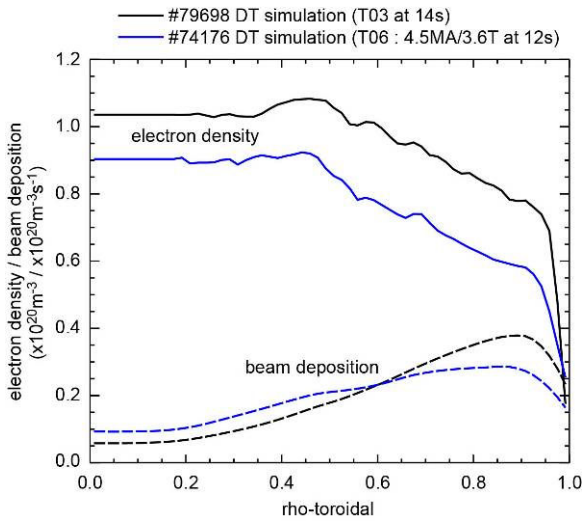

Fig. 4.7: Typical density profiles for ELMy H-mode plasmas #79698 and #74176 and deposition profiles for EP2 DT beams assuming the same density.

heating power. The ion and electron temperature profile shapes were conserved and simply multiplied by a scalar to increase $<T_i>$ and $<T_e>$. The resulting simulation gives and extrapolated fusion performance of $Q_{DT,total}$~0.25 at 4.5MA/3.6T, which scales to $Q_{DT,total}$~0.2 when the neutron discrepancy of the interpretive simulation is taken into account.

A key reason for the modest fusion yield obtained in these high current ELMy H-mode simulations is high plasma density. The relatively poor neutral beam penetration directly affects the beam-target fusion yield as the majority of the beam generated fast ions slow down in the relatively cool plasma periphery. It is plausible the thermal fusion yield is also affected indirectly due to the relatively weak core ion heating and torque, the latter of which may affect the ion heat transport in the plasma interior. If operation with the ILW were to allow a greater degree of density control compared with the previous JET carbon wall, it would be well worth investigating the fusion yield potential for high current ELMy H-mode plasmas with somewhat lower density.

4.1.2 Summary of results of ELMy H-mode extrapolation

The prediction of fusion performance in ELMy H-mode plasmas is fairly robust because such plasmas were obtained in DTE1 and recent experiments have again demonstrated safe operation at high plasma current. Extrapolations to DT operation based on the more recent ELMy H-mode experiments yield similar fusion performance to the DTE1 results in terms of steady Q_{DT} (i.e. $Q_{DT,total}$~0.16-0.2). The main source of uncertainty concerns the effects of any measures required to achieve compatibility with the ILW. This point is discussed further in section 4.5. Further improvement in terms of steady total fusion power compared with DTE1 (i.e. P_{fusion}~4MW) can be expected due to the increased neutral beam heating power available with the EP2 upgrade. Although, to first-order, Q should be relatively insensitive to neutral beam power, the total fusion power should increase with heating power provided that MHD stability can be maintained at higher β (β_N~1.4-1.5 in #79698). Further optimisation in terms of confinement and density control should be investigated with the ILW.

4.3 JET DT fusion yield projections using hybrid plasmas

Hybrid scenarios at JET are now capable of achieving $H_{IPB98(y,2)}$~1.3 at β_N~3 using a plasma current overshoot technique to form a q-profile with q_0 close to unity and a wide region of low magnetic shear in the plasma core at the start of the main heating phase [Joffrin E. *et al* 2010 IAEA EX/1-1]. Fusion yield predictions indicate that a considerable fusion yield at JET would be achieved if the improved plasma performance of present hybrid experiments on JET at $I_P \leq 2$MA could be extended to high plasma current ($I_P \geq 3.5$MA). The TRANSP simulations presented in this section were performed by Ian Jenkins and the CRONOS simulations were made by Jeronimo Garcia.

4.3.1) Reference hybrid plasmas

Two plasmas obtained during the 2008-2009 JET experimental campaigns have been selected as reference plasmas for extrapolation to DT. These plasmas have good

confinement and stability ($H_{IPB98(y,2)}$~1.3 and β_N~3), achieved following a plasma current overshoot to prepare the q-profile for main heating. The two hybrid plasmas considered here were heated using neutral beam injection only. Significantly different plasma density was achieved in the two cases due to different plasma triangularity (δ). The differences can be summarised as follows:

- #75225 (1.7MA/2T) with low δ, low density ($n/n_{Greenwald}$~0.49) and high ion temperature (T_{i0}~1.8xT_{e0}). This discharge has a 4/3 NTM during part of the main heating phase;
- #77922 (1.7MA/2.3T) with high δ, high Greenwald fraction ($n/n_{Greenwald}$~0.68) and comparable ion and electron temperatures (T_{i0}~1.3xT_{e0}). The plasma was essentially free of NTMs during the main heating phase.

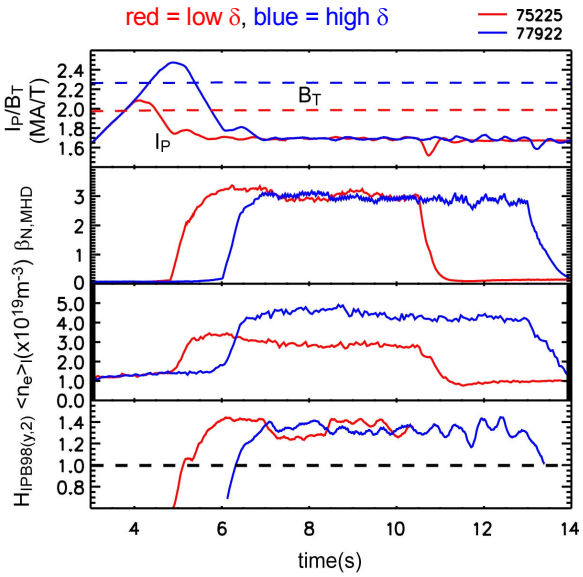

Fig. 4.8: Plasma current, magnetic field, β_N, line averaged density and $H_{IPB98(y,2)}$ for two hybrid plasmas at low (red) and high (blue) triangularity.

4.3.2 Benchmark of hybrid simulations

Interpretive simulations have been made using TRANSP and JETFUSE for the two reference plasmas described in section 4.2.1 to benchmark the neutron yield calculations against experimental data. Both codes calculate the thermal fusion yield from the ion temperature and density profiles. TRANSP realistically models all 16 JET neutral beams with their three hydrogenic species to calculate the NBI deposition and then uses a Monte Carlo fast-ion calculation (NUBEAM) to determine the distribution function for the beam-target and beam-beam fusion reaction calculations. JETFUSE uses a single pencil, single pass beam model including all three hydrogenic species. Arbitrary smoothing is applied in the region ρ<0.34 to prevent a singularity occurring at the

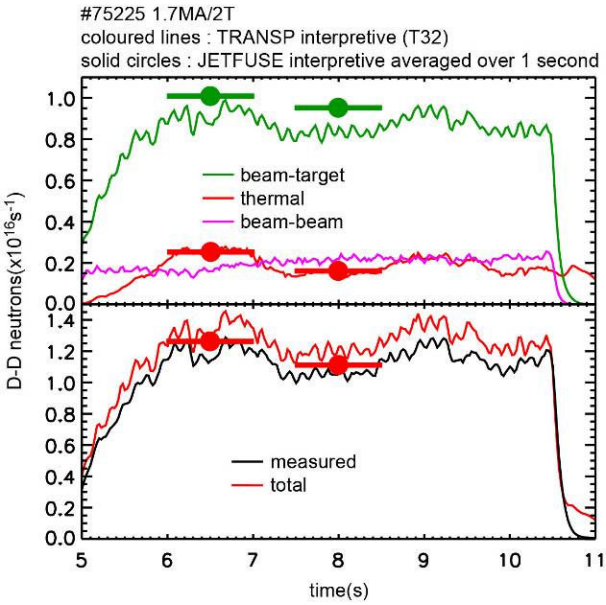

Fig. 4.9: Interpretive simulation of the neutron yield for a low δ hybrid plasma using TRANSP and JETFUSE. The thermal (red – upper box), beam-target (green) and beam-beam (cyan) reactions are shown separately. The total modelled neutron yield (red – lower box) is compared with the measured value (black).

plasma magnetic axis. JETFUSE neglects the effect of plasma rotation on beam deposition and fast ion generation, which results in a slight overestimate in the beam-target neutron yield. Beam-beam fusion reactions are also neglected in JETFUSE, which largely offsets the effect of neglecting rotation. The effect of all of these simplifications is significant for low density plasmas, but good agreement with TRANSP and experimental data is achieved for the hybrid plasmas being considered here. For the low δ hybrid reference plasma #75225 TRANSP reproduces the measured neutron rate to within 12% and JETFUSE achieves agreement with the measurements to within 6%.

In this hybrid pulse a 4/3 NTM is observed from t=6.85s, which results in a 9% drop in $\beta_{diamagnetic}$ and a 12% reduction in the total neutron rate. However, the dominance of the beam-target fusion reactions masks the much larger impact that this core MHD mode has on the thermal fusion yield. The TRANSP simulation shows a 40% reduction in thermal fusion yield when the mode amplitude is largest. This highlights the importance of avoiding core MHD of this sort when designing plasma scenarios suitable for the generation of high thermal fusion yield. The q-profile optimisation techniques used to maximise global performance in the JET hybrid experiments can also play a key role in minimising the impact of core MHD on fusion yield.

A further benchmark has been made of the CRONOS simulations. Here an interpretive TRANSP simulation was used to map the measured temperature and density profiles onto an equilibrium as a reference example. The measured density and rotation profiles, together with the temperature pedestal values, were used as inputs to the CRONOS simulations. The core temperature profiles were predicted using the Bohm/GyroBohm model with an ITB criterion based on a combination of magnetic and rotational shear. The initial q-profile was taken from the experiment and the time evolution was predicted using a poloidal field diffusion model. The CRONOS predictive simulation reproduces the core electron and ion temperature well, giving confidence for the extrapolation to high fusion yield conditions.

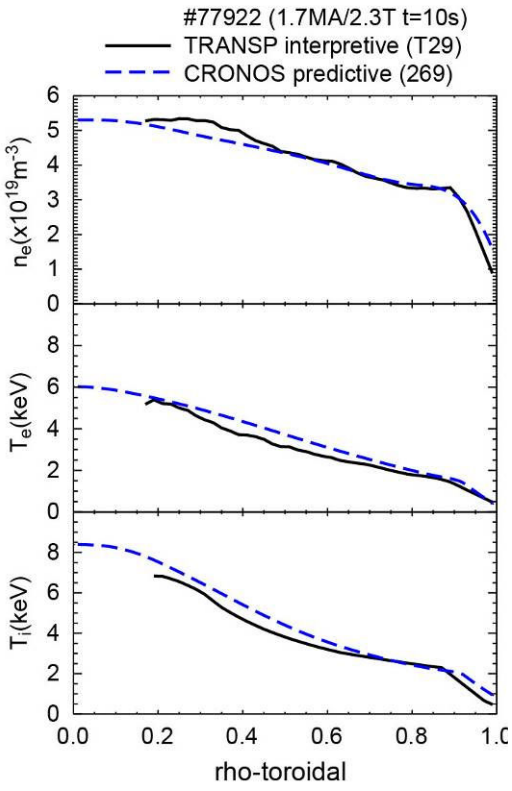

Fig. 4.10: Typical electron density, electron & ion temperature profiles for a high δ hybrid plasma using TRANSP (black) to map the measure profiles to $\rho_{toroidal}$ and CRONOS (blue) to predict the core temperatures from the density profile and temperature pedestal values.

4.3.3 Scaling projections of hybrid performance to DT

JETFUSE has been be used to map out the extrapolation domain by running simulations with different scaling assumptions, while TRANSP was used at points of particular interest to validate the JETFUSE predictions.

Compared to the reference case the JET EP2 beam upgrade will provide much higher beam power and JET can routinely operate with higher toroidal magnetic field values of B_T=3.45T or even as high as B_T=4T for a limited number of pulses. Hence it is desirable to extrapolate the achieved hybrid performance to these conditions where the fusion yield is expected to be much higher. Three reference cases have been used to extrapolate to hypothetical JET DT scenarios using the hybrid plasmas described in preceding sections:

- #75225 at t=6.5s : low δ hybrid with no n=1, 2 & 3 NTMs;
- #75225 at t=8s : low δ hybrid with a 4/ 3 NTM;
- #77922 at t=10s : high δ hybrid with no n=1, 2 & 3 NTMs.

It is assumed that the good confinement and stability ($H_{IPB98(y,2)}$~1.3 and β_N~3) of these reference plasma can be maintained for the most optimistic predictions (case A below), Z_{eff} is assumed to be conserved at the value determined from visible Bremmstrahlung measurements for the reference plasmas (1.73-2.12). Extrapolation to increased plasma current is represented in the following figures and tables as the mid-point of the range of values from these three hybrid reference cases, with the range expressed as an error bar.

The JETFUSE hybrid DT extrapolation was made by scanning the plasma current up to 4.1MA with the following assumptions.

- The toroidal field is increased with I_P (i.e. constant q_{95}) until B_T=4T, then I_p is increased at fixed B_T=4T.
- The following are conserved from the interpretive simulations of the reference plasmas:
  - plasma flux surface geometry;
  - n_e, T_e, T_i profile shapes, including the T_i/T_e ratio;
  - Z_{eff} & impurity composition.
- The density is scaled to either:
  - maintain $n/n_{Greenwald}$ constant;
  - maintain n_e constant.
- Power is scaled to maintain β_N until power limit reached assuming 34.8MW of NBI plus 5.2MW of extra heating (i.e. ICRH is assumed, but not modelled).
- The temperature is scaled to maintain $H_{IPB98(y,2)}$.
- No credit taken for α-heating.
- The EP2 DT NBI specifications are used (as described in section 4.2.1):
  - deuterium beams from NIB-4 with E_b=124keV, P_{max}=16.1MW;
  - tritium beams from NIB-8 with E_b=118keV, P_{max}=18.7MW.

The plasma current can be increased up to I_P~3MA at constant q_{95}, but above this current q_{95} decreases. Extrapolation of hybrid plasma performance to low q_{95} has been achieved at ASDEX Upgrade [Sips A.C.C. *et al* 2007 *Nucl. Fusion* **47** 1485] and DIII-D [Doyle E.J. *et al* 2010 *Nucl. Fusion* ***50*** 075005]. Access to good confinement and stability in this domain would need to be demonstrated on JET to validate the assumptions of these extrapolations.

Another key uncertainty in the extrapolation is the density dependence of confinement. It was shown in section 4.1.2 that the density in JET hybrid experiments tends to increase with plasma current at roughly constant β_N. The ELMy H-mode simulations already illustrate the problem of poor beam penetration at high density and analysis of recent hybrid experiments at JET has suggested that the density dependence may be much weaker than the IPB98(y,2) scaling law, perhaps closer to $\tau_E \propto n^{0.03}$ [F. Crisanti – JET TFS2 meeting 28/4/2010]. This could, indeed, be consistent with an effective loss of core torque and heating due to the effect of density on beam deposition. Since

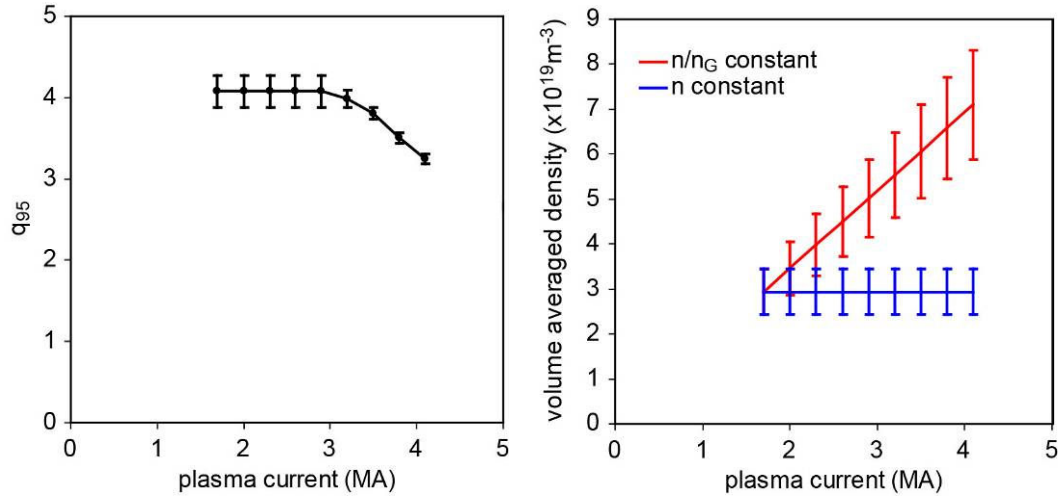

Fig. 4.11: q_{95} (left) and volume averaged density (right) versus plasma current for the hybrid extrapolations using JETFUSE. Two density assumptions: constant $n/n_{Greenwald}$ ((red); and constant n_e (blue) are illustrated. The error bars indicate the range of values due to the extrapolation from three separate reference cases.

hybrid plasmas have essentially no gas fuelling during the main heating phase, the density rise with plasma current is mainly due to increased recycling at the higher heating powers required to maintain β_N, and therefore was not easy to control with the carbon wall.

To take into account the uncertainty in the confinement dependence on density, the

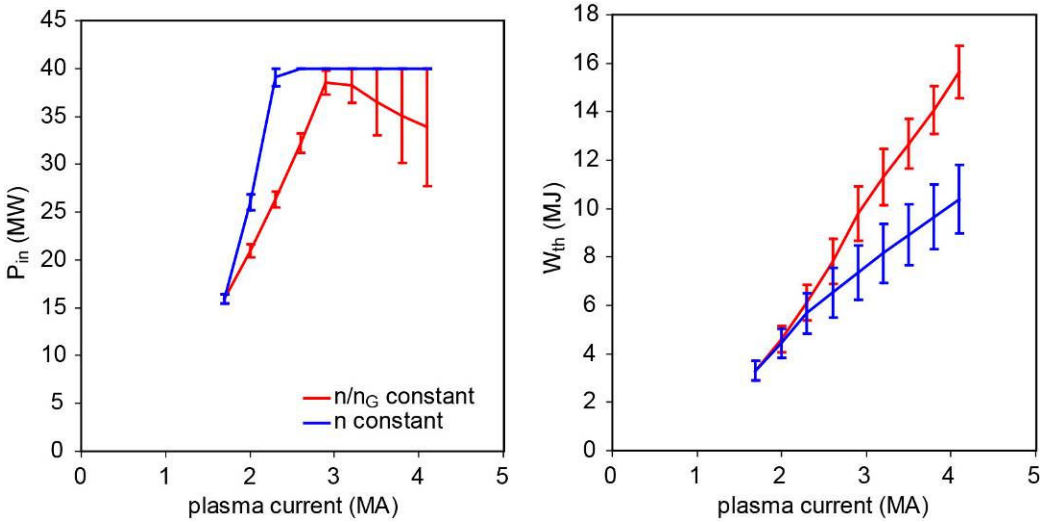

Fig. 4.12: Heating power required to maintain β_N (limited at 40MW - left) and thermal plasma stored energy (right) versus plasma current for hybrid extrapolations using JETFUSE. Two density assumptions: constant $n/n_{Greenwald}$ ((red); and constant n_e (blue) are illustrated.

hybrid reference plasmas were extrapolated to high plasma current with two density assumptions: constant $n_e/n_{Greenwald}$; and constant n_e. Simulations show that the assumption that n_e remains constant yields a similar fusion yield in the extrapolation to high plasma current as the assumption that $n/n_{Greenwald}$ remains constant, but that $\tau_E \propto n^0$. This is not surprising given that the global confinement time extrapolates identically to high plasma current under these two assumptions. So the results shown for constant density can be taken as indicative of the very weak density dependence of confinement suggested by the recent hybrid experiments.

The extrapolation shows a substantial difference in projected fusion performance at high plasma current depending on the assumed confinement scaling with density. Increasing plasma density with plasma current, as is seen in present experiments, and relying on the IPB98(y,2) scaling of $\tau_E \propto n^{0.41}$ yields a plasma stored energy at high plasma current that is 50% larger than the case where no density rise is assumed. This means that, in some cases, the assumed full available power of 40MW is not required to maintain β_N at high plasma current, whereas for the extrapolation without density increase the simulation becomes power limited at I_P~2.3MA.

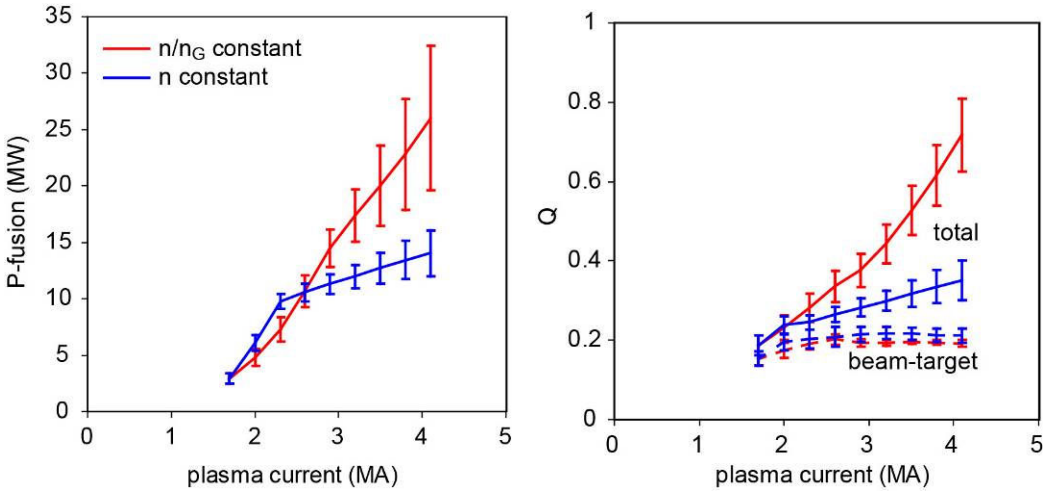

Fig. 4.13: Total fusion power (left) and Q (right) versus plasma current for hybrid extrapolations using JETFUSE. Two density assumptions: constant $n/n_{Greenwald}$ ((red); and constant n_e (blue) are illustrated. Q is shown for beam-target reactions (broken lines) and summed over all reactions (solid lines).

The fusion gain due to beam-target DT reactions saturates at $Q_{DT,beam\text{-}target}$~0.2 when the plasma current is significantly above 2MA. The effect of the discrepancy in the plasma stored energy due to the different density assumptions is amplified in terms of the fusion power giving a range of P_{fusion}~13-20MW at I_P=3.5MA and P_{fusion}~14-26MW at I_P= 4.1MA. This corresponds to a total fusion gain in the ranges Q_{DT}~0.32-0.53 and Q_{DT}~0.35-0.72 for the same plasma currents, respectively.

4.3.4 Predictive projections of hybrid performance in DT

Given the large uncertainty in the effect of density, TRANSP simulations were performed based on the high triangularity hybrid reference case (#77922 at t=10s). The plasma current and magnetic field were set conservatively at 3.5MA/3.45T and the heating was modelled only from neutral beams with the maximum expected DT power of 34.8MW. The density, temperature and toroidal rotation profiles were

conserved with the temperature being scaled to keep $H_{IPB98(y,2)}$ constant. The density was scaled to three values to provide a coarse density scan assuming:

- n conserved (low density);
- $n/n_{Greenwald}$ conserved (high density);
- intermediate density with (~1.5 times the density in the reference plasma).

The magnitude of the rotation was scaled assuming $\tau_\phi \propto \tau_E$.

The neutral beam deposition varies strongly over this density scan with relatively poor beam penetration to the plasma centre for the highest density case compared with a relatively peaked beam deposition profile for the lowest density case, which has unscaled density profile from the reference plasma. It is questionable whether the good core performance achieved in the JET hybrid plasmas could be maintained in circumstances where the core heating is very poor. So predictive modelling has been performed to assess the effect of the variations in beam deposition at different densities on the overall fusion performance.

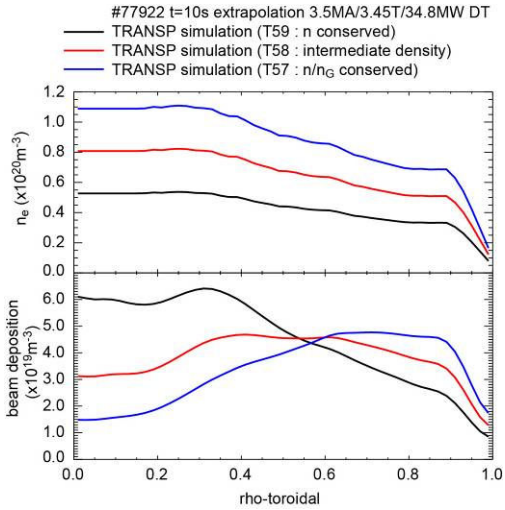

Fig. 4.14: Scaled density profiles for high triangularity hybrid extrapolation from 1.7MA to 3.5MA assuming: n conserved (black); $n/n_{Greenwald}$ conserved (blue); intermediate density (red). DT beam deposition profiles from TRANSP simulations are illustrated for each density assumption.

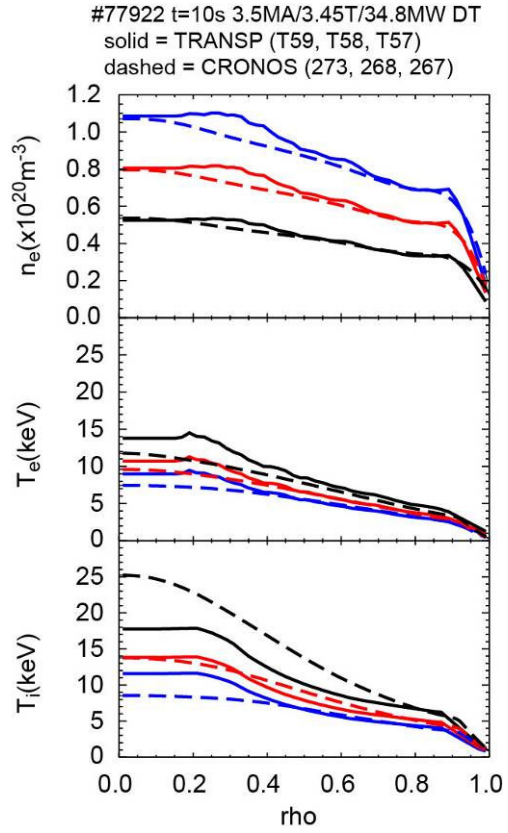

Fig. 4.15: Scaled density profiles for high triangularity hybrid extrapolation from 1.7MA to 3.5MA assuming: n conserved (black); $n/n_{Greenwald}$ conserved (blue); intermediate density (red). Temperature profiles are scaled assuming $H_{IPB98(y,2)}$ (solid lines – TRANSP) and predicted taking the temperature inside the pedestal as a boundary condition (broken lines – CRONOS).

Three CRONOS simulations have been performed to match the coarse three point density scan at 3.5MA/3.45T simulated using TRANSP. The density was scaled in the same way as for each of the three TRANSP simulations (the slight profile differences may be due to different techniques for mapping the measured profile data onto the model equilibria). The electron and ion temperature just inside the pedestal are taken from the TRANSP scaled simulations and applied in CRONOS as a boundary condition for the predictive transport simulation using the Bohm/GyroBohm model coupled with

an ITB model with a combined magnetic and rotational shear threshold, as described above. The plasma toroidal rotation profile was taken directly from the reference plasma in the CRONOS simulations and the initial q-profile was scaled from the reference plasma to match q_{95} at 3.5MA/3.45T.

At the intermediate density the TRANSP scaled temperature profiles are comparable to the predicted CRONOS profiles. At the highest density the poor beam deposition results in a reduction in the temperature peaking in the CRONOS predictive simulations, supporting the concern expressed above that the good core performance of the existing hybrid experiments might be difficult to extrapolate to high density with the JET NBI system. At the lowest density the CRONOS simulation generates a hot-ion core plasma with a peaked ion temperature profile that is quite favourable for fusion performance.

The fusion yield for the CRONOS simulations was calculated using JETFUSE. The variation in total fusion power with plasma density is systematically different for the CRONOS scan with predicted temperature profiles and the TRANSP scan using scaled profiles. The fusion yield increases with density in the case of the scaled profiles because of the $\tau_E \propto n^{0.41}$ dependence in the IPB98(y,2) scaling assumed. The fusion yield is substantially reduced at high density in the predictive simulation because of the loss of ion temperature peaking produced by the poor beam penetration. On the other hand, the increased ion temperature peaking and the generation of a hot-ion plasma core at low density results in a higher fusion yield than was achieved in the scaled simulation.

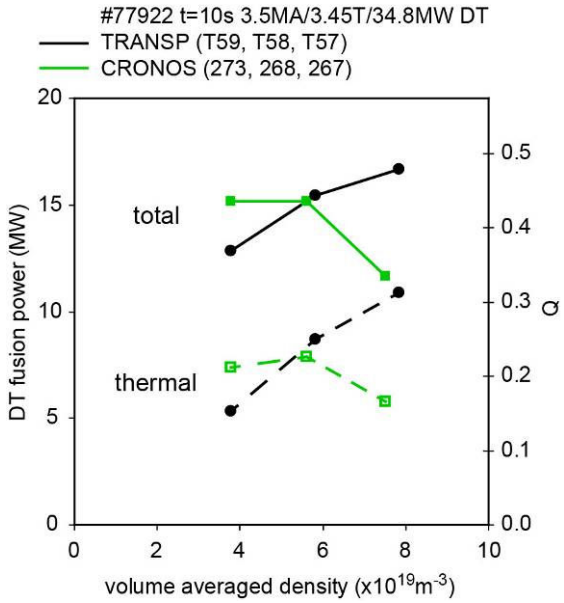

Fig. 4.16: Total and thermal fusion yield for the simulated density scan at 3.5MA assuming: scaled density and temperature profiles to conserve $H_{IPB98(y,2)}$ (black – TRANSP); scaled density and predicted core temperature assuming the same pedestal conditions (red – CRONOS).

The fusion gain obtained from the CRONOS simulations at intermediate and low density was Q_{DT}~0.44, which is close to the middle of the range obtained from the JETFUSE analysis (Q_{DT}~0.32-0.53) in section 4.3.3 at the same value of plasma current.

It should be noted that, although an ITB model was used in the CRONOS simulations, neither the toroidal rotation nor the q-profile have been optimised to maximise the effect of this feature. The rotation was taken directly from the reference plasma, which is pessimistic for the low density case since the power (and torque) is much higher in the extrapolated plasma while the density is the same. The q-profile was scaled to lower q_{95}, whereas experimentally one might try to broaden the current density profile to maintain q_0 close to unity while reducing q_{95}. This would have the effect of reducing the magnetic shear compared with the simulations presented here.

Further work is in hand to assess the effects of further optimisation in both of these directions.

4.3.5 Prospects for Q_{DT}~1

It is possible to estimate the approximate level of plasma performance that would be required to generate high Q_{DT} in JET on the basis of the extrapolations described above. JETFUSE has been used to scan the requirements for Q_{DT}~1 in terms of plasma current and $H_{IPB98(y,2)}$. The density and temperature profile shapes were taken from the high triangularity hybrid pulse #77922. The simulations assumed a magnetic field of 4T and 25MW of DT neutral beam power. The volume averaged density was set to $5.6 \times 10^{19} m^{-3}$, which was the mid-point of the density scan from section 4.2.4. Two cases were simulated: one with the same ratio T_i/T_e as the original plasma; and one with the same pressure profile shape, but with $Ti=T_e$.

The results show that, to obtain Q_{DT}~1, it would be necessary to achieve H_{98}~1.55-1.8 at high plasma current (at 4MA). This would represent an increase in normalised confinement by a factor of almost 2 compared with the recent ELMy H-mode experiments at high plasma current, also necessitating the achievement of MHD stability at higher β_N and compatibility with the ILW.

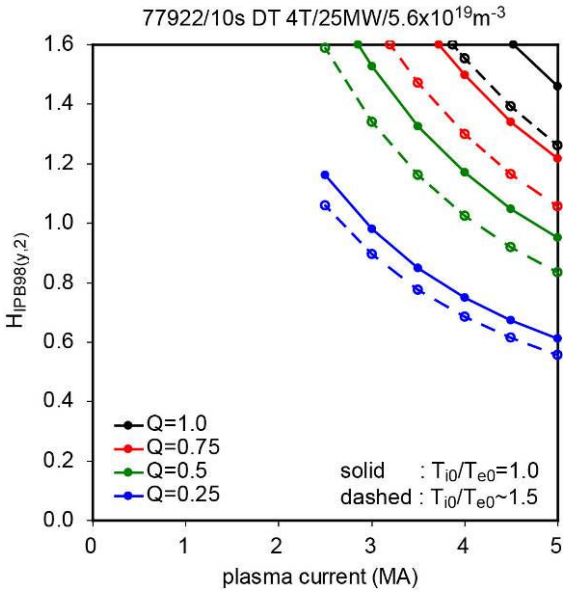

Fig. 4.17: Contours of $Q_{DT,total}$ as a function of plasma current and $H_{IPB98(y,2)}$ for density and temperature profiles from a high triangularity hybrid reference case assuming: T_i/T_e from the reference plasma (broken lines); $T_i=T_e$ (solid lines).

Further simulations are required to assess any potential benefits of the high torque capability of the EP2 NBI upgrade, but even if the recent improvements in $H_{IPB98(y,2)}$ of JET hybrid plasmas could be extended to high plasma current, the projected fusion yield would not reach the required level for Q~1. Therefore proposals for a future JET DT campaign should be assessed on the basis of more modest projections from existing experiments such as those discussed above.

4.3.6 Projections for β_α

Projections in terms of the achievable β_α are subject to considerable uncertainty. In addition to the uncertainty in the fusion yield, which affects the α-particle source rate, β_α is sensitive to the α-particle slowing-down time, which depends on the plasma density and temperature, as well as fast ion orbit effects and any anomalous transport mechanisms.

To illustrate the approximate values that could be expected if the improved confinement of the JET hybrid plasmas could be extrapolated to high plasma current,

the value of β_α at the plasma centre has been obtained from TRANSP using the simulated density scan discussed above. These simulations assume no anomalous fast ion redistribution. The simulation at the intermediate density gives a value of $\beta_\alpha(0)$~0.35% and higher values are indicated at lower density. Clearly the question of density control and compatibility of low density plasmas with the ILW should be assessed in future deuterium experiments to allow a more robust estimate of the potential β_α that could be achieved in JET. The DT simulation at I_P=1.7MA using the original unscaled temperature and density profiles is shown for reference.

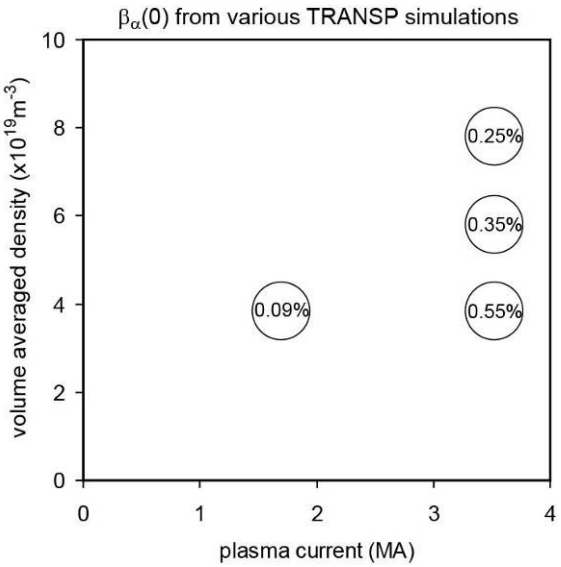

Fig. 4.18: Values of $\beta_\alpha(0)$ as a function of plasma current and volume averaged density for the high triangularity hybrid reference pulse #77922 at 1.7MA and the density scan extrapolated to 3.5MA.

4.3.7 Summary of results of hybrid extrapolation

The recent improvements in plasma confinement in JET hybrid plasmas provide a valuable basis for extrapolation to high fusion gain plasmas in DT. If it were possible to maintain the normalised performance (i.e. H_{98}, β_N, T_i/T_e, $p_o/\langle p\rangle$, etc.) at high plasma current (i.e. $I_P \geq 3.5$MA) then the simulations indicate the possibility to achieve fusion gain in the region of Q_{DT}~0.4-0.5, which is a factor of two larger than was projected for ELMy H-mode plasmas at high current in section 4.1.

However, compared with ELMy H-mode plasmas, there are significant uncertainties associated with this extrapolation which would have to be addressed during deuterium operation before a DT campaign. It should be noted that, in the recent JET campaigns, maintaining the good normalised performance achieved in the initial low current hybrid experiments to higher plasma current and magnetic field was not easy. However, higher beam power is expected due to the EP2 NBI upgrade, which will be a valuable tool for optimising performance at high plasma current and magnetic field provided that conditions for good core beam deposition can be achieved. For this reason density control is likely to be a key issue for the optimisation of fusion yield for the hybrid scenario. In the reference experiments the plasma shape had a significant influence on the density of hybrid

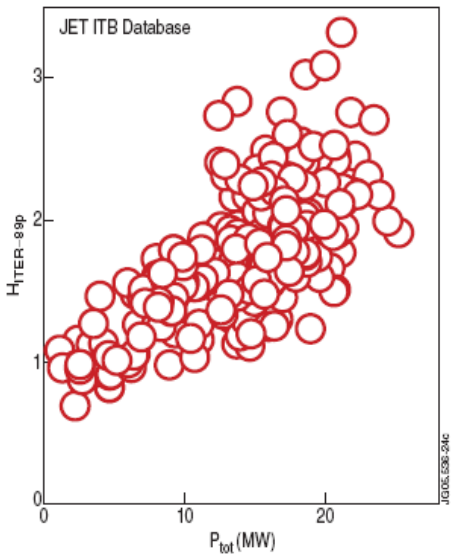

Fig. 4.19: $H_{ITER89L\text{-}P}$ versus heating power for a JET ITB database at B~3.45T, q_{95}=4.5-6.5, δ~0.2, n_l=2-4×$10^{19}m^{-3}$. [from Litaudon X. *et al* 2007 *Nucl. Fusion* **47** 1285*]*

plasma, but an investigation of the effect of the ILW on the density behaviour of these plasmas will be necessary to determine the accessible domain of operation. As with the ELMy H-mode, a key source of uncertainty is the effect of measures required to achieve compatibility with the ILW. This point is discussed further in section 4.5.

4.4 DT fusion yield projections for AT scenarios

In previous JET campaigns it has been noticed that the energy confinement time of plasmas with internal transport barriers generally improves compared with the ITER89L-P L-mode scaling as the input power to the plasma is increased. This led to a predictive analysis of the potential performance of JET experiments to deuterium ITB plasmas at high plasma current, magnetic field and heating power, which was published in [Litaudon X. *et al* 2007 *Nucl. Fusion* **47** 1285]. These simulations concentrated on the goal of a fully non-inductive demonstration on JET and relied heavily on the use of LHCD to shape the q-profile. Although the LHCD power assumed in the modelling was high compared with that presently available at JET for routine operation in ELMy plasmas, the results of the simulation still give an impression of the fusion performance that could be expected if an ITB could be sustained at large plasma radius for some fraction of a resistive time. The JETTO simulations presented in this section were performed by João Bizarro.

4.4.1 Benchmark of AT simulations

The AT scenario modelling benchmark using JETTO is described in [Litaudon X. *et al* 2007 *Nucl. Fusion* **47** 1285]. The key boundary conditions used were the initial q-profile and the values of temperature and density at the edge pedestal. The core temperature, density and toroidal rotation profiles were predicted using a Bohm/GyroBohm model coupled with an ITB model based on a threshold condition in terms of magnetic shear and ω_{ExB} flow shear, as described in [Tala T. *et al* 2006 *Nucl. Fusion* **46** 548] and assuming $\chi_\phi=0.3\chi_i$. The current density profile was evolved assuming neoclassical resistivity and bootstrap current and various externally driven non-inductive current sources.

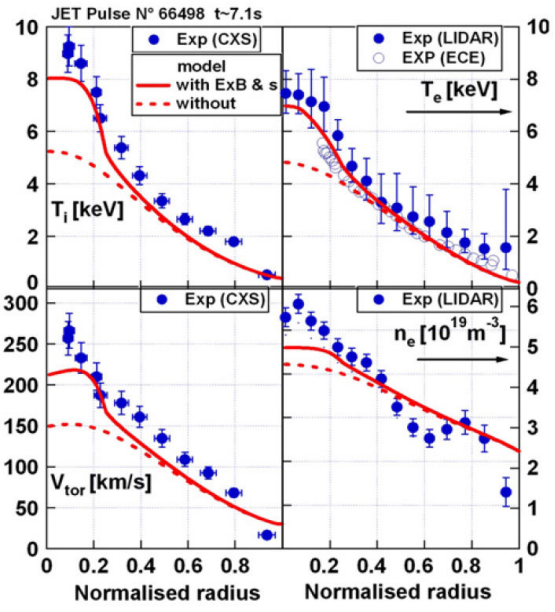

Fig. 4.20: Experimental (closed symbols) and simulated T_i, T_e, n_e and V_{tor} profiles of the JET pulse #66498 using the Bohm/Gyro-Bohm model with either the combined E × B and magnetic shear stabilization effects for the ITB formation (full line) or without (dashed line). [from Litaudon X. *et al* 2007 *Nucl. Fusion* **47** 1285*]*

The benchmark simulation was made for JET AT pulse #66498 at 1.9MA/3.1T with 27MW of additional heating power. The simulation shows good agreement

for the temperature, density and rotation profiles. However, if the ITB model is turned off, the simulation underestimates the core peaking on all transport channels.

4.4.2 Predictive projections of AT performance in DT

Predictive simulations have also been made using JETTO for AT plasmas at JET using the same plasma model as for the benchmark case. These simulations are described in [Litaudon X. *et al* 2007 *Nucl. Fusion* **47** 1285].

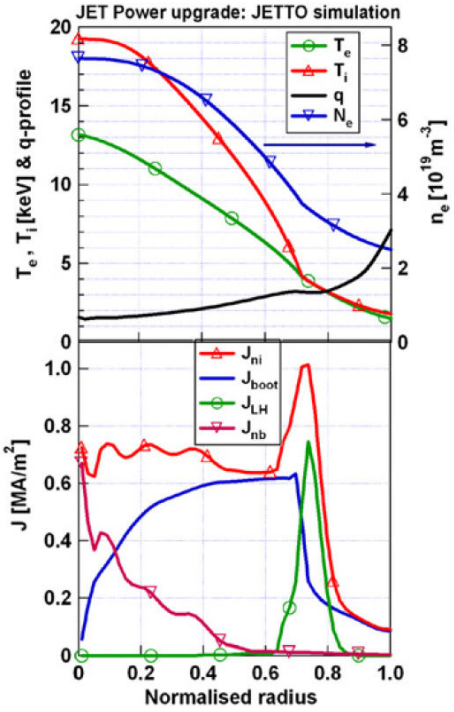

Fig. 4.21: Simulated T_i, T_e, n_e, q and non-inductive current profiles of a fully non-inductive JET plasma at 2.3MA/3.5T with P_{tot}=45MW (P_{LHCD}=3MW, P_{ICRH}=10MW, P_{NBI}=32MW). [from Litaudon X. *et al* 2007 *Nucl. Fusion* **47** 1285*]*

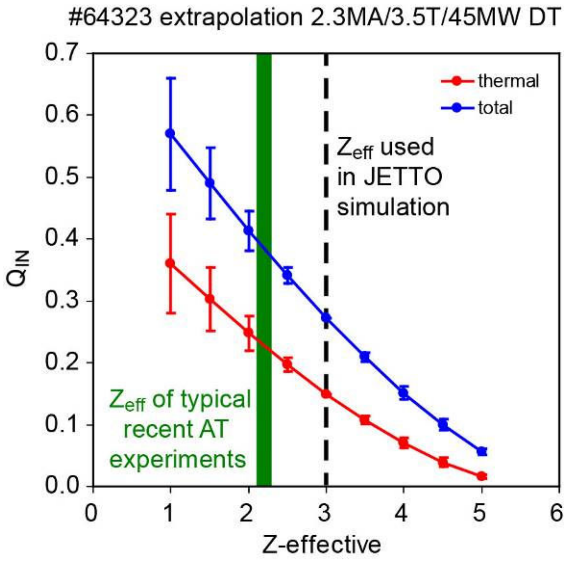

Fig. 4.22: Q_{DT} total (blue) and thermal (red) based on a JETTO predictive AT plasma simulation at 2.3MA/3.5T with 45MW of heating power. Z_{eff} was varied in JETFUSE where the fusion yield calculated. n_e was conserved and the error bars indicate the result of additionally conserving either temperature or $W_{thermal}$ while varying Z_{eff}.

The extrapolation has been made to 2.3MA/3.5T with 45MW of additional heating power (P_{NBI}=32MW; P_{ICRH}=10MW; P_{LHCD}=3MW) based on a deuterium plasma, #64323. In this case the density at the edge pedestal was chosen to be $2.5x10^{19}m^{-3}$ and the pedestal temperatures were chosen so that the simulation achieved H_{98}~1 with the ITB model turned off ($T_{i,ped}$=1.8keV and $T_{e,keV}$=1.5keV). $Z_{effective}$ was set at 3. The ITB criterion was met in the model by using LHCD to provide a low magnetic shear region at ρ~0.7. This provided the ITB at large radius that is favourable for good global confinement.

The simulation shows an intermittent ITB at this level of LHCD power. The model predicts that the ITB can be stabilised with higher LHCD power (P_{LHCD}~6MW) [see Bizarro J.P.S. *et al* 2007 *Nucl. Fusion* **47** L41]. Such a high LHCD power is unrealistic for the present JET LHCD system but, with good launcher conditioning and coupling optimisation, power levels of 3MW or above could be envisaged.

During the ITB phase of the simulation described above the ITB at ρ~0.7 generates a significant confinement improvement, resulting in H_{98}~1.7 and β_N~2.8.

JETFUSE has been used to estimate the potential fusion yield that could be expected if it were possible to produce an ITB of the sort generated in the JETTO simulation. The temperature and density profiles were taken from the JETTO predictive simulation at the time when the intermittent ITB is present. The deuterium beams and plasma were changed to DT using the EP2 NBI specification. No credit was taken for any mass scaling effects of α-heating power. The JETFUSE calculation yields a total fusion of ~12.3MW, which corresponds to Q_{DT}~0.27, and the thermal fusion yield was 6.7MW.

Since $Z_{effective}$=3 is significantly higher than the value typically obtained in recent JET AT experiments, a scan was made over a range of $Z_{effective}$ values using JETFUSE to see if higher values of fusion gain could be achieved by modelling a plasma with lower dilution. In these simulations the dominant impurity was assumed to be carbon.

The $Z_{effective}$ scan shows a significant improvement for plasma simulations at a level more typical of recent AT experiments ($Z_{effective}$~2.2), giving a total fusion gain of Q_{DT}~0.38. In this case the total fusion power was ~17MW with ~10MW due to thermal reactions.

4.4.3 Summary of results of AT extrapolation

Despite recent progress in terms of access to good confinement and stability in the development of advanced tokamak plasmas in JET, the basis for extrapolation to DT plasmas with high fusion gain remains uncertain. The levels of $H_{IPB98(y,2)}$ and β_N achieved now approach the values obtained in hybrid plasmas at JET, and predictive simulations have been performed to investigate the potential plasma performance if the high input power available from the EP2 neutral beams were to produce ITBs at large plasma radius (ρ~0.7) giving access to $H_{IPB98(y,2)}$~1.7. If it were achievable, such a plasma is predicted to generate $Q_{DT,total}$~0.27-0.38 at β_N~3 using 45MW of heating at 2.3MA/3.5T. However, such a high normalised confinement has not previously been maintained in steady condition at JET and plasmas with steep temperature and density gradients due to ITBs can also be limited in terms of fusion performance due to MHD instabilities [see Challis C.D. *et al* 2002 *Plasma Phys. Control. Fusion* **44** 1031] and impurity accumulation [see Dux R. *et al* 2004 *Nucl. Fusion* **44** 260].

It should be noted that the predictive AT simulation discussed above was originally optimised for fully non-inductive current drive rather than high DT fusion gain, leaving open the possibility to increase the plasma current in order to mitigate the need for such a high normalised confinement. The achievement of $Q_{DT,equivalent}$~0.4 has been reported from earlier JET deuterium ITB experiments at high plasma current (3.4MA/3.4T), although the duration was limited to ~1s [see Gormezano C. 1999 *Plasma Phys. Control. Fusion* **41** B367]. It is considered, therefore, that $Q_{DT,total}$~0.4 represents an upper limit on the range of uncertainty for ITB scenarios. In terms of presently available plasma scenarios, the estimated $Q_{DT,equivalent}$ for recent JET AT plasmas at much lower plasma current (1.8MA/2.7T) is of the order 0.1-0.14 maintained for ~5s.

Further experiments in deuterium with the EP2 neutral beam power upgrade would be required to investigate the potential for AT plasmas at high Q. It should be noted that ITBs in JET AT experiments are commonly associated with rational q-surfaces, which calls for a different approach in terms of ITB location control that the magnetic shear control suggested by the transport model used for the simulations above. As with the other plasma scenarios, a key source of uncertainty is the effect of measures required to achieve compatibility with the ILW. This point is discussed further in section 4.5.

Despite being the extrapolation with the greatest uncertainty of the three plasma scenarios in terms of possible fusion yield and potential for sustainment, it may be of interest for AE investigations due to the potential for significant alpha pressure in the plasma core with $q_{minimum}$ above unity.

4.5 Uncertainties and conclusions

As mentioned in the sections above, a key uncertainly for the extrapolation of all plasma scenarios is the impact of measures that may be needed to achieve compatibility with the ILW. These could include ELM mitigation techniques, gas puffing to raise the pedestal density to avoid tungsten sputtering from the divertor, impurity seeding to reduce the divertor heat load between ELMs and disruption mitigation or avoidance. Previous experiments on JET have suggested that all of these techniques can degrade the plasma performance.

It is not clear at this point precisely what measures will be required. The accumulation of tungsten in a tokamak with a tungsten divertor and beryllium main chamber wall has not been investigated experimentally and the performance of the JET ILW divertor has not yet been characterised. For this reason it is not clear how to account for these effects in the modelling at this point. It will be necessary, therefore, to investigate the impact of compatibility with the ILW on plasma scenario performance at high plasma current and heating power during the forthcoming deuterium campaigns in order to re-evaluate the performance potential of all plasma scenarios for DT operation.

There are also uncertainties in the potential DT performance of the different plasma scenarios in terms of extrapolation to high plasma current. This extrapolation is most robust for ELMy H-mode plasmas because examples already exist in the JET database. However, further work is required to assess the prospects for robust $H_{IPB98(y,2)}$~1 operation at the highest plasma currents and the potential to reduce the plasma density. The possibility that the performance of the hybrid scenario could be approached as an optimisation from the existing high current ELMy H-mode plasmas rather than the lower plasma current hybrid examples should not be over-looked.

In order to assess the validity of the extrapolation assumptions used for the hybrid scenario it will be necessary to perform extensive scenario development using deuterium plasmas with the EP2 NBI upgrade. In particular, the following points should be addressed:

- development of high current hybrid scenario (including the optimisation of plasma shape within coil limits, disruption risk, etc.);

- confinement enhancement at low q_{95} (including q-profile tailoring without current overshoot, avoidance of NTMs, effect of sawteeth, β-limits, etc.);
- density scaling & optimisation (including density control and compatibility with ILW, effect of NBI deposition, T_i/T_e, rotation, etc.).

The uncertainties are greatest for the advanced tokamak scenarios due to the complex interplay between current drive, transport physics and MHD stability. Also the lower density often assumed for AT scenarios to maximise non-inductive current drive may increase the uncertainty in term of ILW compatibility. Nevertheless, the potential use of these plasmas for DT experiments concerning the stability of AE modes agues that they should evaluated for use in a DT campaign.

Further simulations should be performed to reduce the uncertainty in the extrapolation of fusion performance, taking into account the results from new JET experiments with the ILW. In this report simple scaling projections have been supported by predictive simulations using a Bohm/GyroBohm model coupled with an internal transport barrier model based on a threshold condition in terms of magnetic shear and ω_{ExB} flow shear. While this predictive approach describes the reference plasma conditions well, the possibility to use alternative transport models should be considered.

5. Isotope effects (H, D, T)

5.1. Access to H mode
5.2. Energy confinement scaling
5.3. Dependence of pedestal characteristics and ELMs on isotope composition
5.4. Local transport physics
5.5. Fuelling and density limit issues
5.6. Isotope effect on current ramp and Internal Transport Barriers (ITB's)

Key points:

Dedicated experiments in hydrogen, deuterium, tritium and deuterium-tritium mixtures would provide key results for:

- Isotope mass scaling for energy in stationary ELMy H-mode, hybrid & advanced scenarios.
- Separation of isotope scaling into pedestal and core components.
- Isotope mass scaling for H-mode transition with the ITER-like Wall and in ITER-relevant plasma conditions.
- Isotope mass scaling for ELM size & frequency.
- Test of ELM mitigation techniques in T and DT plasmas, complemented with data for hydrogen, deuterium and helium.
- An assessment of control requirements (including MHD) with different isotope mixtures.

No data are available from previous DT campaigns at JET on the isotope dependence of performance in hybrid scenarios and advanced scenarios being prepared for ITER.

The dependence on isotope composition of the L-H transition, the confinement time and possibly the density limit are of high importance for the performance of ITER. In particular, there is evidence of a strong dependence of pedestal transport on hydrogen isotope composition, which calls for detailed investigations using the much improved pedestal diagnostics JET is now equipped with. We therefore propose to conduct isotope campaigns in hydrogen and pure tritium (and hydrogen-tritium mixtures) before a DT campaign. Those campaigns would be preceded by reference discharges and scenario development in deuterium. In addition to providing isotope scaling results, the isotope campaigns would allow anticipating the effects of isotope composition on discharge evolution in DT, thereby cutting the fraction of the neutron budget spent on scenario adjustments during the DT campaign.

In the following sections we discuss the necessity of improvement over DTE1 on the basis of published DTE1 results in ELMy H-modes. Many of these would today not be considered as stationary, having strongly rising densities throughout the heating phase. There were also very few pure tritium discharges in DTE1 because of the fear that wall pumping and retention would lock away too much of the precious isotope. A future isotope campaign should allocate a generous campaign for pure T (and H-T mixtures), assuming prior gas balance measurements do not indicate an unexpectedly high retention.

5.1 Access to H mode

The figure below (Fig. 5.1, left) shows slow NBI power scans for an H, a D, a DT and a T plasma for establishing the L-H threshold (Jacquinot, Nucl. Fusion 39 1227). The threshold powers range from 1.7MW in T to 3.8 MW in H. The latter also has a soft, dithering transition. The right figure of Fig. 5.1 shows the threshold power scaling obtained from DTE1 data, which includes a mass exponent of -0.9 (Righi, NF 39, 1999 p309). Closer examination of the figure suggests that with ICH heating (i.e. electron heating, open symbols) the inverse mass scaling may be even stronger. At the transition, the pedestal electron temperature, believed to be a key transition parameter, was seen to decrease with ion mass as $M^{-0.6}$.

The transition form the type III ELMy H-mode to the type I ELMy H-mode regime, which has better confinement, typically occurred about 30% above the threshold, except with hydrogen plasmas, where this transition was not always found.

The L-H transition is very sensitive to vessel conditions and results may be different in an all-metal vessel. This provides a strong incentive for revisiting the threshold scaling in an isotope campaign. Transition physics can and should now be addressed with improved and new edge diagnostics, such as HRTS, the Li-beam, the poloidal CXRS system and the profile reflectometer. Moreover the experiments should be extended to ITER-like conditions, i.e. with a larger fraction of electron heating, low rotation and spanning a larger range of densities.

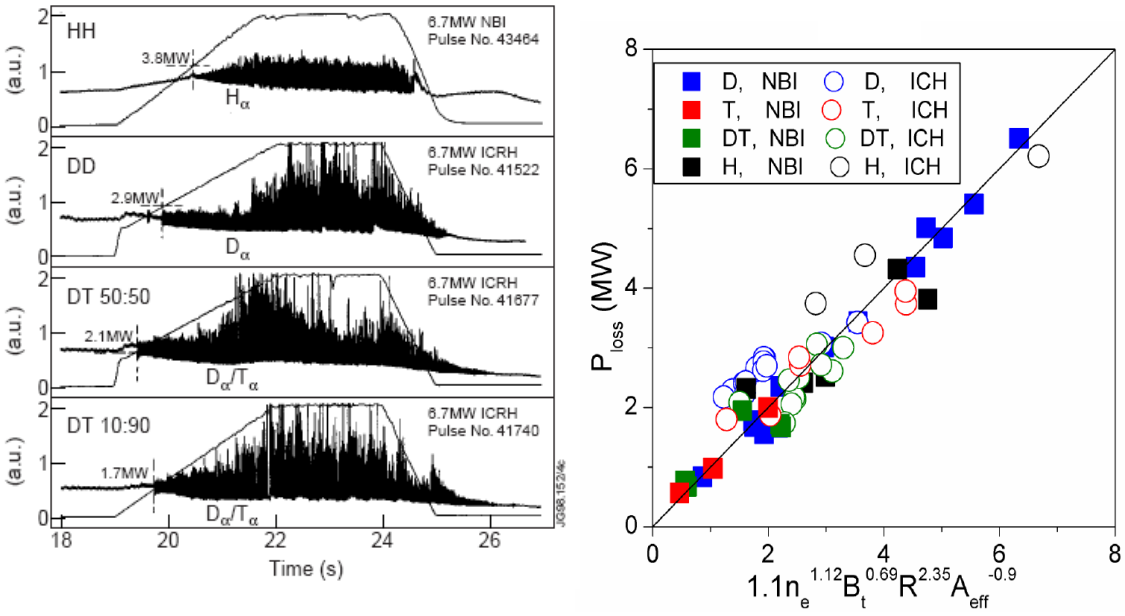

Fig. 5.1: Left: L-H transition studies at 2.6T/2.6MA (Jacquinot, NF, 1999).
Right: Scaling of L-H threshold in DTE1 plasmas (Righi, NF 1999).

5.2 Energy confinement scaling

The bulk of the ELMy H-mode confinement data from the DTE1 experiment turned out to be consistent with the pre-existing IPB97(y,2) multi-machine scaling law, which has a mass scaling $\tau_E \propto M^{0.2}$ (Cordey et al, NF 39, 1999, p 301. ELM-free scaling results will not be addressed in this report). This is still essentially the same in the latest recommended ITPA scaling law IPB98(y,2). When the DTE1 dataset was restricted to pairs of similar discharges, this scaling essentially disappeared with $\tau_E \propto M^{0.03}$ (Fig. 5.2).

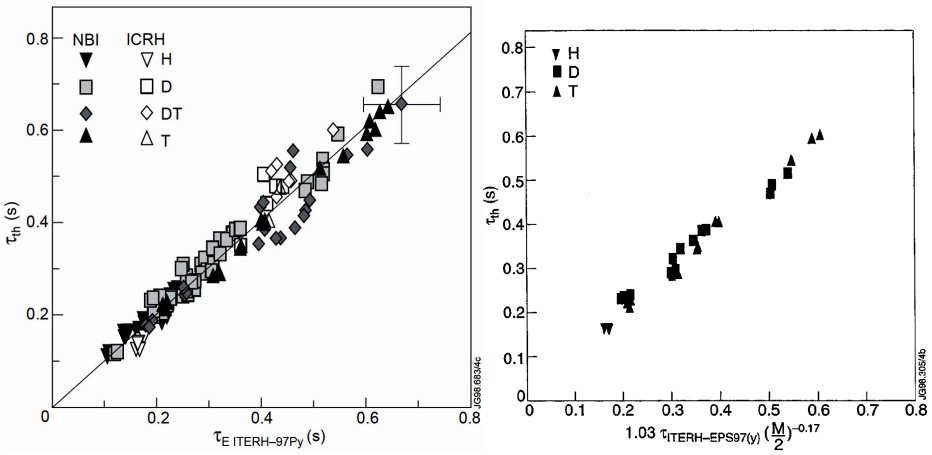

Fig. 5.2: Left: Experimental thermal confinement time in DTE1 JET ELMy H-modes versus IPB97(y,2) scaling. Right: Same for restricted set of matched pairs versus corrected scaling, implying $\tau_E \propto M^{0.03}$ (Cordey et al, NF,1999).

Table 5.I shows the mass scaling of global confinement for several empirical studies, as well as for the Bohm and GyroBohm expectations.

Scaling	year	Mass exponent	
IPB97(y,2)	1997	0.2	Multi-machine
IPB98(y,2)	2007	0.19	Multi-machine
DTE1 reduced	1999	0.03	Matched pairs
DB3v13 (ITPA)	2005	-0.04 to +0.16	Multi-machine 1.83<M<2.17
Bohm		0	theory
GyroBohm		-0.2	theory

*Table 5.I: Mass scaling exponents from several scaling laws. DB3v13 was reported by Cordey et al, Nucl. Fusion **45** (2005) 1078.*

A detailed analysis of the international database in 2005 provided exponents in the range -0.04 to 0.16, depending on data selection and regression techniques, albeit in a narrow range of effective isotope mass. Overall, this leaves us with an uncertainty of 0.2 for the mass exponent. An uncertainty of 0.2 may seem small, since it translates in an uncertainty of only 4.6% in confinement time when extrapolating from M=2 to M=2.5. However it translates into an uncertainty of approximately 30% on Q for a burning device with a target Q of 10. We should point out that the above empirical confinement scalings are for ELMy H-modes only, i.e., there is an urgent need to establish databases and scalings for the increasingly attractive hybrid and AT regimes too, which will have to include isotope dependencies.

Two term confinement scalings were also undertaken, motivated by observations of particularly high pedestal pressures in T plasmas. Fig. 5.3 (left) shows that the core confinement time is some 10% less in T than in D. Pedestal data on the right of Fig. 5.3 were used to argue that pedestal confinement time may scale as strongly as proportionally to M. This result is at odds not only with Bohm and GyroBohm scaling, but also with our understanding of profile stiffness. The dataset underlying this result is unfortunately very small and vulnerable to errors and the data leave much to be desired because of the hypothesis that pedestal ion and electron temperatures are equal and particularly because of the poor resolution of the LIDAR Thomson scattering (15cm) and CXRS systems (9cm) at the time, making an accurate separation of core and pedestal contribution very difficult. Nonetheless, there is compelling evidence of a significant positive scaling of the pedestal confinement with ion mass, even if the exponent remains very uncertain.

The two term scaling approach was revisited in 2002 (Thomsen et al, PPCF 44, 2002, A141) on a multi-machine database, yielding small positive exponents for both core confinement (0.2) and pedestal confinement (0.13). The authors however noted that the database quality was severely limited by poor data conditioning and data quality. JET is now in an excellent position for creating a high quality confinement and profile database suitable for separating core and pedestal contributions using the HRTS Thomson scattering system and an improved CXRS diagnostic. The scaling of turbulent spectra (scales and frequencies) with isotope species would be valuable for comparisons with theory and could be undertaken using correlation reflectometry, correlation ECE and the fast pulsed profile reflectometer.

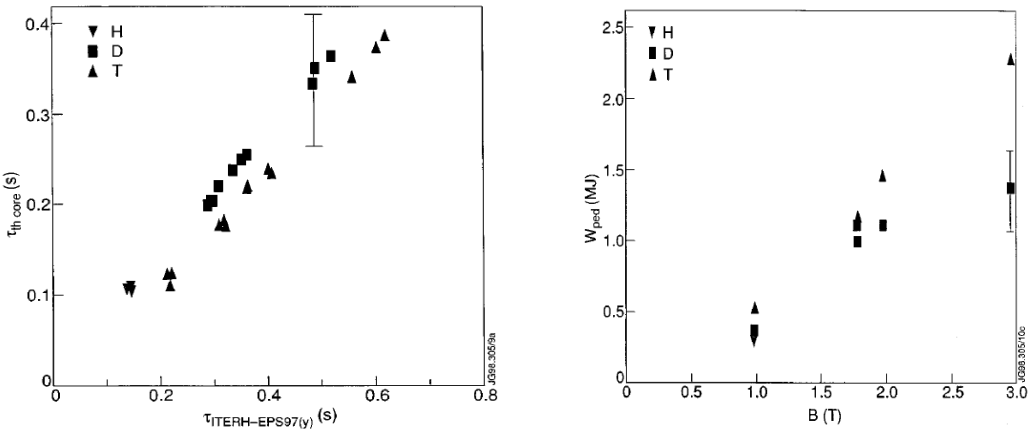

Fig. 5.3: Left: Core thermal stored energy in DTE1 ELMy H-modes versus IBB97(y,2) scaling. Right: Pedestal energy in a B_T scan at fixed q_{95} for matched power within the dataset on the left (Cordey et al, NF, 1999).

Although not reflected in any of the accepted scaling laws, it is of general notoriety in the experimental plasma physics community, that H-mode performance improves when the threshold for the L-H is significantly exceeded, allowing access to the type I ELMy regime. Fig. 5.4(left) shows the confinement improvement factor of the H89 (L-mode) scaling as a function of power for the three species (Righi, NF 39, 1999, p309). For each species, the lowest power points shown are obtained just after the L-H transition. The H89 factor approximately doubles as the ratio P_{loss}/P_{thres} doubles for D and T, but barely improves for H.

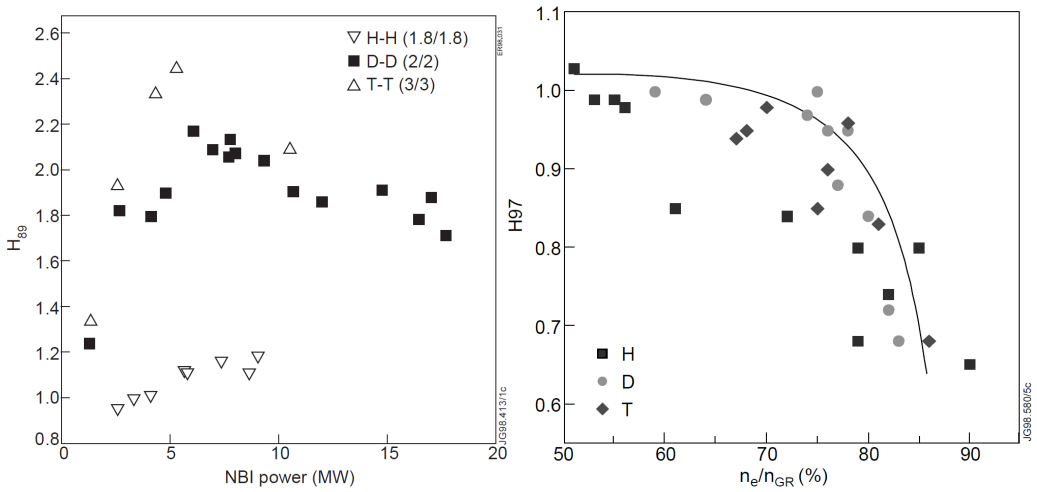

Fig. 5.4: Left: Dependence of H89 factor on NBI power for H, D and T (Righi, NF, 1999). Right: Dependence of H97 factor on normalised density (Saibene, NF 1999).

An additional difference is that in those cases where hydrogen H-modes achieved H97 factors near unity, they only did so at low densities (Fig. 5.4 (right), Saibene, NF 39, 1999, 1133), H97 dropping rapidly at higher densities. As the Greenwald limit was approached, the performance of all three isotopes was similarly poor. Confinement time and ELM amplitudes also strongly depended on fuelling (dropping with strong fuelling) and triangularity (increasing with triangularity, Saibene, NF 39, 1999, p1133). This behaviour is likely to change in the recycling conditions of the new

metallic ILW, the higher triangularity of the recently developed 'ITER-like' plasma shape, as well as thanks to the higher NBI power now available (16MW for H, against 10MW for H in DTE1), justifying a revisit of these issues.

The DTE1 campaign was dominated by transient hot ion ELM-free H-modes (not addressed in this report) and ELMy H-modes, albeit often not nearly as stationary as achieved in more recently. However the mission of future experiments should go well beyond revisiting unsatisfactory or incomplete experiments in DTE1. Future isotope campaigns and DT experiments should not only focus on confinement and transport in the ELMy H-mode, but aim at qualifying all scenarii of ITER interest, i.e. the advanced and hybrid scenario and if possible on JET, the advanced inductive scenario, which has been demonstrated in AUG and DIII-D with far better performance than the baseline ELMy H-mode.
Assuming meaningful electron heating power (LHCD, ECRH, ICRH) will be available in addition to the upgraded NBI, the effect of the electron/ion power ratio should also be assessed, as this would help extrapolating towards ITER conditions, where electron heating is dominant and plasma rotation is reduced compared to existing NBI dominated devices.
Since most of the isotope confinement experiments are not expected to require operating at maximum device parameters, there is considerable flexibility in adapting them to the operating space of JET in its new configuration, as will be explored in the coming campaigns.

5.3 Dependence of pedestal characteristics and ELMs on isotope composition

Pedestal pressures, ELM amplitudes and ELM periods were larger in tritium plasmas, than in deuterium and especially hydrogen plasmas (Bhatnagar, NF 39, 1999, p353; Saibene NF 39, 1999, p1133), exceeding the core stored energy in some of the tritium plasmas (Fig. 5.5, left). The right figure in Fig. 5.5 suggests that this may in part be attributable to the higher densities reached in tritium plasmas (Saibene, NF, 1999).

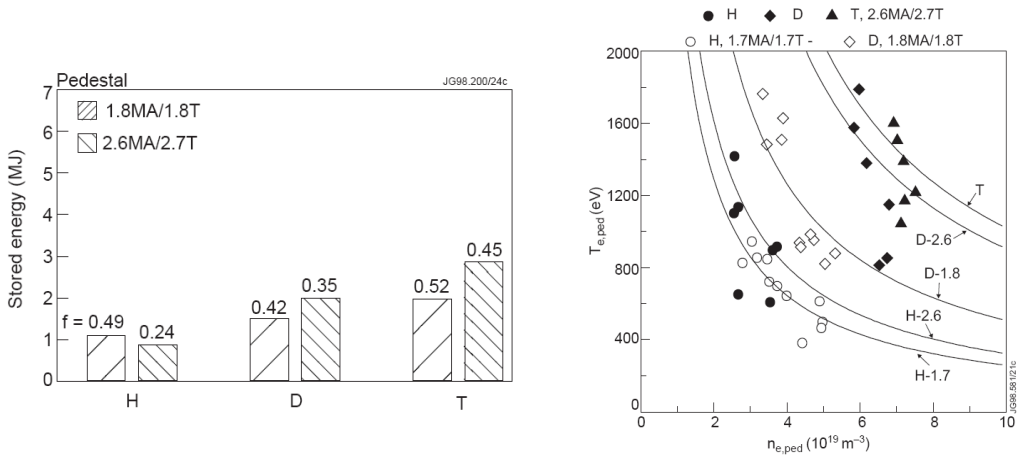

Fig. 5.5: Left: Pedestal stored energies in ELMy H-modes in DTE1 for the three isotopes and for two current/toroidal field combinations. The labels refer to the fraction of the total stored energy attributable to the pedestal (Bhatnagar, NF, 1999). Right: Pedestal electron temperature versus density for 10-12MW of NBI heating. (Saibene NF 1999).

Since MHD limits do not directly depend on isotope mass, the higher edge pressures may result from differences in the edge current profile, the origin of which would warrant further investigation. Another explanation would be a scaling of pedestal width with ion Larmor radius, which could now be investigated with the HRTS Thomson scattering system and the new profile reflectometer.

In Fig 5.6, the left figure below shows the ELM signatures (Saibene NF 39, 1999, p1133) and the middle figure shows the time evolution of the pedestal pressure using ECE and interferometry (Bhatnagar NF 39, 1999, p353). In the case of T, the first ELM is clearly very much larger ($\Delta W_{ELM}/W_{pl} \approx 18\%$) in the T shot, subsequent ELMs are of similar magnitude in T and D. The edge pressure drops in H are of higher frequency and smaller, albeit not as small as suggested by Fig.5.6, which appears to be limited by the poor time resolution of the density diagnostic (FIR interferometer). The D and T examples shown in Fig. 5.6, taken from the available literature, may not be entirely comparable, because the density in T increased strongly during the entire heating phase, despite the absence of a gas puff. ELMs in T discharges are reported to be of lower frequency and to affect a larger portion of the plasma cross section, raising concern about how to mitigate them in ITER (Bhatnagar, NF 1999). Hydrogen plasmas, on the other hand, are clearly not in the type I ELMy regime and therefore should not be compared to D and T in this dataset. The difference between H and D is a warning that the behaviour or T (or DT mixtures) cannot be extrapolated simply from observations in H and D only.

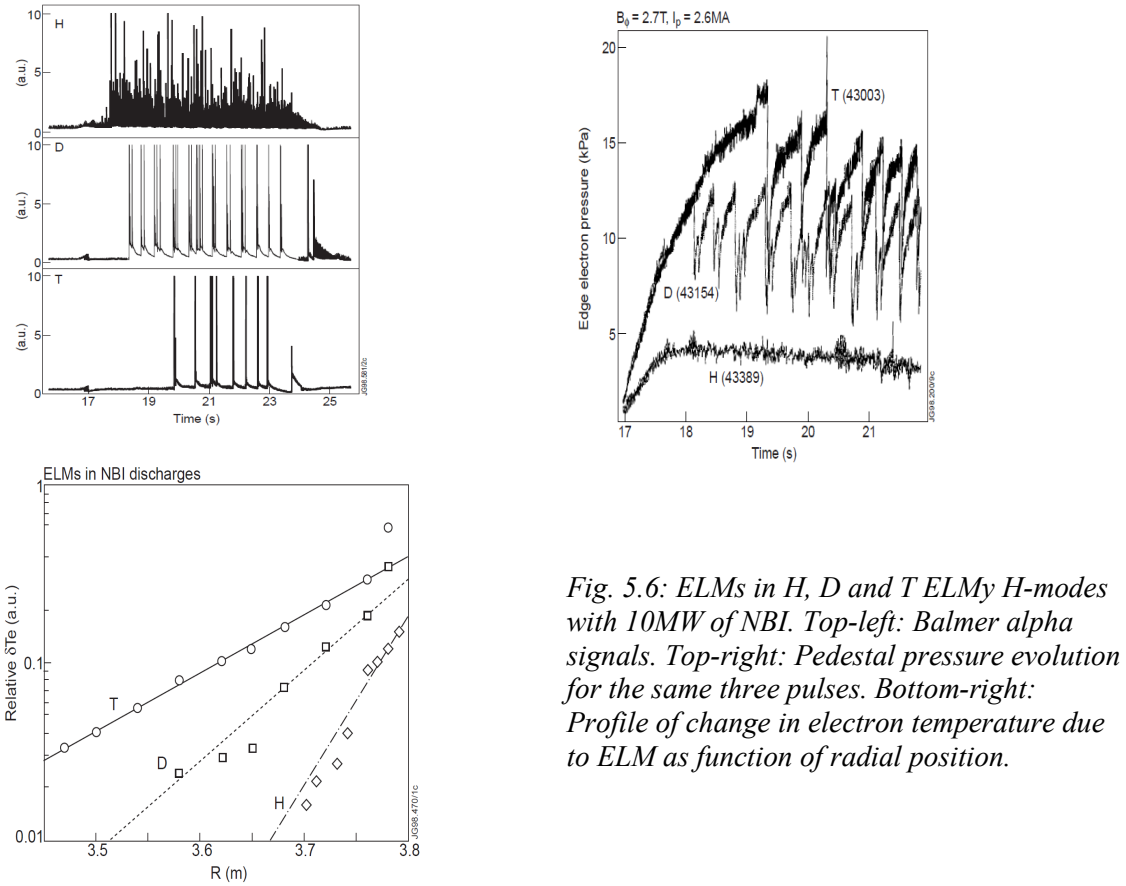

Fig. 5.6: ELMs in H, D and T ELMy H-modes with 10MW of NBI. Top-left: Balmer alpha signals. Top-right: Pedestal pressure evolution for the same three pulses. Bottom-right: Profile of change in electron temperature due to ELM as function of radial position.

In a new isotope (and DT) campaign JET will be in an excellent position for addressing pedestal and ELM physics with ITER relevant PFC's and plasma shape,

increased NBI power and improved edge diagnostics. JET will also be able to test the effectiveness in T and DT plasmas of the various methods of ELM mitigation under development: Pellets, vertical magnetic 'kicks', fuel and impurity gas puffs, n=1 and n=2 resonant magnetic perturbations (and higher n numbers if the RMP enhancement project is approved and implemented in time). Also the isotope campaign should be long enough to develop and study truly stationary ELMy H-modes in tritium, which was not possible in DTE1.

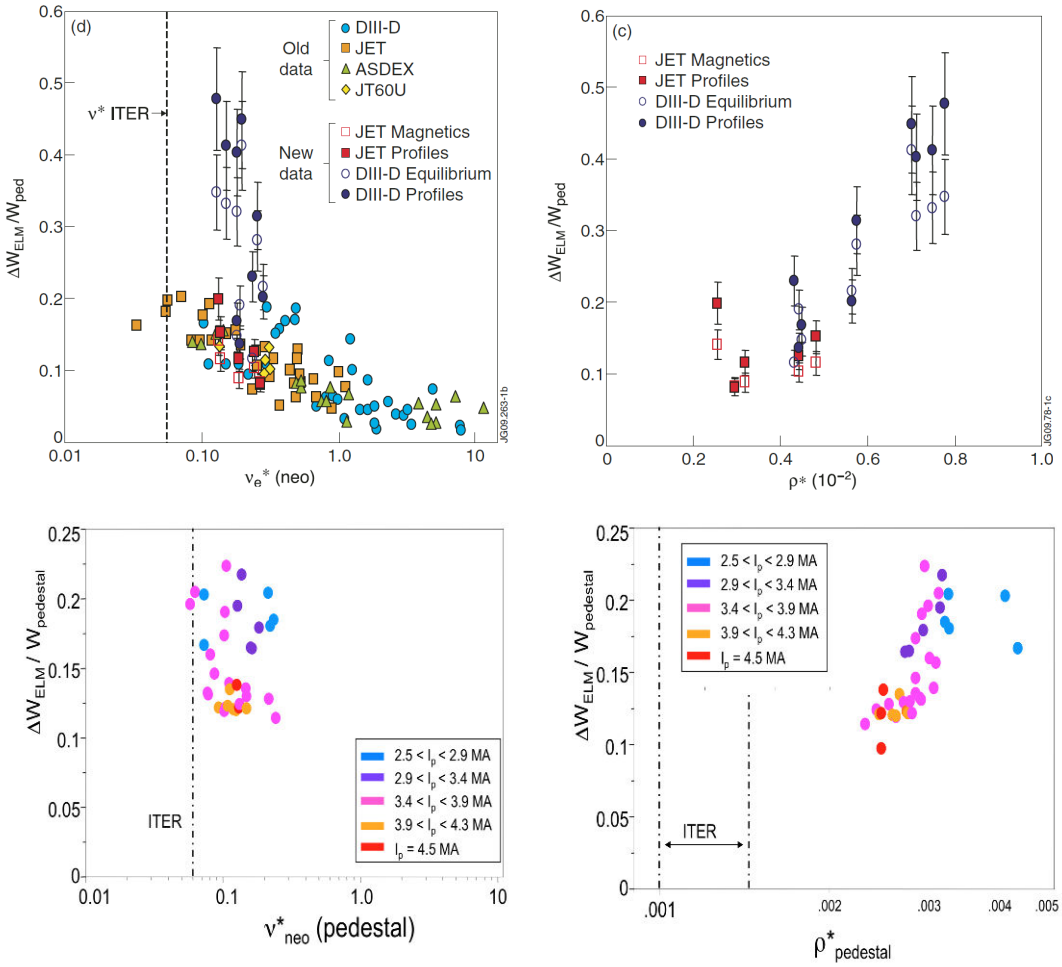

Fig. 5.7: Top left: Multi-machine ELM size trends with collisionality. Top right: Trend with normalised Larmor radius from JET and DIII-D (Beurskens et al, PPCF 2009). Bottom: same for JET data only.

The issue of ELM size is one of the most serious challenges for the lifetime expectations of the ITER divertor PFC's. Observations over a range of devices (top left of Fig.5.7) suggest that relative ELM amplitudes increase as collisionality drops towards ITER values (A. Loarte et al, PPCF 45, 2003, 1549). However, a recent comparison of JET and DIII-D data (M. Beurskens et al, PPCF 51, 2009, 124051) suggests that ELM amplitudes drop with ρ*, which is favourable for ITER (top right in Fig. 5.7). The bottom figures in Fig. 5.7 are for JET data only and show a better correlation of ELM size with ρ* than with ν*, indicating for the least, that other parameter dependencies than ν* have been overlooked in the past. This recent realisation calls for a broader multi-machine approach to determine the probably multiple parametric dependencies of the pedestal characteristics and ELM size

scalings. The future JET isotope campaigns, by supplying high quality data in H, D and T, would be the cornerstone of such an endeavour.

5.4 Local transport physics

The above issues with the H-mode threshold, global confinement and pedestal/ELM behaviour relate directly to performance expectations for ITER. Here we would like to mention a number of transport physics issues, which are likely to benefit from the proposed isotope campaigns.

- Non-dimensional scaling studies (as ongoing in the ITPA Transport TG) can be expected to benefit from improvements in the ρ* scaling brought by data from the three isotopes in similar conditions, both concerning core and pedestal physics.
- These studies could be complemented by turbulence measurements using diagnostics not available in DTE1 (correlation reflectometer, pulsed profile reflectometer, correlation ECE), to check whether turbulent length scales scale as the ion Larmor radius.
- Particle and impurity transport is likely to be affected by the background isotope. Related investigations and experiments may produce valuable data for theory (in)validation.

5.5 Fuelling and density limit issues

A topic of particular interest is fuelling, which is often feared to be a major issue in ITER because of the expected (or rather required) high density and pedestal width in the face of a very short mean free path of the neutrals. Since penetration depths depend on neutral velocity and hence mass, experiments using all three isotopes may help answer the question of whether fuelling is dominated by neutral penetration into the main plasma or by plasma transport processes (such as a pinch) in the pedestal. Strong convection is known to occur in the pedestal for impurities (CMOD, Pedersen NF40, 2000, 1795), but has never been demonstrated unambiguously for hydrogen isotopes. It should also be noted that operation at the Greenwald limit, where the overall density is clamped, is not an obstacle to efficient substitution of deuterium by puffed (trace) tritium, which occurs at the same time scales as energy transport (Matthews et al, Journal of Nuclear Materials 266-269 (1999) 1134).

A related issue is the density limit, which was achieved to 95% in H, D and T ELMy H-modes in DTE1, albeit with poor confinement. Results from DTE1 showed that the density limit in L-mode (defined by the onset of an X-point MARFE) decreases with increasing ion mass in vertical target configurations, whilst being insensitive to isotope mass in horizontal configurations (Maggi NF 39, 1999, p979). Both cases are qualitatively consistent with an analytical model for detachment (K. Borrass et al, NF 37, 1997, p523), where neutral velocity is a key parameter. Also, a combined density limit study on AUG and JET in ELMy H-mode, which appears to be consistent with the Borrass model, has cast doubts on the ability of ITER to attain its projected working density in H-mode (Borrass et al, NF 44, 2004, p752).

More important than the absolute highest operating density is the highest density allowing good H-mode confinement. Recent observations suggest that confinement degradation with density is not always as severe as experienced in DTE1. Factors which influence confinement at higher densities include the plasma shape and the wall recycling, both of which will be different from DTE1. In an isotope campaign, JET would provide the possibility for investigating this issue for all isotopes and in conditions closer to those of ITER.

5.6 Isotope effect on current ramp and Internal Transport Barriers (ITB's)

Keilhacker et al (NF39, p225, 1999) reported that current ramps for the optimised shear regime obtained higher q(0) values in DT compared in D plasmas, i.e. current diffusion appeared to be slower in DT plasmas (Fig. 5.8). This effect was not explained, but may be a result of improved confinement in DT plasmas, leading to higher electron temperatures. It was compensated by altering the ramp rate and the ICRH power, allowing ITB's to be triggered at the q=2 surface in DT plasmas. It is noted that ramp-up modelling is challenging even in D plasmas, as recently experienced in the ITER reference discharges (ramp-up) and hybrid discharges; for both the current penetration is slower than expected from modelling.

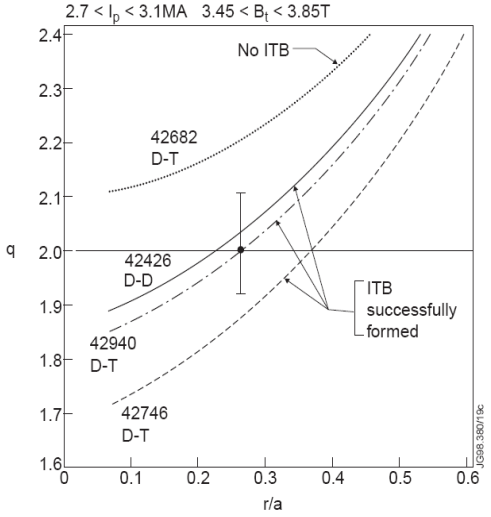

Fig. 5.8: Safety factors in D and DT plasmas. Discharges 42682 (DT) and 42426 (D) used identical ramp-up scenarios with very different results. Subsequent scenario adjustments allowed lower safety factors and ITB's to be obtained in DT plasmas. (Keilhacker, NF 1999)

Understanding and modelling current ramps has so far received little attention. It is of importance for ITER, since ramp-up and ramp-down are major items in the discharge flux budget. Isotope composition may play a role, although probably not a direct one in the conductivity. Ramp-up and ramp-down scenarios in ITER will also have to deal with the isotope dependence of the L-H threshold, confinement and the alpha power generated by fusion reactions.

Related to this is that ITB's have been achieved in only a few DT plasmas in DTE1 during the early L-mode edge phase of the discharge. The H-mode transition led to their disappearance. These ITB's had lower electron densities than in D and cannot

meaningfully be compared to any of their intended D counterparts, because of scenario alteration which were required to fasten current penetration and delay the H-mode

Most of the previous points were written with mainly H-modes and hybrids in mind. However, to some extent they apply to ITB's as well. Specific ITB experiments during the isotope campaigns and the DT campaign proper should also be considered. They may provide comparisons of conditions for ITB formation and ITB quality in different isotopes, in analogy with the H-mode ETB.

6. Alpha particle physics

Key points:

Experiments in DT at high performance will also provide:

- An assessment of alpha particle heating in stationary conditions. This includes the classical electron heating and the direct ion heating through the so called "alpha channelling" effect, possibly already observed during the DTE1 as well as the effect on impurity and particle transport.
- Documentation of the interaction of alpha particles with core MHD, such as fishbones (generated by heating ions), NTM's and sawteeth.
- Measurement of TAE spectra in ITER relevant scenarios and measurement of alpha particle drive on TAE modes for TAE code validation.
- Measurement of transport produced by unstable TAE modes in advanced modes of operation with elevated central q-values (q_0~2).

During DTE1, Alfvén Eigenmodes were identified in advanced scenarios with elevated central q-values, in so called 'switch-off' experiments (stepping down the additional heating power). Calculations suggest that in these conditions alphas were the dominant drive for Alfvén Eigenmodes.

The simulation of high performance scenarios (provided by the performance projections described above) are currently being used for detailed code calculations performed by the ITPA Topical Group on Energetic Particles to provide clear answers as to the studies that should be performed at JET on TAE's in the presence of alpha particles.

A modelling effort has been initiated, with aim to predict TAE spectra and stability properties for the scenarios presented in chapter 4, as well as for comparable ITER conditions. This will help optimising experiments aimed at code validation and eventually improve predictions for TAE stability in ITER.

6.1 Introduction

Transient hot ion H-modes in DTE1 led to significant alpha populations with $\beta_{fast} \approx 0.7\%$, as compared to $\beta_{fast} \approx 1.2\%$ expected in the ITER baseline scenario. Both JET and ITER have supra-Alfvénic alpha populations with $v_\alpha/v_A \sim 1.6$ in DTE1 and $v_\alpha/v_A \sim 1.9$ expected in ITER. Unavoidably, the relative orbit size, ρ^*_α, is nearly four times as large in JET as in ITER, which has profound implications for TAE stability. However, the non-observation of TAE's in high performance DT plasmas in DTE1 does not appear to be due to the large ρ^*_α in JET, but rather to the high plasma pressure achieved. DTE1 also demonstrated electron heating by alphas and unexpectedly, ion heating or an ion confinement improvement, albeit in transient conditions. No alpha particle transport investigations were undertaken in DTE1, largely for lack of adequate diagnostics.

TFTR however has conducted a range of alpha particle transport studies, briefly summarized here. In the absence of MHD activity, alpha transport in the gradient zone of TFTR was reported to be consistent with classical orbit losses and stochastic ripple diffusion with dependences on alpha energy, q and ripple amplitude. Reversed shear plasmas had significantly broader alpha profiles than normal shear plasmas, consistently with orbit calculations.

TFTR measurements have demonstrated alpha particle transport by sawteeth (Fig. 6.1) and fishbone modes, as well as by TAE's. (Medley et al, 1998).

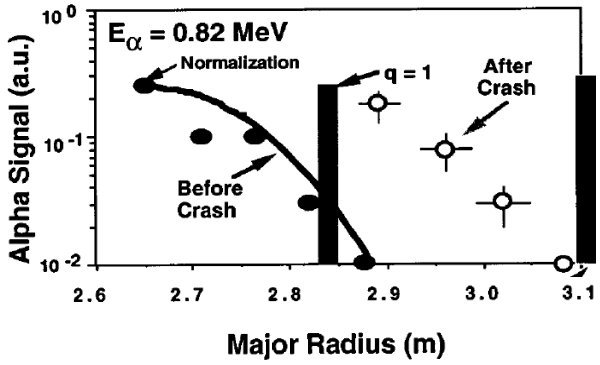

Fig. 6.1: Redistribution of 0.82 MeV slowing down alpha particles in TFTR by a sawtooth, measured using the Li pellet charge exchange diagnostic.

The TAE's were observed in reversed shear discharges in TFTR with $q_0 \approx 2$, $v_\alpha/v_A \approx 0.7$ and attributed to resonant trapped alphas, causing observable redistribution (Fig. 6.2).

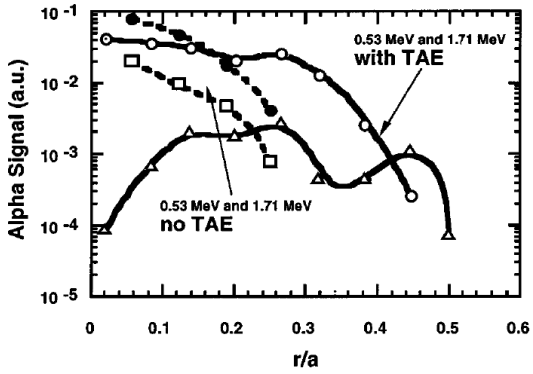

Fig. 6.2: TAE redistribution of alphas in TFTR. Comparison of alpha particle profiles with and without TAE for two energies

6.2 TAE's in DTE1 and possible investigations in a future DT campaign

Ideal core TAE modes in high performance DT plasmas were not observed. This is consistent with the fact that they were not found in the Alfvén Wave spectrum (not found to exist, as opposed to found to exist, but being stable because of damping) using CASTOR stability calculations, as a result of high plasma pressure. Only in one case was marginal TAE instability indicated (by the CASTOR code) before the peak kinetic pressure was reached (Fig. 6.3), but no mode activity was detected. Kinetic TAE's (KTAE's) were found to exist (CASTOR), but were always heavily Landau damped (mostly by NBI & thermal ions) and therefore stable.

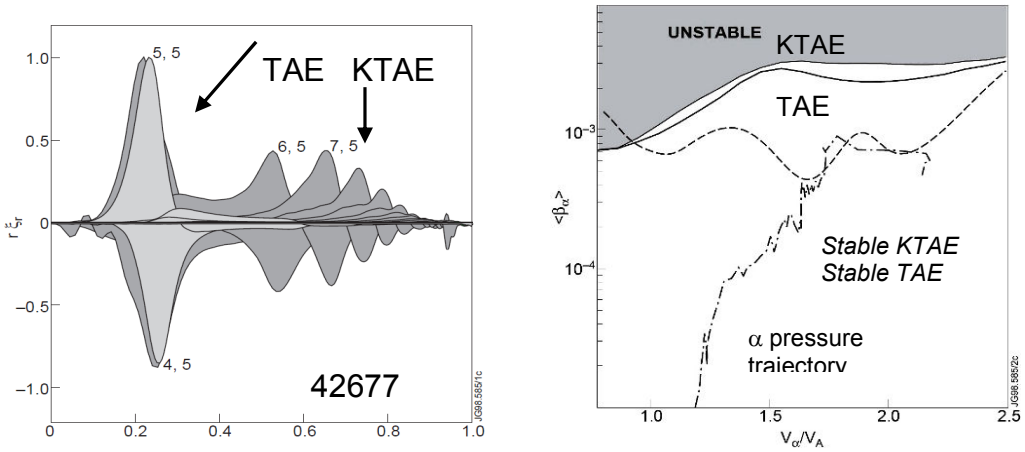

Fig. 6.3: TAE stability analysis for JET DT hot ion H-mode 42677, which produced 10 MW fusion power for 21 MW of NBI and was marginally unstable to TAE's. Left: TAE and KTAE mode structures. Right: trajectory of discharge in v_α/v_A -$<\beta_\alpha>$ space. The dotted line is represents the minimum TAE's stability boundary. The two boundaries for KTAE correspond to including and not including Landau damping on beam ions.

AE's were only observed in optimised shear discharges with ICRH, but destabilisation could be ascribed to ICRH fast ions only. AE's were also identified in 'switch-off' experiments, as the pressure had dropped and fast particles from NBI, ICRH and alphas were still slowing down. Calculations suggest that in this case alphas were the dominant drive, together with residual ICRH ions.

JET is the only magnetic fusion device which can produce and confine alpha particles, i.e. with an isotropic distribution and $v_\alpha/v_A>1$. Simulations for high performance hybrids and 'advanced inductive' scenarios at full power suggest that normalised alpha pressures up to some 0.5% may be possible in stationary conditions (see chapter 4). This is lower than expected in ITER (>1%). However it first remains to be seen, by simulations and eventually by experiments, whether these scenarios have plasma pressures allowing TAE's to exist and what the critical plasma pressure for their appearance is. If they exist, but sufficiently high alpha pressures for instability are not obtained, TAE investigations can still be carried out in specific experiments at lower density (i.e. with longer slowing down times and hence higher β_α) and/or using the active TAE antennae, as detailed below.

Even if normalised alpha pressure gradients velocities match those of ITER, TAE modes expected to be unstable in ITER may not be so in JET, because of the large relative orbit size, which leads to a quasi-adiabatic alpha particle response, i.e. alphas interacting only weakly with smaller scale TAE modes (Zonca & Chen, PPCF Plasma Phys. Control. Fusion 48 (2006) 537, Plasma Phys. Control. Fusion 48, 2006, B15, Chen & Zonca, Nuclear Fusion 47, 2007 S727). Large fast ion orbit sizes are not an impediment to TAE instabilities per se, but they lead to instability at lower radial/toroidal mode numbers. Indeed, TAE's are observed in all NBI heated discharges in MAST and NSTX, where NBI ions are supra-Alfvénic. When this issue was recognized earlier in 2010, a modelling effort was started in several Associations and a similar initiative was started at the Fast Particle Topical Group of the ITPA. The aim of this effort is to investigate to which extend TAE observations in JET (or the documented absence of TAE's) can be used for code validation in view of extrapolations to ITER. Another question is to which extend such observations on JET would or would not be unique, i.e. not replaceable by experiments using the non-isotropic, sub-Alfvénic ion distributions produced by ICRH. So far no output from these studies has been made available to the work group. We nonetheless provide a few elements for discussion:

- The existence of a critical plasma pressure for unstable TAE's to exist at all, suggest that scenarios developed for ITER be tested for the existence of these modes, even if no TAE activity is detected. This can already be done during scenario development prior to any DT campaign, by using the JET active TAE antenna system, which can excite AE's with toroidal mode numbers up to n~30 and determine their damping rate in the absence of fast particles. In the presence of a fusion alpha population it can of course also determine their existence and effective growth rate ($\gamma-\alpha$), as long as the drive doesn't exceed the damping. Hence, for prospective ITER scenarios without fusion alphas, the system can assess whether potentially deleterious modes are present and how strongly they are damped. In the DT campaign it can then quantify the destabilising effect of the alphas, even if the net effect is that the modes remains stable, as may well be the case for inductive and hybrid scenarios with $q_0\approx1$. The effect of the alphas can be obtained very simply by measuring the apparent damping of modes with opposite toroidal mode numbers, since only TAE's propagating in the direction of the magnetic field interact with the alphas. This can be achieved with the JET TAE antenna system, for which an upgrade involving significant non-EFDA collaborations is underway. The difference between the effective damping rates is a direct measure of the alpha drive. The so obtained plasma damping and

alpha drive are key ingredients for code validation (and developments, if agreement is founds unsatisfactory). The larger ρ^*_α in JET makes modelling more difficult than the ITER case, where ρ^*_α is small. JET DT discharges would therefore constitute a stringent theory test, which if successful, would bode well for predicting TAE behaviour in ITER.

- Since the TAE growth rate scales as q^2, we can expect to observe TAE's in advanced scenarios with $q_0, q_{min} \sim 2$, as previously observed in the presence of fusion alphas in TFTR and other fast particles in several devices. This may potentially lead to so called 'massive TAE instabilities' produced by a large number of simultaneously unstable TAE modes, with a large range of mode numbers, affecting a large portion of the minor radius, as observed in NBI heated reversed shear discharges with an ion ITB in DIII-D (Nazikian et al, PRL 96, 2006**,** p 105006). These modes are localised in the weak magnetic shear region and are destabilised by a wide range of ion energies, all the way down to the thermal range. Although they don't require alpha particles for instability, it may be desirable to study the effect of alpha particles on these modes in JET for the purpose of model validation and for assessing their potential relevance to ITER advanced scenarios. Such experiments would also allow assessing the effect of these modes on alpha particle transport.

- Finally power switch-off experiments, where pressure, beam ions and alphas decay (as already performed in DTE1), would allow further investigations of alpha particle physics. Such experiments could be done parasitically after the main experiment's heating phase and would not require a specific neutron budget allocation.

6.3 Passive alpha particle transport and losses

By passive transport we mean that the alphas are not to a large extent responsible for increasing their own transport, as in the case of TAE's and Energetic Particle Modes. Many of these effects can be studied in plasmas having only a modest alpha particle population, as long as it is sufficient for detection of alpha particles by the neutron/gamma cameras (using nuclear reactions between alphas and impurities), neutral particle analysers and scintillator probes (for lost alphas). The effects to be studied would include:

- Effects of sawteeth in H-modes (inductive scenarios):
  - Alpha particle redistribution (measured using γ cameras, NPA)
  - Losses to walls (measured using scintillator probes)
  - Observation of reduced α heating (for high fusion power scenarios)

  The alphas may themselves contribute to stabilising sawteeth, which may eventually lead to 'Monster' sawteeth with very large crashes. Suitably phased ICRH or localised ECCD (if available) may be attempted to reduce the sawtooth period and crash amplitude.

- Effects of fishbones and NTM's in hybrid scenarios

Hybrid scenarios (or advanced inductive scenarios) would have the advantage of avoiding 'Monster' sawteeth. They would however remain susceptible to fishbones and NTM's. The former do not in general appear to affect plasma confinement, whilst the latter can seriously compromise confinement and fusion performance. A future DT campaign would allow studying the effect of these modes on fusion alpha particles. These effects are likely to result in a broadening of the alpha profiles and in alpha losses to the walls, as observed in TFTR in the case of fishbones (Fig. 6.4).

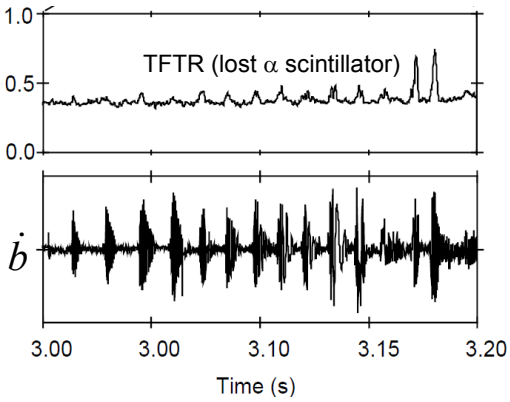

Fig.6.4: Signal from lost alpha scintillator in TFTR (top pane), showing bursts of lost alphas coincident with bursts of fishbone activity measured using external magnetic probes and shown in the lower pane.

- Other losses may be considered for investigations in MHD quiescent discharges, but are not likely to constitute priority items:
  - classical orbit losses
  - ripple losses
  - turbulent transport losses

The former two processes would provide an irreducible background transport level, mainly depending on the plasma current and current profile. These processes are well understood and there is probably no urgent need to validate them using fusion alphas in JET.

It is generally assumed that turbulence does not affect energetic alpha particle transport. Because of their large Larmor radii, alphas are not believed to interact with small scale turbulence. This is consistent with TFTR not having reported any evidence for turbulent alpha transport. Recent theoretical studies (Estrada-Mila et al, POP 13, 2006, 112303, C. Angioni et al NF 49, 055013) corroborate this view. The results suggest that for ITER conditions, alpha particle and energy transport coefficients by ITG turbulence are at least one and two orders of magnitude smaller, respectively, than for thermal Helium. Besides not being relevant to fusion performance, such small effects would be impossible to measure.

6.4 Alpha particle heating and possible effect on energy confinement

The demonstration of alpha particle heating concurrently with the production of substantial fusion power was one of the main goals of DTE1. Alpha particle heating in DTE1 was observed in a short T/(D+T) ratio scan in the range 0 to 92% (Thomas, PRL 80, 1998, p5548) and 10MW of NBI power. The results (see Fig. 6.5), show

alpha particle electron heating corresponding to approximately 1keV central temperature increase per MW of alpha heating. This effect is the same as obtained for the same amount of ICRH in D discharges. A difficulty with this experiment is that the discharges were transient and time histories differed somewhat from shot to shot.

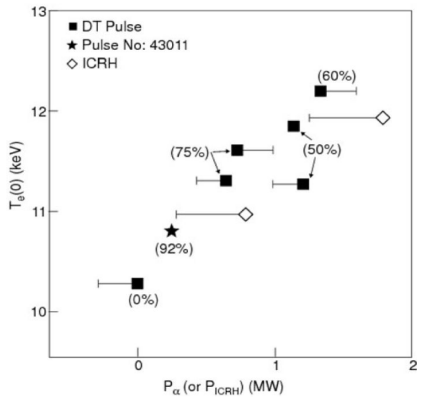

Fig. 6.5: Electron temperature response to alpha heating (black squares) and ICRH heating (open squares). The bars indicate the variation of NBI power with respect to #43011, which was chosen as a reference. For assessing the performance, the barred end should be chosen, rather than the symbol.

Although the electrons behaved as expected, the ions provided a surprise, with a temperature increase nearly three times as large as that of the electrons, when only an increase similar to that of the electrons was expected. This is shown in Fig. 6.6. The corollary is that the confinement time in alpha heated discharges was slightly better than in comparable NBI+ICRH discharges.

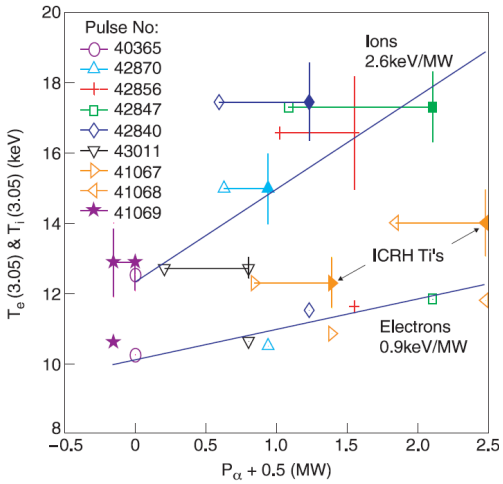

Fig. 6.6: Ion (top) and electron response to alpha particle heating. The barred ends of the ions symbols should be considered for accounting for shot-to-shot variations of beam power. (Sharapov, FST, 2008)

Figure 6.7 shows the overall stored energies and the confinement time as a function of the T/(D+T) ratio. The thermal confinement time is highest at maximum total power (i.e. max fusion power), just the opposite of what is expected from power degradation.

Two explanations have been suggested for the ion temperature increase. The most likely seems to be the formation of a modest ion ITB with a foot near the q=3/2 surface and is supported by a measured steepening of the ion temperature gradient (S. Sharapov, Fusion Science and Technology, 53, 2008 p 989). No evidence of an alpha specific mechanism for ITB formation has been reported; there are e.g. no changes in toroidal rotation.

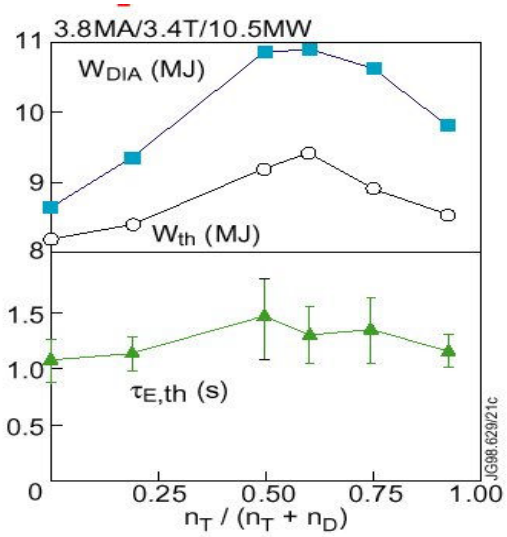

Fig. 6.7: Diamagnetic and thermal energies, as well as thermal confinement time versus the D/T mixture. P. Thomas et al, 28th EPS, ECA Vol. 25A (2001) 929-932, P03.001

Another explanation put forward is ion heating via Compressional Alfven Waves (CAW), excited by the alpha population at ion cyclotron harmonics. These waves may gain energy through their interactions with fast ions and transfer it to the thermal ions. No corresponding ion cyclotron emission (ICE) measurement was available in DTE1. The explanation should however not be dismissed out of hand, because ICE emission up to high harmonics of ω_{ci} clearly related to fusion alphas, was observed in the Preliminary Tritium Experiment, PTE (Cottrell et al, NF 33 , 1993, 1365). Similar observations were made in TFTR (Gorolenko and Cheng, POP 2, 1995, p 1961). Observations of CAW are produced by energetic (supra-Alfvénic) ions have also been made in NSTX (Gorolenko, NF42, 2002, 977) and MAST (private communications at MAST forum, Dec 2010). The fact that such effects have only been reported from spherical tokamaks and in the presence of fusion products in JET and TFTR, suggests that supra-Alfvénic ions may a key ingredient for this instability.

Experimental evidence of the importance of this effect could be obtained from a thorough assessment of alpha slowing down population and slowing down time, which would be lower than predicted without this effect. The physics likely affects beam ions too, if supra-Alfvénic. In spherical tokamaks lower than expected beam-beam and beam-plasma neutron yields would be a tell-tale sign of this effect on beam ions and appear to have been observed in some high power NBI discharges in MAST (private communications, 2010). MAST also reported problems establishing a meaning ion power balance (i.e. obtained $\chi_i<0$), suggesting that part of the ion heat source was unaccounted for. Whether CAW's in the ion cyclotron range of frequencies are the smoking gun, is one of the most intriguing issues to be investigated in a future DT campaign on JET.

Even if this radiative process caused ion heating in DTE1, it is still necessary to invoke a confinement improvement, since any non-collisional transfer of power from the alphas to the ions would remove the equivalent amount from the electrons.

The observation of ion heating and of a confinement improvement in the alpha particle heating experiment is potentially the most important result of DTE1. Since it is not understood and potentially very important, a future JET DT campaign should perform alpha heating experiments in stationary conditions (possibly a hybrid

scenario), equipped with better diagnostics able to identify the causes of any ion confinement improvement, if reproduced. They should also allow for the assessment of the possible role of ICE and CAW's by direct emission measurements and by a quantitative assessment of the alpha population (by e.g. gamma spectroscopy) and slowing down time. Both confinement improvements due to alphas and the possibility of ion heating mediated by CAW's are important physics issues susceptible of affecting ITER and eventually reactor performance.

6.5 Alpha particle sawtooth stabilisation

Fast particles generally lead to longer sawtooth periods and larger, potentially deleterious crashes, followed by large ELMs or NTM's. Mitigation techniques include fast particles from suitably phased ICRH and local ECRH/ECCD.

Experiments to mimic the expected sawtooth triggering of NTMs in ITER require at the same time very long sawtooth periods with large crashes, which can be produced at JET by fast ion populations generated by ICRH or alternatively by a fast of alpha particles in DT plasmas. Such experiments may be difficult to conduct in smaller devices. The difficulty in obtaining monster sawteeth in smaller machines can be understood theoretically [White, Phys. Fluids B 2 (1990) 745] and has been observed experimentally in attempts to perform similar experiments on machines other than JET, TFTR and JT-60U.

In a DT campaign JET could test sawtooth mitigation techniques using ICRH and if available, localised ECRH/ECCD. However this motivation and the priority are under discussion, since the process of (de)stabilisation is fairly well understood and can be (and has been) tested in other JET campaigns and in other devices. One would also have to consider that the contribution of alphas to sawtooth stabilisation may in practice be difficult to distinguish from that of the beams.

6.6 Impact of Alpha heating on particle and impurity transport

Density peaking and impurity accumulation have a strong impact on fusion performance. It has been reported from JET and from several other devices that density profiles in H-modes and hybrids tend to become more peaked at lower collisionality and higher T_i/T_e or NBI fuelling, which is correlated to T_i/T_e (Angioni et al, PPCF 51 2009 124017, Maslow et al, NF49, 2009 p075037), in fair agreement with gyrokinetic theory. This is due to a convective component, the direction of which depends on the dominant type of micro-instability (TEM or ITG) and therefore on the electron and ion heat fluxes (i.e. auxiliary heating and equipartition), which will be different in ITER.

Central ICRH and ECRH, even at modest power, have been reported to reduce electron density peaking in most cases. Fusion alphas in JET provide a centrally very peaked electron heating source, with a core electron heating power density exceeding that from NBI heating, suggesting that this may lead to a core density flattening. As an example, for the intermediate case scenario simulation shown in figs 4.15 & 4.16 (TRANSP run T58, 2.5MW of alpha power) alpha particle electron heating provides

more than half of the electron heating for r/a<0.6 and more than 70% of the electron heating for r/a<0.37). Recent observations and numerical simulations in AUG (Angioni et al, NF to be published) indicate however that, depending on circumstances, core electron heating can also lead to increased central peaking, the T_i/T_e ratio being again a key parameter. We therefore do not expect that a possible influence of the alpha particle heating on density peaking in JET can be extrapolated in a simple way towards ITER. This issue, like many other physics issues, needs to be resolved in the framework of a maturing theoretical understanding, buttressed by a broad experimental database.

More importantly, central ICRH and especially ECRH, even at modest power, effectively counteract central impurity accumulation (Puiatti et al, PoP 13, 2006 p 042501; O. Gruber et al, Nucl. Fusion 49 (2009) 115014). It is important to assess whether alpha particle heating has the same effects, especially with respect to tungsten impurities. The expected alpha power matches the range of ICRH powers over which a beneficial effect of ICRH on core impurities has been observed.

7. RF heating scenarios and RF physics

Key points:

The effectiveness of ICRH scenarios in DT for plasma heating in ITER must be demonstrated and quantified at JET, in order of priority:

- Full characterisation of the 2nd harmonic tritium scheme.
- Using this scenario, demonstrate the minimum level of ^{3}He required to provide effective ion heating.
- Assess deuterium minority ICRH in tritium-rich plasma.

JET discharge conditions during flat top offer absorption conditions for ICRF similar to the ITER ramp-up phase. By using tritium beam injection, the absorption conditions for the flat top phase of ITER can be reproduced, allowing:

- Assessment of the impact of these scenarios on H-mode accessibility and fusion performance.
- Assessment of parasitic absorption effects by impurities and alpha particles.

7.1 RF heating scenario studies for ITER

It should be emphasised that all ICRF scenarios have their own characteristics and the studies referred to below could therefore not be replaced by experiments in plasmas without tritium. The three scenarios to study in a possible second DT campaign are in order of priority:

- Second harmonic tritium (ω=2ω_{cT}) *ICRF heating,* which is the main heating scenario for ITER:
    - Exploration of absorption at ω=2ω_{cT} in plasmas representative of the phase between the end of current ramp-up phase and transition to H-mode in ITER. In this phase the absorption strength is relatively weak and is close to flat top conditions in JET;
    - assessment of absorption in cases where the projected absorption strength should be good, i.e. more representative of the flat top phase of ITER. The necessary conditions in JET could be achieved by Neutral Beam Injection; and
    - much of the investigation could be done during a pure tritium campaign, with a final (brief) verification in DT. For the latter, especially the influence of the fundamental D cyclotron resonance (on the high field side of the ω=2ω_{cT} resonance, see Fig.1) is important to investigate.
- Combined ^{3}He minority, (^{3}He)DT, and second harmonic tritium (ω=2ω_{cT}) heating:
    - Pure second harmonic tritium heating is expected to give predominant electron heating (via collisional transfer from the resonating tritons to the thermal electrons and ions in the plasma);
    - addition of ^{3}He minority ions could significantly increase the absorption strength and the fraction of ion heating, which could be beneficial in the phase before the transition to H mode to maximise the alpha heating. Further experimental information on appropriate levels of ^{3}He ions in this scenario should be valuable for preparation of ITER scenarios; and
    - it is important to assess the interplay between the absorption mechanisms, especially when the ^{3}He concentration is diminished (in the flat top phase of ITER one should avoid dilution of the fuel ions, while ion heating is no longer critical).
- Minority heating of deuterium in a tritium rich plasma, (D)T:
    - Heating at the fundamental cyclotron frequency of deuterium is one of the possibilities catered for by the planned ITER ICRF system. The crucial question is how high one can go in deuterium concentration. To be a practicable scenario, the deuterium concentration must be at least 30-40% when entering into the flat top phase of an ITER discharge. However, weak damping and mode conversion phenomena associated with such concentrations leave significant uncertainties with the present level of knowledge, especially on the experimental side;
    - the possibility of using a tritium rich scenario in the ramp-up phase of ITER before transition to H-mode (which may itself be during ramp-up) should be investigated. In this case (D)T ICRF heating could provide a good ion heating fraction and a significant enhancement of

the DT yield due to non-thermal deuterons accelerated to the 100 keV range;

- moreover, an early T-rich phase in the ITER discharge would also lower the L-H threshold; a balanced fuel ratio could be restored as soon as H-mode is achieved; and
- issues to be documented include mode conversion at high deuterium concentrations, parasitic absorption of ICRF power by alpha particles and beryllium impurities.

Together with various diagnostic enhancements since DTE1, as given in Chapter 3 of this report, it should also be noted that during the past few years, Break-in-Slope (BIS) methods have been developed to deduce the power deposition profiles from the temperature measurements variation during ICRF power modulation. BIS analysis is now extensively used at JET and would provide new insights into the analysis of ITER relevant DT ICRF schemes. Thus, new experiments on ICRF scenarios for DT plasmas should allow one to create a much more solid and targeted database with relevance for ITER preparation.

ICRF scenarios	**ITER B_t / ICRF frequency**	**Comment**	**Corresponding JET B_t / ICRF frequency**
$2\omega_{cT}$ $(= \omega_{cHe\text{-}3})$	53 MHz @ 5.3T	Main scenario for DT phase. This 2nd harmonic T scenario can be combined with ^{3}He minority heating to increase ion heating	28 MHz @ 2.6-2.8 T 33 MHz @ 3.1-3.3 T 37 MHz @ 3.5-3.7 T 42 MHz @ 4 T
ω_{cD}	40 MHz @ 5.3 T	Minority D heating in T rich plasma.	28 MHz @ 3.7T/
FWCD	55 MHz @ 5.3 T	Fast Wave Current Drive.	28 MHz @ 2.6-2.8 T 33 MHz @ 3.1-3.3 T 37 MHz @ 3.5-3.7 T
$\omega_{cHe\text{-}3}$	45 MHz @ 5.3T	Sawtooth control with ^{3}He fundamental resonance layer near q = 1 surface (outboard).	28 MHz @ 3.1-3.3 T 33 MHz @ 3.5-3.7T
$\omega_{cHe\text{-}3}$	40 MHz @ 3.7T to 55 MHz @ 5.3T	Minority ^{3}He heating in H (inverted scenario), D, ^{4}He or DT	28 MHz @ 2.6-2.8 T 33 MHz @ 3.1-3.3 T 37 MHz @ 3.5-3.7 T
ω_{cH}	40 MHz @ 2.5T / to 55 MHz @ 3.8T	Minority H heating in D, ^{4}He or DT	From 28 MHz @ ~1.8 T up to 51 MHz @ 3.4 T

Table 7.I: ICRF scenarios foreseen for ITER, compared to the capabilities of the ICRH systems at JET

The ICRF system planned for ITER [P. Lamalle, AIP Conf. Proc. 1187 (2009)] is designed to couple 20MW of power in the frequency range of 40-55MHz and allows for a variety of heating scenarios, as summarized in the Table 7.I and illustrated by Fig. 7.1, where the main absorption/conversion layer of the fast wave are schematically represented.

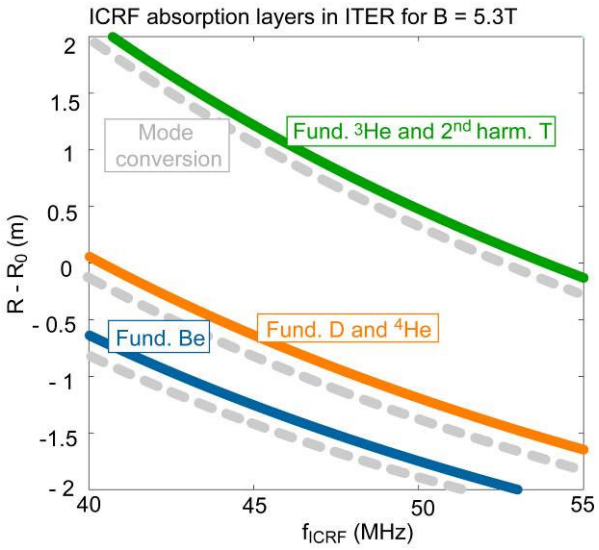

Fig. 7.1: Cyclotron and mode conversion (ion-ion hybrid layer and associated cut-off) layer foreseen in ITER at 5.3T. Note that the Mode Conversion layers are schematically represented and their position depends on the exact plasma composition.

The first two scenarios, $\omega=2\omega_{cT}$ and $\omega=\omega_{cD}$ are the most relevant ones for ITER preparation in a possible DT campaign on JET. In fact both these scenarios were tested in the first full DT campaign in JET, DTE1 [D.F.H. Start, Nucl. Fusion (1999)]. A significant amount of information on the heating scenarios was obtained, and the main features were reasonably well understood [L.-G. Eriksson, Nucl. Fusion (1999), V. Bergeaud, Nucl. Fusion (2000)]. However, as will be outlined below, a significant benefit for ITER preparation could be obtained by further experiments, especially for the application of heating after the current ramp-up phase of an ITER discharge, or even during it if electron heating can contribute to saving volt seconds. New experiments on JET should extend the database of discharges, especially since the discharges in DTE1 were mainly aimed at enhancing the performance in JET rather than directly studying features of relevance for ITER. For this reason the database from DTE1 on the main ICRF heating scenario for ITER, $\omega=2\omega_{cT}$, is very limited (it did not perform well in terms of enhanced DT yield).

Another important aspect affecting the heating scenarios is the amount and type of impurities present in the plasma, which can affect their efficiency. For example, the presence of Be can lead to parasitic minority cyclotron layer on the plasma high field side. The presence of C carbon (or of any other impurities with a Z/A ~1/2) can enhance the mode conversion efficiency in minority scenarios, such as (^{3}He)DT and (D)T, [Van Eester, Nucl. Fusion (2002), M.-L. Mayoral, Nucl. Fusion (2006), D. Van Eester, 37th EPS (2010)]. Since the impurity concentrations with the new Be/W wall is likely to be different than with the C-wall, pursuing the development of the ICRF heating scheme for ITER in a C-free environment is highly relevant. Of course, both measurement and control of the minority concentrations are critical. Real-time control of the ^{3}He concentration has been operational at JET since 2003 [D. van Eester, (2004)] and it has proven to be an essential tool for heating scenario development. It could be of significant benefit in a potential DT campaign at JET, especially for (^{3}He)DT heating experiments.

Finally, it is important to mention that for the A2s antennas, the ICRF frequencies to be used in JET (see table 1) to test these DT heating scheme are the ones giving the lowest antenna loading. This is particularly true for frequencies below 30 MHz. In previous experiments, a high level of ICRF power (up to 6 MW at 28 MHz and 8.7 MW at 37 MHz), was achieved due to operation with a relatively small separatrix-limiter distances (~ 4cm) and a long period of antenna conditioning that allowed operation at 35kV to be achieved. During the recent JET campaigns, the time

allocated during restart period allowed one to only to marginally reach 30kV. In order to maximise the performance of ICRF in a future DT campaign this aspect should be taken into account. Additionally, the repair of the ITER-like ICRF antenna (frequency range between 29 and 47 MHz) could be envisaged as it would provide additional power between 3 and 5 MW depending on the plasma condition, especially if safe operation with the new Be-wall prevents operation at low plasma-wall distances. The options for repair (schedule and costs) of the ILA have been assessed and presented in section 2.3 of this report.

7.2 Second harmonic tritium absorption, $\omega=2\omega_{cT}$

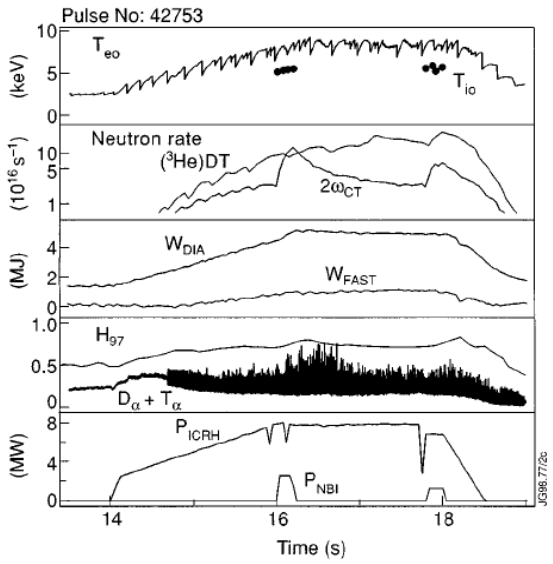

Fig. 7.2 (from [D.F.H. Start, Nucl. Fusion (1999)]): Highest neutron reactivity obtained with `pure' $2\omega_{cT}$ heating. The neutron rate of a comparable ^{3}He minority case is also represented and illustrating that without ^{3}He, a neutron rate a factor of 6 lower is obtained. Note the logarithmic scale for the neutron rate.

The main heating scenario for ITER relies on the fast wave absorption at the tritium second harmonic cyclotron resonance, $\omega=2\omega_{cT}$. The absorption mechanism for this scenario is a Finite Larmor Radius (FLR) effect, making the damping on the tritons to lowest order proportional to $n_T(k_\perp\langle v_{\perp T}^2\rangle/\omega_{cT})^2$. The perpendicular wave number of the fast wave scales roughly with the electron density, indicating that the damping roughly vary like $n_e^2 w_{\perp T}/B$, where $w_{\perp T}$ is the energy density of the triton population in the absorption region (obviously simply proportional to the triton temperature in a thermal plasma). Since the temperature and density in ITER should be significantly higher in the flat top phase of a discharge than at JET (typically $n_e \sim 1\text{x}10^{20}$ m^{-3} and T_i ~ 20 keV in ITER compared to $n_e \sim 4\text{x}10^{19}$ and T_i ~ 5 keV JET), the conditions in JET and ITER should be quite different for the $\omega=2\omega_{cT}$ scenario during that phase. In particular, while the single pass absorption should be high in the flat top phase of ITER, it is low in JET. Results are available from DTE1 (se Fig. 7.2), however, there are two factors that make it relevant to extend the database for this scenario on JET in preparation for ITER: (i) at the end of the current ramp-up phase of an ITER discharge the absorption conditions for $\omega=2\omega_{cT}$ are close to those in the flat top phase in JET; (ii) improved $\omega=2\omega_{cT}$ absorption in JET can be achieved by injection of neutral beams (this was not done DTE1), which should allow to achieve absorption conditions approaching those during the ITER flat top phase.

Predictive simulations of the discharge evolution during the first hundred seconds of an ITER discharge [D. Van Eester, 15th Conf. on Radio-Frequency Plasmas (2004)] indicate an almost linear rise of the density, which reaches central values around $4\text{x}10^{19}$ m^{-3} at the end of the current ramp phase; the central electron temperature at

this point is simulated to be close to 10 keV. During ICRF experiments in DTE1 with $\omega=2\omega_{cT}$, similar densities were used while the temperature was somewhat lower (around 8 keV electron temperature and 5 keV ion temperature). The difference in the magnetic field (see the simple scaling above) compensates for the lower temperature in JET, leading to similar single pass absorption fractions in the two cases. Simulations using the parameters above indicate that the single pass absorption coefficient on the tritons is around 5%, which is low.

In order to assess in more detail then potential of JET as a "test bed" for $\omega=2\omega_{cT}$ scenario in ITER a number of simulations have been carried out with the full wave code EVE. The parameters and global results of two simulations, one for ITER DT plasmas and one for JET DT plasmas, are shown in table 7.II.

	ITER (L-mode start-up)	**JET**
Input:		
n_e [m^{-3}]	$4\cdot10^{19}$	$4\cdot10^{19}$
T_{e0} [keV]	10	6
T_{i0} [keV]	8	5
$n_{He3}/(n_D+n_T)$	0.1%	0.1%
f [MHz]	53	37
N_{tor}	50	25
Simulated fractions of absorbed power:		
P_T/P_{ICRF}	5.3 %	6.94 %
P_D/P_{ICRF}	0.1%	1.12 %
P_{He3}/P_{ICRF}	81.2 %	74.86%
P_e/P_{ICRF}	13.4 %	17.08%

Table 7.II: Simulation results from the full wave code EVE for ITER and JET for parameters where JET could be used as a "test bed" for ITER in simulating $\omega=2\omega_{cT}$ ICRF heating in the phase before transition to an H-mode in ITER.

The contours of the E_+ component of the electric field are shown in Fig. 7.3 for the two cases. As can be seen in Table 7.II, the partition of the power between the different species is very similar in the ITER and JET cases. It is especially important to notice that the power absorbed on the tritons is small. In the simulated cases the ^{3}He ions absorb most of the power despite their low concentration (similar results were found in [Van Eester, Nucl. Fusion (2002)]. Furthermore, even in the absence of ^{3}He the power absorbed on them would not dominate, instead the electrons (via TTMP/ELD) would absorb the lion's share of the power. The wave fields displayed in Fig. 7.3 show many similarities, it is clear that the wave lengths are similar (which is not surprising since the densities and parallel wave numbers are almost the same). Consequently, it is clear from Table 7.II and Fig. 7.3 that experiments with $\omega=2\omega_{cT}$ during a JET flat top phase can provide crucial information on the performance of this scenario in ITER during the critical phase before the discharge makes the transition into an H-mode.

The delicate balance of the power absorbed by the different species and the weak damping make also shows why this scenario for ITER needs to be understood better than is currently the case. When the damping is low it is also important to assess other parasitic absorption mechanisms, which could have played a role for the poorer performance of the $\omega=2\omega_{cT}$ scenario than others tested in DTE1 [P. Lamalle, AIP Conf. Proc. 1187 (2009)]. In addition, as a tail evolves on the distribution function of

the tritons, their absorption strength increase, this can lead to them absorbing significantly more power [D.F.H. Start, Nucl. Fusion (1999)]. Thus, a number of effects play a role, which presents a real challenge, not least to simulations. Thus, in addition to providing direct information on how the scenario should perform in ITER, possible JET DT experiments with $\omega=2\omega_{cT}$ would also provide very valuable data for validation of ICRF codes, such that one could have significantly increased confidence in their predictions for ITER.

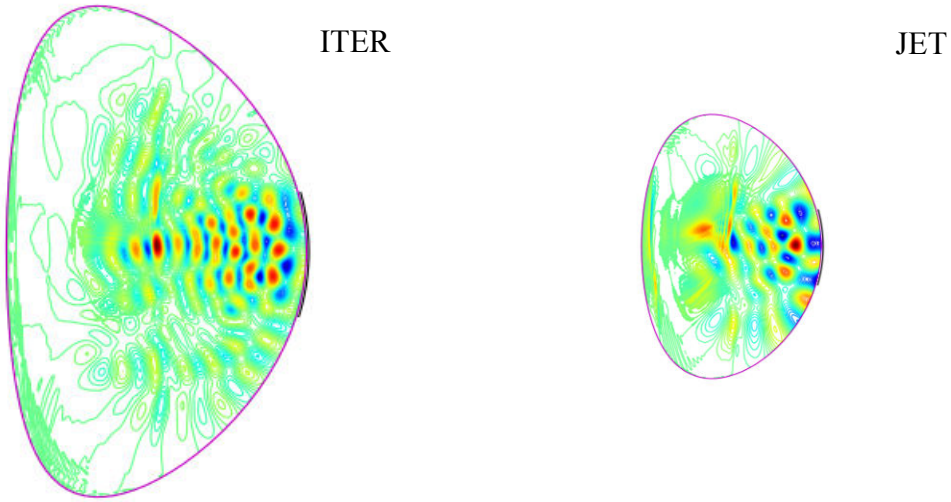

Fig. 7.3: Simulations of E_+ (left hand polarised component of the wave electric field, which to lowest order give rise to the cyclotron absorption) for ITER (left) and JET (right).

In order to simulate the increase of temperature in ITER one can, gradually, add deuterium Neutral Beam Injection (possibly also Tritium injection) and thereby increase the absorption strength on the thermal tritons to levels approaching those in the ITER flat top. Simulations of H-mode JET plasmas with 30MW NBI injection indicate that this should lead to an increase of absorption strength by ~factor 5.

The issues to study include:

- Assessing the fraction of direct electron heating by ICRF power modulation and fast ICRF switch-off; and also other possible parasitic absorption mechanisms;
- try to quantify the enhancement in $\omega=2\omega_{cT}$ damping as a non-thermal tail on the triton distribution function develops with ICRF alone and combined with T NBI injection;
- role of mode conversion near the deuterium fundamental resonance on the high field side of the $\omega=2\omega_{cT}$ resonance;
- documenting the loss of confinement and energetic triton losses as input to code simulations (RF codes, fast particle loss codes and transport codes);
- assessing the role of sawteeth in the $2\omega_{cT}$ heating efficiency by operating in sawtooth-free discharges (mode B breakdown);
- reducing direct electron heating by operating at $k_{||}\sim 3m^{-1}$ ($-\pi/2$ phasing for smaller sawteeth).

With the improved diagnostic techniques now available it is feasible to quantify these effects experimentally, which should be important information for preparation of ITER. The new diagnostics and methods include: gamma-rays with the possibility of

tomographic reconstruction for detailed studies of the confined fast ion populations [S. H. Kim, PPCF (2009)], fast ion loss detectors, new algorithms for analysing modulation experiments [V. Kiptily, Nucl. Fusion (2002)].

One should remark that the beneficial effect of NBI on the $\omega=2\omega_{cT}$ absorption has been documented in TFTR [V. Kiptily, Nucl. Fusion (2002)], where they used very strong tritium NBI heating, which enhanced the $\omega=2\omega_{cT}$ absorption significantly. In JET, however, the increase in the fast triton beta due to tritium injection would be small compared to the increase in the thermal beta; and according to the simple formula for the damping strength above, the benefit from tritium injection on the triton absorption would be small compared to simply inject deuterium. The advantage with deuterium only injection is that it is consistent with ITER and it would make diagnostic information on fast tritons easier to interpret.

To summarise, an extended coherent and well diagnosed database of shots in JET should focus on exploring $\omega=2\omega_{cT}$ absorption in conditions of low to intermediate $\omega=2\omega_{cT}$ damping strength representative of the phase before an ITER discharge transits into an H-mode. In DTE1, $\omega=2\omega_{cT}$ was used in ICRF only plasmas, i.e. the absorption was weak. Moreover, the existing JET database is very limited since the scenario was not used much due to its poor performance in terms of DT yield in JET. It should be emphasised that most of the issues listed above can be studied in a pure tritium campaign. Thus, for the point of view of ICRF studies, a significant campaign in pure tritium with a shorter campaign in DT for final verification would be appropriate.

7.3 Fundamental ^{3}He minority heating in DT plasmas, (^{3}He) DT

Application of ICRF power in the pure $\omega=2\omega_{cT}$ scenario tends to lead to a tail of few but very energetic tritons, which give rise to predominant electron heating when the absorbed power is redistributed by collisions to the thermal species. However, it might be more desirable to have a significant ion heating fraction (after collisional redistribution) to enhance the thermal fusion reactivity in the phase leading up to the H-mode transition in ITER. Furthermore, as the simulation above illustrates, even a very small residual amount ^{3}He can take a significant fraction of the power before transition to H-mode in ITER, making the scenario more unpredictable.

A stable scenario capable of producing a significant ion heating fraction is obtained by adding a small amount of ^{3}He, typically 2%, to the plasma (still using the $\omega=2\omega_{cT}$ frequency) this will lead to a combination of ^{3}He minority heating, (^{3}He) DT**,** and second harmonic tritium heating. With a few percent of ^{3}He the damping on the minority ions should dominate and the ion heating fraction can be significantly increased [V. Bergeaud, Nucl. Fusion (2000)]. This effect was clearly observed in DTE1, see Fig. 2. An extended database on the use of (^{3}He) DT should be helpful for ITER preparation, not least to provide those designing ITER scenarios with hard facts of what can be achieved. In JET experiments the ^{3}He concentration could be varied at the start of the application of ICRF power. Since in ITER one would like to minimize the ^{3}He concentration after the transition to H-mode (to keep the cost of using ^{3}He and the dilution down), one should study how the partition on absorbing species evolves as the ^{3}He concentration decays. In addition, also in this case it is of interest to add

NBI injection to assess the influence of an increasing $\omega=2\omega_{cT}$ absorption as the temperature in ITER increases.

Thus, questions to study include:

- Optimum ^{3}He concentration, in terms of providing ion heating, in conditions similar to the phase after the current ramp but before transition to H-mode. This is an important point because of the high cost of procuring ^{3}He;
- partition among the absorbing species (^{3}He, T, electrons); also the absorption by residual levels ^{3}He should be assessed;
- other absorption mechanisms such as mode conversion and parasitic absorption should be documented;
- polychromatic heating to optimise the ion heating fraction.

7.4 Deuterium minority heating in T plasmas: (D)T with D concentration up to mode conversion

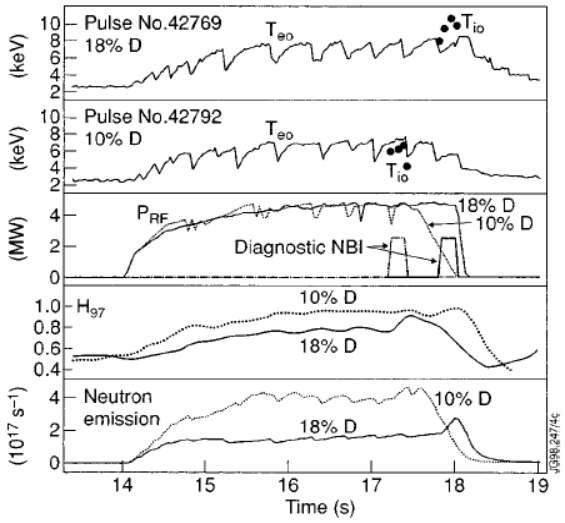

Fig. 7.4 (from [D.F.H. Start, Nucl. Fusion *(1999)]): Comparison of discharges with 10% deuterium (#42792) and with 18% of D (#42769).*

During DTE1 substantial ion heating was demonstrated using D minority heating in tritium rich plasmas (3.3MA/3.8T, 28MHz). The experiment also established the record steady state Q=0.22 with ICRH alone using 6MW of power (Fig. 7.4).

Numerical simulations reproduced fairly well the experimental results as long as the D concentration remained below 10% [P. Lamalle, AIP Conf. Proc. 1187 (2009)]. At higher D concentrations, however, the deuteron tail temperature was reduced to such an extent as to indicate that the power was not absorbed any more by the minority ions. It is possible that either mode conversion or absorption by ^{9}Be impurities could be responsible this observation. Since it is a tritium rich scenario it is clearly not suitable for the flat top phase of an ITER discharge. However, it might be possible use tritium rich plasmas in the phase between the end of the current ramp and the transition to H-mode (but need further investigation). The advantages of this would be a good ion heating fraction; an enhanced DT fusion yield due to ICRF accelerated non-thermal deuterons, combined with a lower L-H threshold. Even if this is not the reference scenario for ITER at the moment, it should be considered as a fall-back scenario in the case H-mode access in ITER is marginal. Moreover, during the ramp-down phase of ITER the use ICRH may be essential to ensure safe exit from H-mode and soft termination of the burn (by regulating the amount of ion-heating supplied to the plasma). So far no proposals for the use of ICRH during the ramp down phase of ITER have been developed.

Thus, if this is a possible scenario one should carry out experiments aiming at exploring the optimum D concentration in the phase before the H-mode transition.

Furthermore, information on the behaviour when the D concentration is increased to levels consistent with flat top operation in ITER (around 40% or more) should be obtained. The aim of the experiment should be to achieve a higher steady state Q value and to establish whether the fraction of RF power that is mode converted, absorbed by alpha particles and by ^{9}Be impurities or other parasitic mechanisms.

Consequently, issues to study include:

- Assessment of bulk ion and electron heating by means of RF modulation and RF fast switch off (break of slope method) at different D concentrations;
- documentation of mode conversion at high D concentrations;
- investigation of the parasitic absorption of RF power by the energetic α population ($\omega=\omega_{cD}=\omega_{c}{}^{4}_{He}$), and other parasitic mechanisms.

7.5 Other RF scenarios and experiments for a JET DT campaign

Fast Wave Current Drive

The Fast Wave Current Drive scenario in ITER cannot be well simulated at JET since the densities and temperatures in the flat top are too dissimilar (the direct damping on the electrons is much weaker in JET than in ITER). Furthermore, since direct electron absorption is the key factor for the current drive, there is not much to be gained by testing it in DT plasmas as compared to e.g. D plasmas on JET.

H Minority Heating in DT Plasmas

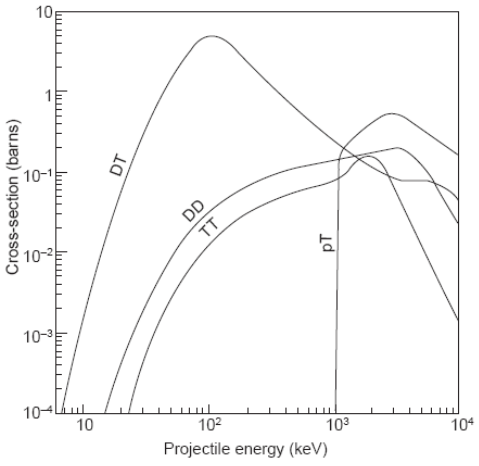

Fig. 7.5: Cross section of the p-T reaction.

For the first time in a tokamak, high power ICRF heating of H minority in T plasmas during DTE1 generated a total neutron rate about 40% larger than the 14 MeV neutron rate originating from fusion reactions between bulk tritium and residual deuterium ions. The reaction $T(p,n)^{3}He$ has been identified as responsible for the anomalous neutron rate. This reaction occurs only if the H ions have energies (in the laboratory frame of reference) above 1MeV, and the cross-section peaks at energies around 3MeV (see Fig. 7.5).

Measurements of both gamma-rays and high energy NPA confirmed the presence of this very energetic minority tail. Simulations using the PION code however show that the fast ion energy content and the p-T fusion reactivity should be even higher than those observed experimentally. The discrepancy is probably due to degradation of fast ion confinement caused by the presence of bursts fishbone-like MHD activity (n=1, with chirping frequency). With the improved fast particle and neutron diagnostics available in JET, the present experimental proposal aims at studying more in detail this heating scenario and the loss mechanisms for the fast proton population.

Comparison with alpha particle losses in the same discharges may provide insight into to pitch-angle dependence of fast ion losses.

Parasitic absorption of Lower Hybrid power by alpha particles

Lower Hybrid power is used on the JET tokamak for current drive, and its use is also foreseen in ITER because of its higher efficiency. Therefore, it is important to analyse possible parasitic absorption mechanisms that could reduce this efficiency. Fast ions and α's can absorb LH power through perpendicular Landau Damping. Different mechanisms are invoked for this process, thus different amounts of LH power are predicted to be absorbed by fast ions and α's. Previous experiments carried out on the JET tokamak have shown that parasitic absorption of LH power by MeV energy protons (whose energy per unit mass is equivalent to that of α's) is due to mode conversion of a fraction of the launched LH spectrum to high harmonic Bernstein-like waves. Operating conditions for the LH antenna were also found where such parasitic absorption could be reduced. Experiments would study parasitic absorption of LH power by α's under different operating conditions of the LH antenna, particularly with respect to the antenna phasing and power spectrum. The diagnostic capability of JET is such that even changes to a relatively small alpha pollution can be observed.

ICRF Assisted Wall Conditioning

A recent assessment of the Ion Cyclotron Wall Conditioning (ICWC) technique has been performed on many experiments including TORE SUPRA, TEXTOR, ASDEX Upgrade and JET. ICWC discharges were produced using the standard ICRF heating antennas, at different frequencies and toroidal fields, either in continuous or pulsed mode. Intrinsic ICWC discharge in-homogeneities could be partly compensated by applying a small vertical magnetic field, resulting in the vertical extension of the discharge in JET. The conditioning efficiency was assessed from the flux of desorbed and retained species, measured by means of mass spectrometry. ICWC scenarios have been developed in D or H plasmas for isotopic exchange. In ITER, the toroidal magnetic field, generated by superconducting magnets, will be continuously maintained and GDC is not stable in the presence of high magnetic fields. Hence, ICWC was recently added to "Functional Requirements" of the ITER ICRF system and approved for integration into the ITER baseline. In ITER, the toroidal magnetic field will be 5.3 T during the DT phase. With RF frequencies of the ICRH generators ranging from 40 to 55 MHz, Ion Cyclotron Resonance layers for D^+ ions at B_T = 5.3 T lie on the magnetic axis (above the divertor), and on the high field side respectively. Such a scenario can only be simulated in JET for deuterium, with ITER-relevant f/B_T values of 7.0 – 10.5 MHz/T, at B_T = 3.3 T and f = 25 MHz. Deuterium discharges created by ICWC would then be used at JET to study the tritium removal efficiency (see ITER relevant cleaning methods in Chapter 8.1).

8. Fusion Technology

8.1. Tritium retention studies in DT
8.2. Tritium processing and AGHS
8.3. Neutronics and Activation
8.4. Safety and waste management

Key points:

An extensive fusion technology programme can be implemented in parallel with a DT programme, covering:

- Tritium retention with the ITER-like wall, including retention by co-deposition, formation of (tritiated) dust, the study of long term retention by taking samples and validation of tritium accountancy methods.
- The assessment of tritium removal using cleaning techniques proposed for ITER:
  - Clean-up discharges
  - Divertor bakeout
  - ICRH glow discharge cleaning
  - Hot and cold temperature venting
  - Laser detriation in the divertor area

A DT campaign at JET can give a 14 MeV neutron flux in excess of 10^{12} n/s·cm^2 and a fluence in excess of 10^{14} n/cm^2 on the first wall, which are significantly larger than what is achievable in any other existing experimental facility, allowing:

- Test/rehearsal of ITER calibration procedures for neutron diagnostics in the DD, TT and DT neutron energy ranges and possibly providing tests of novel neutron monitor concept proposed for ITER.
- Irradiation tests of ITER relevant material samples by 14 MeV neutrons, including neutron damage to critical ITER diagnostic component and possibly including (small) breeder blanket mock-ups.
- Validation of neutron transport codes in realistic geometries/materials and operational experience in safety and waste management technologies.

8.1 Tritium retention studies in DT

The JET activities in support of ITER include also technology R&D with particular focus on activities which aim at providing support for ITER.

- Tritium retention studies of in-vessel tiles, on introduced materials (beryllium, tungsten etc) are important not only for ITER, but also for the Operator (decommissioning information for JET);
- tritium accountancy: Validation of gas balance method through post mortem analyses on tiles and on deposits (rotating collectors, capacitive balances). Benchmark methods for tritium accountancy in ITER;
- documenting the fuelling and reprocessing requirements with the ILW of scenarios envisaged for ITER, including isotope mixture control, the use of tritium gas, seeding and cleaning techniques; and
- characterisation of dust including its activation, tritium retention in dust, and removal of tritium from dust (including tritium out-gassing). Assessment of local tritium measurement (dust catcher, speckle interferometer, capacitive diaphragm balance, marker coupled with spectroscopy);

The behaviour of the JET carbon wall has been well documented in DTE1 and in more recent hydrogen and deuterium retention experiments. During DTE1, 35g of tritium were introduced into the vessel, of which about 11.5g remained after the last tritium pulse (see Fig. 8.1). In a typical pulse some 0.05g of tritium was retained, representing some 30% of the tritium introduced.

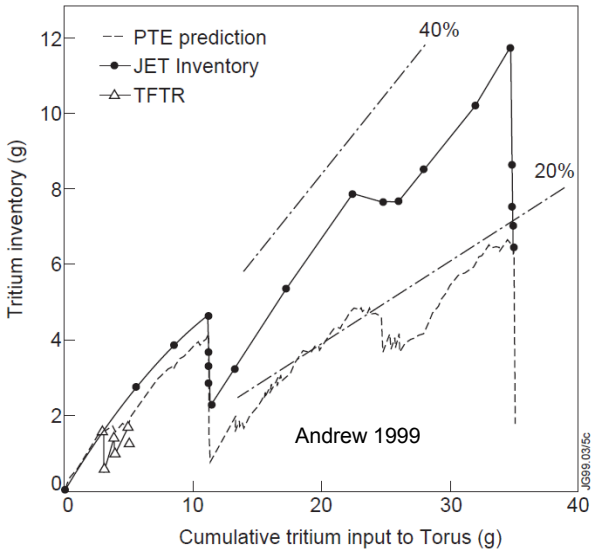

Fig. 8.1: Evolution of tritium inventory as a function of input into torus during DTE1. The drops after 11g and 35g of T input are the result of cleanup pulses.

After DTE1 the tritium in-vessel inventory decreased to 6.2g or 18% of total T input using clean-up pulses. Fig. 8.2 (Loarer et al, J.Nucl.Mat. 337–339 (2005) 624) shows the evolution of the amount of tritium removed in Ohmic cleanup pulses after the last DT pulse, up to pulse 41790, when ICRH was applied. ICRH only transiently improved T removal. The removal rate of ~10^{21} T atoms per cleanup pulse was very low, compared to the in vessel inventory of about 10^{24} tritium atoms.

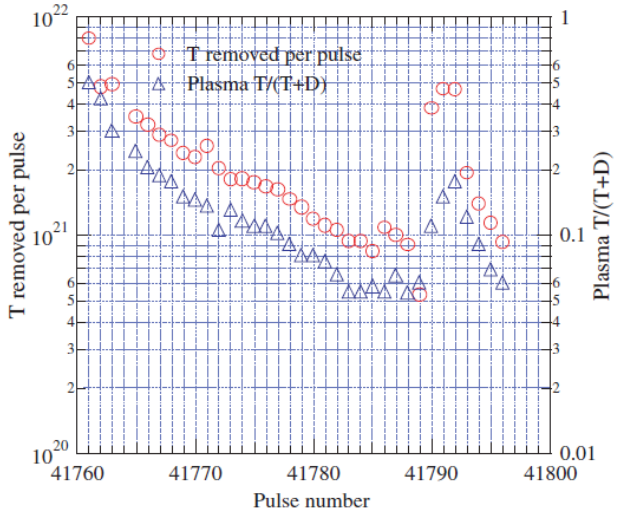

Fig. 8.2: From Loarer et al, J.Nucl.Mat. 337–339 (2005) 624: Tritium atoms removed and plasma isotopic ratio (T/(T+D))as a function of the pulses performed after the last 100% tritium pulse (#41760). After 20 pulses, the number of tritium atoms removed per pulse has dropped by more than 10 i spite the presence of more than $9.53x10^{23}$ T particles in the vessel.

Most other clean-up efforts, such as 'deuterium soaking' (no plasma), Glow Discharge Cleaning and divertor baking to 135^0C were ineffective. Venting, with a vessel temperature in the range 120-150^0C for 2 days allowed removing a further 0.6 g of tritium in form of HTO. Further venting at room temperature for several months during the post DTE1 shutdown released another 1.9 g tritium in the form of HTO. The remaining 3.7g of tritium (10.6%) was mostly in the form of Carbon co-deposits in cooled parts of the inner divertor, out of view of the plasma. Most of the deposits had flaked off and fallen below the divertor (N. Bekris et al., Journal of Nuclear Materials 337–339 (2005) 659–663). Some of those flakes, containing 0.5g of T, were recovered during the shutdown, but the main part, containing 3g of T at the end of DTE1 remained at the bottom of the vessel. An estimated 0.1 g was retained in the divertor tiles (strike point areas) and another 0.1g elsewhere in the vessel. An overview is given in Table 8.I.

Table 8.I: Tritium inventory during post DTE1 clean-up (Courtesy of Th. Loarer)

JET DTE Campaign 1997-1998	T Vessel inventory
End of DTE1 campaign Injected-Exhausted (35g – 23.5g)	11.5 g
Clean up phase (D, H, He, Disrp, GDC…) →Remove 5.3g	6.2 g
Venting → Remove 2.5g	3.7 g
Flakes →Remove 0.5g	3.2 g
Inner and Outer wall → Remove 0.1g	3.1 g
480 Tiles of Divertor → Remove 0.1g	3.0 g still remaining (flakes)

Following DTE1, tritium has been found not only in surface deposits and flakes, but at all depths inside the PFC's and virtually all materials inside the torus. The surface and bulk content of sample graphite tiles was analysed following DTE1 (Penzhorn et al, Journal of Nucl. Mat 288, 2001, p170), example profiles are shown in Fig. 8.3.

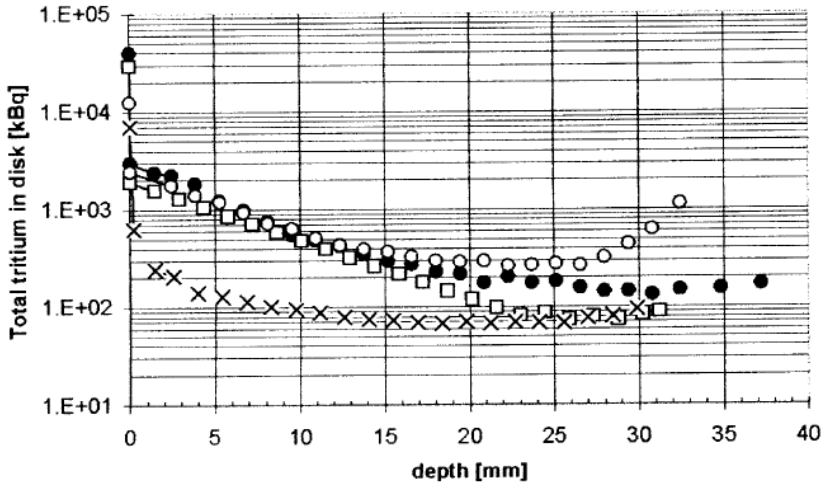

Fig. 8.3: Examples of tritium content profiles from divertor CFC tiles from various locations. (Penzhorn et al, Journal of Nucl. Mat 288, 2001, p170).

An estimated 0.2g retained in the bulk of the JET PFC's may seem negligibly small. However, one can see from the profiles above, which suggest ongoing diffusion, that tritium concentrations are far from saturated due to the relatively short exposure of the PFC's to tritium during the DTE1 campaign. Penzhorn et al. concluded that this previously unrecognised type of tritium retention represents an inventory with a long time constant that is inaccessible to any surface treatment technique and may be significance for next step machines with permanent exposure to tritium.

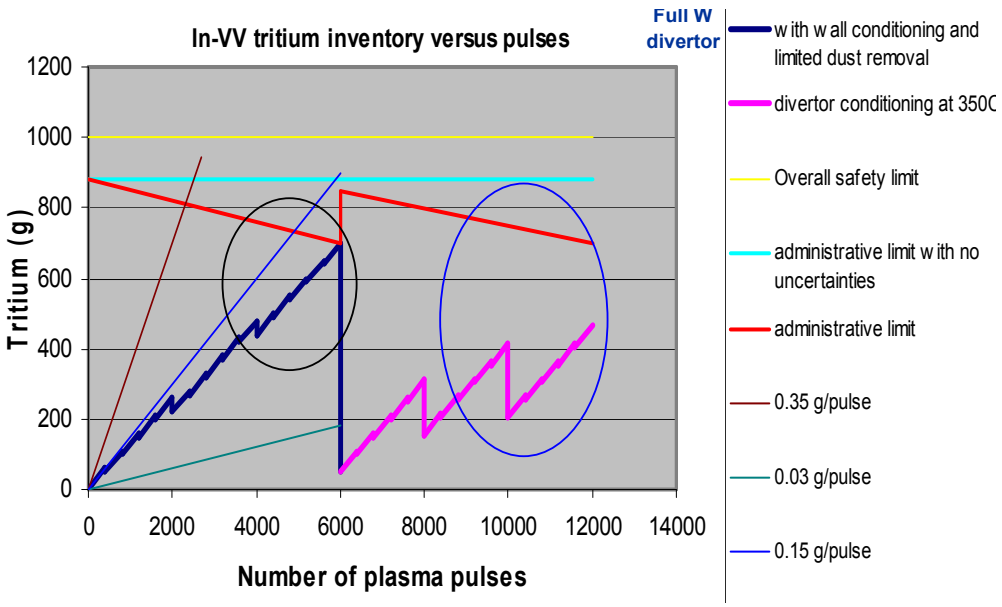

Fig. 8.4: Tritium inventory build-up for different retentions per pulse. From a presentation by S. Ciattaglia, ITER Safety Division, 11 June 2010.

The ITER operating time will be limited by the tritium inventory build-up in the vessel, the maximum permitted, after taking into account uncertainties, being about 700g. Fig. 8.4 shows tritium inventory build-up in ITER as function of pulse number using various assumptions as to the amount of tritium retained. Fig. 8.4 shows that for being able to operate for campaigns of several thousands of pulses, the inventory

build-up per shot must not be larger than a few times the retention in JET DTE1 (~0.05g) despite the much larger requirement for tritium due to the larger device size and longer pulse duration. Another requirement is the ability to drastically reduce inventories by effective cleanup procedures.

The expectation of significantly lower tritium retention, both at the surface and in the bulk, of metallic PFC's, is the main motivation for the ITER-like Wall at JET. A tritium isotope campaign and a DT campaign will allow direct comparison of retention by a full metal wall and by a carbon wall and should be helpful for the choice of PFC's used in ITER (W/Be or W/C/Be or even full W, should there be excessive co-deposition with Be).

Dedicated experiments of fuel retention on deuterium (during 2011-2014), followed by retention measurements in hydrogen and tritium would allow full assessment on diagnosing the retention for the various hydrogen species. Moreover, the results will give guidance on how to translate the results obtained in hydrogen to tritium, important for preparing DT operation in ITER, based on results from the non-active phase, using hydrogen and helium plasmas.

First figures for short term deuterium retention will become available fairly early (2011-2012) during the exploitation of the ILW, using gas balance measurements. Unfortunately, accurate figures for long term trapped deuterium cannot be obtained, due to inherent uncertainties in deuterium gas balance measurements. Tritium balance and accounting measurements are substantially more accurate. The presence of long term retained tritium in (and on) PFC's can be measured using samples retrieved after the campaign, allowing an accurate assessment of the various retention mechanisms. In the shutdown preceding tritium operation, special samples will have to be installed (free of tritium produced in D-D reactions or from tritium used in previous DT campaigns) to provide accurate references for long term tritium retention studies.

Wall pumping is expected to be stronger than with a carbon wall, i.e. more gas will have to be injected to achieve a given density, but this is not generally expected to lead to increased long term retention (R Sartori et al, Journal of Nuclear Materials, 176-177 (1990) pp 624-629). Retention in the tungsten divertor tiles by implantation is expected to be much lower than in Carbon, as already observed in AUG (M Mayer et al., J. of Nucl. Mat., 390-391, p538). Most of the retention would be in co-deposits with beryllium and oxygen. Some co-deposition with residual carbon, or with carbon released by accidentally damaged the tungsten coated Carbon tiles, will probably also occur. Post-mortem analysis will be required to assess the relative importance of co-deposition with residual carbon and with beryllium. The behaviour of possible W-Be alloys with respect to tritium trapping is unknown, as is possible bulk trapping in Be and W. For ITER and especially DEMO, where in-vessel components will have substantially longer exposure to tritium than will ever be possible in JET, these components, due to their sheer volume, may become a significant unwanted long-term repository of tritium. Only the usage of tritium in JET will provide operational experience concerning the potentially important issue of bulk tritium retention, as even very small tritium concentrations can be detected in post mortem analysis. Attention must be given to understanding the deep trapping and diffusion mechanisms, since measured profiles after limited exposure in JET, cannot be extrapolated towards

ITER or DEMO in a simple way (especially for DEMO, since trapping in radiation and plasma induced defects and porosities will probably be important).

Tritium cleanup techniques can similarly be tested in the ILW environment. These include the methods tried in DTE1, mentioned above, as well as new methods, such as:

- Ion Cyclotron Wall Conditioning, is a technique considered for ITER and already tested in JET (see end of Chapter 7). If effective, this technique could be used to keep the tritium inventory low already during the tritium (and DT) campaign.
- The Divertor LIDAR system could be used for testing the proposed technique of in-vessel laser de-tritiation on a small sample surface (20×30cm) on the upper vertical tiles of the inner divertor, where most of the co-deposition is expected to occur.
- Vessel baking under vacuum at 320^{o}C should tell us what to expect from divertor conditioning at 350 ^{o}C in ITER (for the all W divertor option). Increasing the baking temperature in JET to 350 ^{o}C should be considered.
- Hot venting, possibly up to 350 ^{o}C, should be considered for tritium removal, following promising results from DIII-D with the thermo-oxidation technique (S.-L. Allen et al, 23rd IAEA FEC, 2010, EXD/6-4). This experiment achieved 50% D removal by baking in a 2 Torr oxygen atmosphere for 2 hours without compromising subsequent tokamak operation. Lab results at 600 Torr and 350 ^{o}C achieved some 95% removal in 2 hours. Possible deleterious effects and hazards would need to be carefully assessed before an experiment with thermo-oxidation; moreover tritiated water poses a corrosion risk to the Active Gas Handling Systems at JET.

Finally, we would like to caution against relying solely on retention studies in hydrogen and deuterium. The three isotopes differ in their physical and chemical properties (see properties of hydrogen isotopes below) and it is not clear at this moment if this leads to significant differences in retention behaviour or not. Accurate data in these areas should be obtained for ITER and even more so for DEMO.

Properties of hydrogen isotopes:
The hydrogen isotopes differ in their physical and chemical properties. The difference in physical properties (e.g. gas diffusion constant) is due to the mass difference of the different isotopes and can be accounted for in a straightforward manner. However, also the chemical properties of the hydrogen isotopes differ. In the best studied case of super-heavy water the differences between hydrogen and tritium containing molecules are significant ['Lehrbuch der anorganischen Chemie', Holleman-Wiberg, 102nd edition, de Gruyter (2007)], see Table 8.II. The underlying reason for this is the different reduced mass which enters the Schrödinger equation in the nucleus-electron interaction terms. The consequences are negligible for the hydrogen-tungsten interaction as there are no relevant chemical interactions. However, beryllium forms hydrides and the strength of these bonds may be altered. Experimental knowledge on the difference between hydrogen isotopes for bonds with beryllium is extremely limited (or classified?). In a tokamak, the effect on retention is assumed to be small; this assumption however requires testing with the ITER-like Wall on JET.

Table 8.II: Comparing the properties of H_2O, D_2O and T_2O

Chemical property	**H_2O**	**D_2O**	**T_2O**
Temperature of highest density:	3.98 °C	11.2 °C	13.4 °C
pK_value (=pH+pOH) at 25 °C:	7.0	14.9	15.2
Melting temperature:	0 °C	3.8 °C	4.5 °C
Boiling point:	100 °C	101.4 °C	101.5 °C

In general tritium is less reactive in chemical reactions than hydrogen, which, however, may be overcompensated by the effects of radioactive decay; tritium decays by beta-emission with E=18.6keV, which may influence the trapping behaviour (and erosion behaviour) of T-containing materials. The best example is the extreme corrosion of steel by tritiated water, which is unexpected considering the low reactivity of ordinary water.

8.2 Tritium processing and AGHS

During DTE1, the JET torus was pumped continuously through by the Active Gas Handling System (AGHS) and was supplied with tritium (and deuterium) by the gas introduction and neutral beam (NB) systems. The tritium was stored in uranium beds and reprocessed in the AGHS to a purity of 99.4% by gas chromatography. The site inventory of 20 g of tritium was reprocessed eight times by the AGHS, making the equivalent of 99.3 g of tritium available for DTE1, permitting a significant number of tritium and DT experiments.

The Active Gas Handling System (AGHS) at JET is a key part of DT operation as the JET torus is pumped continuously through by the on-site closed circuit. The possibility of testing key ITER technology however, may require intervening in a system controlled by strict safety regulations, and remains to be studied.

8.3 Neutronics and Activation

Accuracy of the neutron diagnostics is of paramount importance not only for determining the fusion power, but for a machine expecting significant tritium burn, also for tritium accountancy. The basis for neutron diagnostic calibration in DTE1 was the activation technique, using plasma discharges as neutron sources and achieved an accuracy of some 10%. Different samples were used for DD and DT neutrons (L. Bertalot et al, Rev. Sci. Instrum., 70, 1999, p1137). Even better accuracies would be required for ITER. A calibration strategy for ITER calls for "(1) a functional link of several types of neutron measurement systems, (2) series of well-planned in situ calibration process and (3) an accurate neutron transport study" (M. Sasao et al, Rev. Sci. Instrum., 81, 10D329, 2010). The in-situ calibration involves a source moved around the torus or placed at a large number of discrete positions for the time required for accumulation of a sufficient number of counts. A ^{252}Cf source with a broad spectrum ~2MeV is only suitable for DD neutrons. D-T neutron generators (small accelerators) with rates of $\sim 10^{11}$n/s are required and are currently under development. Their usage is however challenging because of their size (not too

big for the JET boom though), because of self-shielding by the source material, leading to an altered energy spectrum and anisotropic emission. The non-ideal effects may be mitigated in several ways, such as averaging over source orientations, but ultimately the numerous non-ideal effects will have to be corrected for by intensive neutron transport calculations using an accurate nuclear model of the device and its surroundings together with the source and temporary supporting structures.

Although JET would not need this procedure for a further DT campaign, it would provide a unique (possibly the last and only) opportunity for testing and validating it before application to ITER. The experience gained would likely allow avoiding errors, which would be costly in time (the procedure is time-consuming), money and lost accuracy.

JET could also provide a test for a neutron monitor concept proposed for ITER, which is based on the activation of water by $^{16}O(n,p)^{16}N$ reaction with an energy threshold ~10 MeV. The ^{16}N decays with emission of a detectable γ-ray with a half life time of 7.13 s. This detector involves flowing water through pipes to a position in the vessel with direct exposure to 14MeV neutrons for a duration determined by the desired time resolution and bringing it back outside the vessel within a times shorter than the half life for measurements of the decay gammas. Tests at JET would also allow comparison with other (and already available) neutron detectors.

Activation tests on sample of ITER relevant materials could take advantage of the high 14 MeV neutron flux / fluence that could be obtained in JET DT campaign at the first wall level. Assuming a rate of 10^{19}n/s, and a total budget of $>2\cdot10^{20}$ neutrons, at irradiation ends the 14 MeV neutron flux would be in excess of 10^{12} n/s·cm^2 and a fluence in excess of 10^{14} n/cm^2. Such neutron flux level is not achievable by presently available 14 MeV neutron generators, while the fluence is achievable only after several weeks of irradiation and only for very small volumes. Hence, a DT campaign at JET provides a high level of 14 MeV neutron fluence that can be used to measure:

- The activation of materials foreseen for ITER;
- the activation materials characterised by short term activation (relevant to accident doses and decay heat);
- the activation specific materials of interest and consequent dose rates, such as Ar, N, carbon gases etc; and
- the influence of neutrons on diagnostics materials and instrumentation: New optical fibres, detectors, mirrors and windows, together with testing the stability of electronics.

Using activation samples would allow validation of neutron transport codes in the presence of streaming paths, such as channels, relevant for ITER diagnostics and heating systems at distances far from the neutron source.

Finally, benchmark experiments on mock-ups of the European breeder blankets (HCLL and HCBP, mock-ups already available) could be tested at JET, by mounting the mock up on top of a vertical port at JET. This would test the instrumentation developed for the Test Blanket Modules (TBMs) in the presence of realistic neutron and gamma ray spectra, and magnetic field. This activity is not crucial for ITER operation, but would provide useful information for the ITER TBM program.

8.4 Safety and waste management

A future DT campaign would provide controlled and accurate data for extrapolating to ITER and for licensing of ITER on:

- Database on tritium release in the material and environment in normal operation and in maintenance activities;
- Database on the performance and reliability of tritium handling and on occupational radiation exposure and collective doses during repair, maintenance and shutdown periods;
- Decontamination operations in plant areas following abnormal events; and
- Existing database has been collated from old JET records.

After a tritium and/or DT campaign the tritium removal efficiency from plasma facing components and dust (divertor baking, DD sequence at the end of DT), ICRH conditioning and laser techniques (LIAS/LIBS) will be tested, together with tests on samples removed from the JET machine after the DT campaigns.

The activation of the JET device will provide validation of shutdown dose rate calculations under fusion-relevant DT conditions for ITER. The available, state-of-art codes have been validated using small mock-ups irradiated at 14 MeV generators, but still provide different predictions when applied to the ITER case. Validation of such codes is needed; validation at JET would be extremely valuable.

Moreover, new data may be obtained to validate the PACTITER code for the calculation of activated corrosion products (ACP) in ITER in fusion relevant condition. The feasibility of using JET results needs to be assessed; however, the code has been validated only in fission reactors so far.

Finally, the study waste management and disposal routes for new waste categories will provide input for ITER and DEMO on the:

- Characterization of beryllium wall & tungsten divertor for waste strategy;
- detritiation (thermal annealing under radiation and magnetic field, incineration…), removal of impurities (chloride route…) and disposal or recycling by metallic powder; and
- limitation of outgassing of tritium from metallic waste (tiles, plant material).

9. DT campaign proposals

Key points:

The campaign proposed for the DT phase of JET includes:

- A shutdown and restart period prior to DT operation.
- The sequence of experiments would start with operation with 100% hydrogen, with both neutral beam boxes converted to hydrogen.
- Followed by operation using 100% tritium, with both neutral beam boxes converted to tritium.
- With a 14MeV neutron budget of up to $3x10^{20}$ neutrons, a DT campaign would last ~1 month, allowing ≤10 discharges for ITER scenario demonstrations and limited ICRH physics studies.
- Alternatively, an extended DT campaign of ~6 months (up to $17x10^{20}$ neutrons) would allow optimising fusion performance in ~50 high power discharges towards high fusion gain, including long pulse integrated scenario demonstration in DT, for the studies of alpha particle driven instabilities, together with a detailed ICRF heating scenario assessment.
- An ITER relevant cleanup phase would follow, including some final reference discharges for isotope and retention studies.
- A period of 6 months after the DT campaigns is required to allow entry for sample removal and for essential diagnostic (neutron) calibrations.

In this case study, programme options for DT operation in combination with the installation of RMP and/or ECRH systems have not been considered.

9.1 The JET programme leading up to DT operation

The JET experimental programme will be focused strongly on preparations for ITER construction and exploitation, concentrating in 2011 on the following programmatic Headlines:

1. Characterisation of the ITER-like Wall;
2. Exploration of ITER operating scenarios with the ITER-like Wall; and
3. Physics issues essential to the efficient exploitation of the ITER-like Wall and ITER.

The expansion of the operational domain with the ILW will be progressive and is expected to require several years from 2011-2013, with Experimental Campaigns being interspersed by periods of system commissioning and intervention(s), primarily for the removal of tile samples for post-mortem analysis.

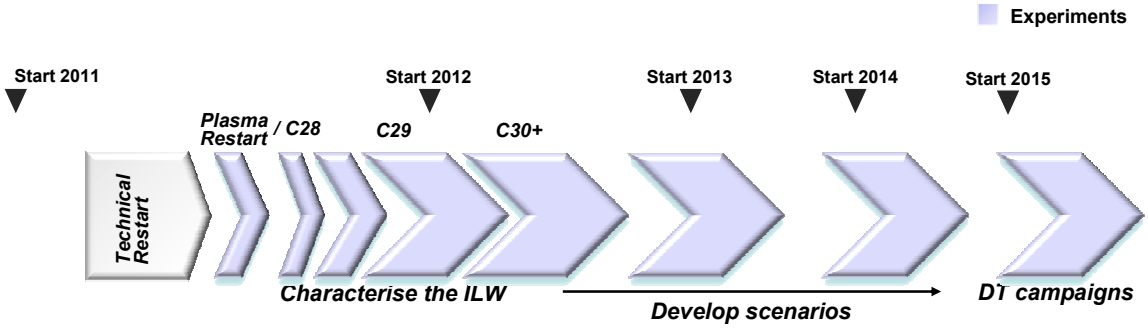

Fig. 9.1: A five-year roadmap for the exploitation of the recent enhancements at JET.

An outline programme sequence leading up to DT operation would include:

- First plasma following the present shutdown in late July 2011;
- Operation until end of June 2012;
- A six month shutdown form July 2012 to December 2012 to remove tile samples using remote handling but with no manned intervention in the machine;
- Operation through the first half of 2013;
- Another six month shutdown, possibly with a remote handling exchange of the bulk tungsten tile. Again, no manned access inside the machine;

To establish a firm basis for defining the sequence and priorities for a (restricted) tritium and/or DT programme, the preparation and milestones prior to high performance DT operation will have to be defined.

During 2013 and early 2014, the experimental campaigns would:

- Demonstrate plasma operation closest to ITER parameters and related physics issues with the full exploitation of EP2 enhancements;
- Consider H/He campaigns, reversed ∇B, TF ripple and W-bulk melt experiments (before the shutdown in 2013); and
- Obtain key objectives required for a successful DT campaign, all compatible with the ILW, including a full rehearsal in deuterium using the AGHS at JET, operation at the highest plasma currents (at least 4.5MA), at maximum input power and B_T=3.4-4T, at the lowest possible plasma density, obtaining low ν^*.

9.2 DT programme assumptions

Operating JET with deuterium-tritium in 2014-2015 would be a final phase in a five year "JET programme in support of ITER", integrating experimentation with an ITER-like wall and the development of plasma configurations and parameters towards the most ITER-relevant conditions achievable. Moreover, it would allow a full exploitation of recently enhanced scientific and technical capabilities.

The DT campaigns assumptions include:

- DT Campaign is performed with W/Be wall. The solid W tile 5 may be exchanged for W-coated carbon tile in 2013;
- Full NB power at 35MW + 5MW from ICRH must have been shown to be available and compatible with ILW (for at least 5s) at high plasma current;
- High performance (hybrid) scenarios must have been developed in DD (3.5-5 MA), including operation up to 4T that is needed for performance optimisation and tests of ITER relevant ICRF heating scenarios; and
- LHCD can be used (in contrast to DTE1);

DT campaign in 2014-2015 would require significant preparation in deuterium, starting as soon as possible, with the development of plasma scenarios that aim for high absolute performance whilst also being compatible with the ILW. Results obtained in reference discharges and high performance discharges could even give a late "go or no-go" milestone for certain elements in the DT programme.

A shutdown prior to DT is mandatory, to remove any equipment that is not tritium compatible or equipment that will be damaged by DT neutrons. Some diagnostics that will be damaged can be left on the machine to have maximum use of their measurements right up to the first high performance DT discharges.

A restart and commissioning phase is required to ensure all systems are tritium compatible. This restart phase could be run in deuterium as a final test before the use of tritium.

A first series of experiments would be run in pure hydrogen, with both NB boxes converted to hydrogen. This would remove any remaining deuterium from the walls, and provide reference discharges for isotope and ITER scenario studies.

The DT campaign would then start with a full tritium campaign. During this campaign the neutron production will depend on (background) deuterium concentration. The TT reactions will produce a similar amount of neutrons compared to deuterium. We estimate that with 1% deuterium concentration the DT neutron production would allow up to 200 high power pulses (using a 14MeV neutron budget of ~$2x10^{19}$). With 10 to 20 high power tritium NBI pulses possible per week (limited by tritium consumption) this results in a total 100% tritium campaign length of ~2 months.

The DT phase itself could be divided in a low power campaign for physics studies, diagnostic tests (neutrons) and may include some test at 10:90 and 20:80 D:T mixtures of full power discharges (short pulse tests). A second phase would then be for high performance DT and alpha-physics studies.

A cleanup phase would follow, and take about 2 months, including some final reference discharges for isotope and retention studies.

9.3 Options for the JET DT programme (campaign proposals)

A limited DT neutron budget of $\underline{3x10^{20}}$ would have $2x10^{19}$ neutrons for full tritium and $2.5x10^{20}$ for a brief DT campaign (20MW of fusion power for 5s would produce $3.55x10^{19}$ DT neutrons), requiring about 1 month of campaign time, allowing ≤10 discharges for ITER scenario demonstrations and limited ICRH physics studies. Up to ~$3x10^{19}$ could be in reserve for clean-up or essential post campaign DD reference discharges, with some tritium background.

Table 9.I: DT campaign proposal with a limited neutron budget (~ $3x10^{20}$ ~ DTE1)

Programme item	Duration	Period
		1st half of 2014
Complete the ILW characterisation and final preparation in deuterium, including reference discharges	6 months	
		2nd half of 2014
Shutdown prior to DT operation	4 months	
Restart, incl. tritium system commissioning	2 months	
Conversion to hydrogen, campaign at 100% hydrogen	1 month	1st half of 2015
100% tritium operation (both NBI boxes)	2 months	
Low yield and high yield DT campaign	***1 month***	
ITER relevant cleanup and final reference discharges	~2 months	
Bring JET to a safe state for decommissioning and entry for tile sample removal	6 months	2nd half of 2015

A full DT neutron budget of $\underline{17x10^{20}}$ would have a much more comfortable $16.5x10^{20}$ neutron budget allowing an extended DT campaign lasting 6 months for optimising fusion performance in ~50 high power discharges towards high fusion gain, including long pulse integrated scenario demonstration in DT, for the studies of alpha particle driven instabilities, together with a detailed ICRF heating scenario assessment..

Table 9.II: DT campaign proposal with a neutron budget up to the JIA limit (~ $17x10^{20}$)

Programme item	Duration	Period
		1st half of 2014
Complete the ILW characterisation and final preparation in deuterium, including reference discharges	6 months	
		2nd half of 2014
Shutdown prior to DT operation	4 months	
Restart, incl. tritium system commissioning	2 months	

Conversion to hydrogen, campaign at 100% hydrogen	1 month	2015
100% tritium operation (both NBI boxes)	2 months	
Extended DT campaign	***6 months***	
ITER relevant cleanup and final reference discharges	~2 months	
Bring JET to a safe state for decommissioning and entry for tile sample removal	6 months	1st half of 2016

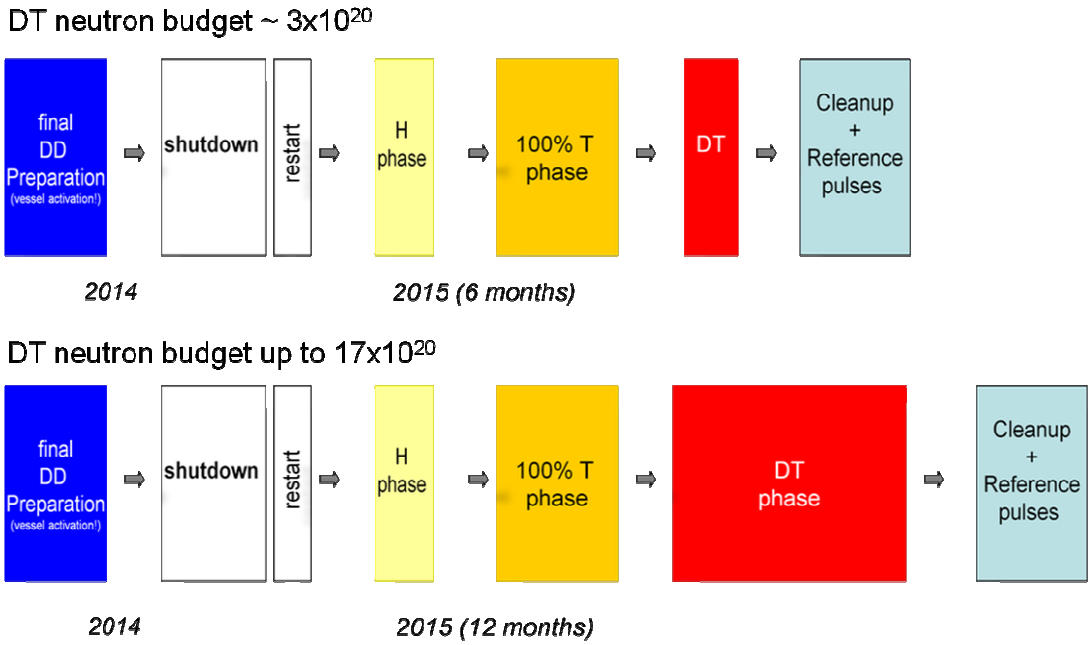

Fig. 9.2: Two options for DT campaigns in 2015.